NASA CONTRACTOR REPORT

NASA CR-1934

LF336 LIFT FAN · MODIFICATION AND ACOUSTIC TEST PROGRAM

by S. B. Kazin and L. J. Volk

Prepared by
GENERAL ELECTRIC COMPANY
Cincinnati, Ohio 45215
for Ames Research Center

NATIONAL AERONAUTICS AND SPACE ADMINISTRATION • WASHINGTON, D. C. • DECEMBER 1971

1. Report No.	2. Government Accession No.	3. Recipient's Catalog No.
NASA CR-1934		

4. Title and Subtitle	5. Report Date
LF336 Lift Fan Modification and Acoustic Test Program	December 1971
	6. Performing Organization Code

7. Author(s)	8. Performing Organization Report No.
S. B. Kazin and L. J. Volk	
	10. Work Unit No.

9. Performing Organization Name and Address	11. Contract or Grant No.
General Electric Company Aircraft Engine Group Cincinnati, Ohio 45215	NAS2- 5462
	13. Type of Report and Period Covered
12. Sponsoring Agency Name and Address	Contractor Report
National Aeronautics & Space Administration Washington, D. C. 20546	14. Sponsoring Agency Code

15. Supplementary Notes

16. Abstract

A NASA-sponsored research program was conducted to investigate lift fan noise reduction by configuration modifications. An existing lift fan, the 1.3-pressure-ratio, 36-inch-diameter LF336/A, was the test vehicle. Modifications tested included three outlet stator vane rows (including one with lean), two rotor-stator spacings, and addition of acoustic treatment and acoustic exit louvers. The tests were conducted at the General Electric Edwards Flight Test Center, using a test site constructed specifically for acoustic testing.

Incorporation of all these modifications reduced the aft quadrant fundamental and second harmonic power levels by 19.6 dB and 10.7 dB, respectively, and reduced the 150-foot arc peak PNL by 13.5 PNdB.

1. V/STOL
2. Noise reduction

17. Key Words (Suggested by Author(s))	18. Distribution Statement
lift fan noise	UNCLASSIFIED-UNLIMITED

19. Security Classif. (of this report)	20. Security Classif. (of this page)	21. No. of Pages	22. Price*
UNCLASSIFIED	UNCLASSIFIED	140	$3.00

*For sale by the National Technical Information Service, Springfield, Virginia 22151

TABLE OF CONTENTS

SUMMARY

A NASA-sponsored research program was conducted to investigate lift fan noise reduction by configuration modifications. An existing lift fan, the 1.3-pressure-ratio, 36-inch-diameter LF336/A, was the test vehicle. Modifications tested included three outlet stator vane rows, two rotor-stator spacings, and addition of acoustic treatment and acoustic exit louvers. The tests were conducted at the General Electric Edwards Flight Test Center, using a test site constructed specifically for acoustic testing.

For a lift fan aircraft, noise radiated in the rear arc is the most important because of the orientation of the lift fan in the aircraft. Thus, noise comparisons were made using data in that quadrant. The tests showed that increasing the vane/blade ratio from 1.07 to 2.14 reduced the aft quadrant sound power level (PWL) of the fundamental blade passing frequency about 7 dB and the corresponding second harmonic PWL about 5 dB. This reduction amounted to a decrease in the 150-foot arc perceived noise level (PNL) between 1 and 4 PNdB. Leaning the stator vane 30° in the direction of rotation reduced the aft quadrant fundamental PWL about 4 dB and reduced the corresponding second harmonic PWL about 5 dB. Selection of the lean angle for this stator was arbitrary, and further analytical effort and testing will be required to optimize the selection of vane lean angle in future fan designs. Increasing spacing from 0.15 to 1 chord significantly decreased the tone noise and broadband noise, and resulted in a sideline peak PNL reduction of 5.4 PNdB. Increasing spacing from 1 chord to 2 chords resulted in an additional PNL reduction of 1.3 PNdB, for a total reduction of 6.7 PNdB. An initial reduction of 4 PNdB was obtained at 0.15 chord spacing by changing from 45 vanes to 90 leaned vanes. Changing to 2-chord spacing reduced the arc peak PNL another 2.5 PNdB; thus, the noise increment due to spacing with a leaned vane row was less than that obtained with a radial vane row. Acoustic treatment was tested with 90 leaned vanes at 2 chord spacing. Treatment was added to the flowpath hub and tip walls and to an acoustic splitter on the surface facing the tip wall. The treatment reduced the aft quadrant peak fundamental sound pressure level (SPL) about 4 dB and the corresponding fundamental power level (PWL) about 3.7 dB. The second harmonic SPL was reduced 5 dB and the second harmonic PWL was reduced 4.9 dB. With the addition of acoustic treatment to louvers used to vector the flow, the peak fundamental tone SPL was reduced 12.5 dB, and the aft quadrant fundamental PWL was reduced 8.1 dB. The corresponding noise reduction was 2 PNdB. Incorporation of all these modifications reduced the aft quadrant fundamental and second harmonic power levels by 19.6 dB and 10.7 dB, respectively, and reduced the 150-foot arc peak PNL by 13.5 PNdB.

LIST OF ILLUSTRATIONS

LIST OF ILLUSTRATIONS (continued)

LIST OF ILLUSTRATIONS (continued)

LIST OF ILLUSTRATIONS (continued)

LIST OF ILLUSTRATIONS (continued)

LIST OF ILLUSTRATIONS (continued)

LIST OF ILLUSTRATIONS (concluded)

LIST OF TABLES

INTRODUCTION

Potentially, one of the most serious problems facing commercial vertical takeoff and landing (VTOL) aircraft is noise. Although no federal regulations exist at this time, noise limits for VTOL aircraft probably will be at least as stringent as those applied to conventional takeoff and landing aircraft. The necessity of bringing the VTOL aircraft into city centers may require that even lower noise levels be obtained. These low noise levels will in many cases have to be obtained without the advantage of extensive use of acoustic treatment. The podded or fan-in-wing lift fan installations do not lend themselves to large treatment areas since these configurations employ shallow inlets and little or no exhaust ducting. The only areas which can be treated are within the fan frame and on the exit louvers. The generation of noise by the lift fan must, therefore, be limited by judicious selection of the fan cycle and geometry if low noise is to be obtained.

An extensive lift fan acoustic research program was conducted using the LF336 as the test vehicle. The objectives of these tests were:

- To better understand the sources and propagation of lift fan noise
- To substantiate analytical noise prediction methods
- To evaluate noise reduction potentials for lift fans for changes in stator configuration, rotor-stator spacing, and acoustic treatments.

The tests were conducted in three phases:

- LF336/A Acoustic Tests
- LF336/B Modification and Acoustic Tests
- LF336/C Modification and Acoustic Tests

LF336/A Acoustic Tests - The LF336/A is the design configuration which has a rotor-stator axial spacing of 0.15 blade chord at the fan tip. Acoustic measurements were taken on one fan under Contract NAS2-4970.

LF336/B Modification and Acoustic Tests - The LF336/B configuration is the same as the LF336/A except the rotor-stator axial spacing was increased to 2 chords at the fan tip. Spacing hardware was manufactured and acoustic measurements were taken on one fan under Contract NAS2-4970.

The LF336/A and LF336/B tests were conducted in January and February, 1969. Test results are given in References, 1, 2, and 3.

LF336/C Modification and Acoustic Tests - The LF336/C denotes the fan in a reduced noise configuration, with changes in vane geometry and spacing, and with acoustic treatments. Hardware was manufactured and 12 tests were conducted under Contract NAS2-5462. Testing began December, 1969 and was completed in July, 1970. Test data are published in Reference 4. The basic areas of investigation on this program were:

- Vane number
- Split vane row
- Vane lean
- Rotor-stator spacing
- Acoustic treatment
- Acoustic exit louvers

LIST OF SYMBOLS

B	Blade number
dB	Decibels
Deg	Degrees
k	Zero or any positive or negative integer
m	Spinning lobe number
PNdB	Perceived noise level units
PNL	Perceived noise level, PNdB
PWL	Sound power level, dB re 10^{-13} Watts
RPM	Fan rpm
SPL	Sound pressure level, dB re 0.0002 dynes/cm^2
V	Vane number

MODEL AND APPARATUS

LF336 Lift Fan

Geometry features offering potential noise reduction were investigated by making practical hardware modifications to an existing lift fan, the LF336/A. Two of these fans were built under the LF336/A High Pressure Ratio Lift Fan Program (Contract NAS2-4130) for use in NASA wind tunnel investigations.

The LF336/A is a single-stage, turbotip, 1.3-pressure-ratio, 36-inch-diameter, rotor-stator lift fan driven by the full flow of one dry J85-5 turbojet engine. A fan cross section is shown in Figure 1. Table I is a fan design point description. There are 42 blades, with a fundamental blade passing frequency of 4230 Hertz at 100 percent rpm. There are 45 vanes, with a rotor-stator axial spacing of 0.15 blade chord.

Special Hardware

Hardware was manufactured to provide the following configuration changes:

Three Vane Rows:

- Split vane row with 90 tip vanes and 45 hub vanes
- 90 vanes
- 90 vanes with 30° lean

Two Spacings:

- 1 chord and 2 chords

Acoustic Treatment:

- Hub and tip walls and acoustic splitter

Acoustic Exit Louvers

Table II lists the tests, test dates, and test configurations. A balanced program was conducted, as shown in Table II, to investigate the effects of vane geometry, vane-to-blade ratio, vane-blade spacing, acoustic treatment, and acoustic exit louvers on lift fan noise.

Test Site

The tests were conducted at the General Electric Edwards Flight Test Center. The test site is in an area free of buildings and obstructions and was constructed specifically for acoustic tests. Figure 2 shows an overhead

view of the test site. Figures 3 and 4 show two ground-level views of the test site. The control room protrudes only 2 feet 6 inches above the ground. The test stand is mounted on a concrete surface. The area surrounding the sound field consists of desert sand and brush.

Figures 5 and 6 show two views of the fan installed on the test stand. The fan bellmouth inlet was mounted flush with a flat steel plate to simulate a wing or pod upper surface. The fan was 10 feet above the ground with the fan flow parallel to the ground. The J85 gas generator was connected to the fan by a pants-leg-duct arrangement which delivered the full J85 exhaust to the fan scroll. A sound suppressor was mounted to the J85 inlet to reduce engine compressor noise far below the lift fan noise.

INSTRUMENTATION AND DATA REDUCTION

Sound Field

All acoustic data measurements were made using Bruel-Kjaer microphone systems. Model Numbers 4133 and 4134 microphones were used for far-field measurements, and Model Number 4136 microphones were used for probe measurements.

Far Field Microphones - Figure 7 is a sketch of the far field microphone arrangement. Seventeen microphones were installed 10 degrees apart along a circular arc. The microphone arc radius was 250 feet for the LF336/A and LF336/B tests. For the LF336/C tests, the arc radius was changed to 150 feet, and one additional microphone was installed at a 250-foot radius at 120 degrees from the fan inlet.

For the acoustic louver test, additional microphones were installed at a 150-foot radius at angles greater than 180 degrees (see Figure 7) to measure noise directivity with the louvers deflected. All far-field microphones were installed in a plane which passed through the fan axis and was parallel to the ground.

Acoustic Probes - For all tests, one fan inlet probe and one fan exhaust probe were used. In addition, for the acoustic louver test, a third probe was used at the louver discharge. Figure 8 shows the fan inlet and exhaust probes installed. The open end of the probe was immersed in the flow passage, with the microphone mounted outside at the end of the probe tube. A 40-foot length of tubing was wound into a coil and attached at the end of the probe mounting block to eliminate reflection and standing waves. The probe assembly was driven by a remote-controlled actuator to translate the sensing end of the probe to any desired immersion setting.

Acoustic Data

Data Acquisition - The output of each microphone was fed to an amplifier for attenuation or amplification. This output was then recorded on a Hewlitt-Packard Model 3900 FM tape recorder operated at 30 inches of tape per second

with a system response of 0 to 20,000 Hertz. Figure 9 shows a schematic of the complete data acquisition system. Figures 10 and 11 are two views of the control room showing the recording equipment used.

Data Processing - All 1/3-octave data processing was performed using a high-speed computerized data system developed by General Electric. The basic components of the system are a Bruel-Kjaer 1/3 octave filter bank, a high-speed electronic scanning system for the filters, an analog-to-digital converter, and an SDS-920 computer. Each data channel was processed for a continuous 30 seconds integration time to obtain the following acoustic data:

1. One-third octave sound pressure levels corrected to sea level standard day conditions

2. Overall sound pressure levels calculated from the corrected 1/3-octave sound pressure levels, and overall sound pressure levels as obtained directly from the tapes

3. Directivity indices

4. Calculated perceived noise levels, using SAE Aerospace recommended practices

5. Extrapolation of the 1/3-octave sound pressure levels, overall sound pressure levels, and perceived noise levels to 200- and 500-foot sidelines

6. One-third-octave sound power levels, corrected to the source

All narrow-band data were processed by a Federal Scientific UA-6A real time analyzer. A 50-Hertz constant bandwidth filter was used for the LF336/A and /B tests, and a 20-Hertz constant bandwidth filter was used for the LF336/C tests. For each narrow-band plot, 256 scans of the entire spectrum were made using a continuous 12.8-second integration time.

Equipment Calibrations - The probes were calibrated in the laboratory to determine insertion loss characteristics. Prior to testing, a frequency response check of the complete recording system was made by inserting a constant voltage at various frequencies into the cathode follower of each far-field and probe microphone and recording the resulting signal on the tape recorder. This tape was used to determine the record and playback characteristics for the 1/3-octave tabulations and the narrow-band plots. This system calibration was repeated during the test program.

Before and after each day's testing, an absolute level calibration was conducted. A known noise level was inserted directly on each microphone using a Bruel-Kjaer pistonphone and the output recorded. Any microphone deviating more than ± one decibel from the manufacturer's output voltage specification was replaced.

Corrections to Acoustic Data - Corrections made to the acoustic data were:

1. System record and playback frequency response, determined from the calibrations

2. Electronic data processing equipment frequency response, determined from the computer data reduction of the calibration tapes

3. Wind screen frequency response. A Bruel-Kjaer Number 0082 wind screen was used on the 160-degree microphone to reduce noise levels caused by fan exhaust impingement. Where additional microphones were installed between 190° and 210°, Bruel-Kjaer UA0237 wind screens were used.

4. Probe insertion loss, measured by laboratory calibrations

5. Atmospheric corrections and ground attenuation corrections were made using SAE Aerospace Recommended Practices.

All data presented in this report contain these corrections except the machine-generated narrow-band plots. The narrow-band analyzer does not have the capability of incorporating data corrections, therefore these plots are "as recorded" uncorrected data.

DISCUSSION OF RESULTS

The acoustic tests results are discussed in the following pages. The effects of acoustic features on fan performance are discussed in Appendix A.

It should be kept in mind that this fan, as studied, is a lift fan. Thus, in flight the arc location nearest the observer is at 180° and the noise in that part of the arc is most important. On the other hand, with the aircraft on the ground, the noise at 90° is most important. Therefore, noise measurements in the aft quadrant are most significant.

Vane Number

The baseline vane configuration was the 45-vane stator originally designed for the LF336. The baseline results were compared to those obtained using a 90-vane stator. The vane rows are shown in Figure 12.

Several investigations[5, 6, 7, and 8] conducted over the last ten years have indicated that noise reductions can be obtained by maintaining a vane-to-blade ratio of 2 or greater. These noise reductions have been shown to result from decreased pure tone generation and from the well-known cut-off phenomenon.

The decreased tone noise generation is a result of the decreased efficiency of energy transfer between the noise source and the modes of propagation within the fan flowpath. In theory, the higher vane/blade ratios produce

spinning lobe patterns which result in less efficient propagation and generation of blade passing frequency noise. The lobe number "m" for the fundamental blade passing frequency is given by:

$$m = B - kV$$

where: B = number of rotor blades

V = number of stator vanes

k = zero or any positive or negative integer

The most important lobe numbers are the lowest numbers resulting from the above equation for various values of k, since the lowest numbered spinning lobe patterns contain the largest part of the acoustic energy. The first four lobe numbers for 45 vanes and for 90 vanes are shown in Table III. It can be seen that with 42 blades, the 45-vane stator has a lowest lobe number of 3, while the 90-vane stator has a lowest lobe number of 42.

The cut-off phenomenon may or may not be operative for the lift fan depending on the theory evoked. In Reference 5, an exhaust duct is required in order to get attenuation. The lift fan has no ducting behind the outlet guide vane; and, therefore, the cut-off mechanism may not commence before the acoustic energy is propagated to the far field. Reference 8, however, proposes a theory which does not require a duct for cutoff. If this theory applies, the spinning modes in the lift fan will decay. The theory of cut-off[5] defines the first mode cut-off speed to be 670 rpm for the 3-lobe pattern and 7590 rpm for the 42-lobe pattern. That is, for all practical fan speeds, the 45-vane configuration is not cut off while the 90-vane configuration is always cut off.

Figures 13 through 17 show the effect of increased vane number at 95 percent speed with one-chord spacing. Figure 13 indicates that both tone power level (PWL) and peak arc sound pressure level (SPL) have been significantly reduced. Figure 14 shows the directivity of the second harmonic of the blade passing frequency for the two configurations. Although the reduction is not as great as it was for the fundamental, there has been a decrease in the aft peak second harmonic SPL of 3 dB and a sound power level (PWL) decrease of 5.2 dB. Figures 15 and 16 are machine-generated uncorrected comparisons of narrow-band (20 Hertz) spectral analysis for the two vane rows. The blade passing frequency and second harmonic decreases previously noted are clearly evident. There has also been a broadband noise decrease.

Figure 17 shows the perceived noise level (PNL) around the 150-foot arc. It can be seen that PNL has decreased all around the arc except in the most forward angles. Noise reductions of up to 4 PNdB were obtained at the most rearward angles. These angles are the most important to lift fan noise, since noise generated at these angles will have the shortest acoustic range relative to the ground plane.

Split Vane Row

Figure 12 shows the split vane row. There are 45 vanes in the hub area and 90 vanes in the tip area. The lower number of vanes in the hub area avoids the weight and performance penalties associated with compromises to optimum vane shapes and solidities usually associated with many small full-span vanes. It was hoped that this stator would acoustically represent the full 90-vane stator, because theoretical calculations and experimental work done by General Electric indicate that the major source of noise occurs in the outer third of the flowpath. Furthermore, when a vane/blade ratio of two or more is used, the propagating acoustic energy tends to concentrate in radial modes with sound pressure level distributions that are highly peaked toward the flowpath outer wall.

Figure 18 shows the distribution of the blade passing frequency SPL around the arc for the 45-, 90-, and split (90/45) vane rows. At a few angles, the 90/45-vane stator shows lower noise than the 45-vane stator; however, at all aft angles, the 90-vane stator is significantly lower than the 90/45-vane stator - the difference ranging from $1\frac{1}{2}$ dB at 120° and 130° to $8\frac{1}{2}$ dB at 140°. The results for the SPL of the second harmonic are shown in Figure 19. Here, the split-vane row shows higher noise than both the 45- and 90-vane rows at angles between 120° and 150°. Figures 20 through 22 show comparisons of the narrow-band spectra. In each case, the 90-vane stator is lowest in both tone and broadband noise content. The 90/45-vane stator also shows a tendency to produce high-frequency noise between 6 and 8 KHz. Figure 23 contains the PNL directivity. In general, in the aft quadrant, the 45-vane stator is lower than the split-vane stator. These test results show that, at least as configured here, the split-vane row was a poor acoustic simulation of a high vane/blade ratio design.

Vane Lean

A leaned vane differs from a conventional vane in that it is nonradial. Leaned vanes reduce noise generation by decreasing the strength of the viscous wake interaction and by phasing that interaction so as to produce a degree of phase cancellation. Small-scale experimental programs have been conducted to determine the effect of nonradial vanes on fan-generated noise[7, 9]. These experiments were all based on inlet guide vane rotor interactions; and, therefore, their results are not directly applicable to the rotor-outlet guide vane lift fan design. In the case of the rotor wake - OGV interaction, some consideration must be made of the lean direction if the most efficient design is to be obtained. The lean angle is defined as the angle between a radial line and the nonradial vane, measured at the fan hub. The lean angle is in the direction of fan rotation in order to increase the amount of the aerodynamic lean (nonradial rotor wakes) inherent in fans and compressors.

Figure 12 shows the leaned-vane row, which has 90 vanes at 30° of lean. Figure 24 shows the blade passing frequency SPL for the leaned and unleaned 90-vane stators at 95% fan speed at the 2-chord spacing. The leaned stator shows significant reduction at angles of 80° through 130°, with the peak aft quadrant sound pressure level dropping 7 dB.

There is, however, an unexplained increase in the front quadrant. This is not as detrimental to the lift fan as it might be to a turbofan, due to the lift fan's vertical orientation. Figures 25 and 26 show the corresponding inlet and exhaust acoustic probe data. Figure 25 indicates an increase in the inlet radiated noise as was seen in the arc data. The exhaust level, Figure 26, shows a large decrease in noise almost all the way across the span. Figures 27 through 29, respectively, contain the arc, inlet probe, and exhaust probe data for the second harmonic. The trends are the same as previously noted for the fundamental. The aft quadrant peak noise decreases about 8 dB, while the inlet probe (Figure 28) shows no net reduction, and the exhaust probe (Figure 29) indicates a large noise decrease.

Figures 30 and 31 are overlays of the 20-Hz, band-pass filter narrowbands at 110° and 140°. Here, as in the case of the 90-vane versus 45-vane stator, the tone noise decrease has been accompanied by a broadband noise decrease. At the 110° location, a new noise source appeared with lean at 1400 Hz. The source of this tone is unknown.

Figure 32 shows the resultant PNL directivity. The PNL is seen to have decreased in the aft quadrant but increased in the front quadrant. The aft quadrant peak reduction was about $1\frac{1}{2}$ PNdB. This reduction was limited by the tone at 1400 Hz. Figures 33 through 41 show similar data at 80% fan speed. Figures 33 through 35 indicate some blade passing frequency noise reduction, particularly as seen in the probe data. Figures 36 through 38, for the second harmonic, show appreciable reduction throughout the aft quadrant. Figures 39 and 40 are narrow-band overlays at 110° and 120° at 80% speed. Once again, the decreased broadband noise is noted. Figures 41 and 42 are the PNL directivities at 80% and 50% fan speed. The reduction in blade passing frequency PWL occurred at all fan speeds, as shown in Figure 43.

These results show lean to be very effective in reducing fan noise. However, further analytical effort and testing will be required to optimize the selection of vane lean angle in future fan designs. The effectiveness of lean is a function of the fan aerodynamic design, rotor-stator spacing, vane number, and blade number.

Rotor-Stator Spacing

It has long been recognized that the most direct method of reducing fan noise is to increase the spacing between the moving and stationary blade rows. The increase in spacing effectively eliminates potential interaction noise and greatly reduces viscous wake interactions. The potential interaction is a result of the interference between the pressure fields associated with moving and adjacent stationary blade rows. When such an interaction takes place, there are actually two noise sources developed. The rotor pressure field disturbs the stator pressure field making it a source of blade passing frequency noise, and the stator pressure field disturbs the rotor pressure field making it a second noise source. In general, for a high vane-to-blade ratio fan, the former is greater than the latter.

Figure 44 is a presentation of some typical theoretical results[6, 11]. The figure shows the magnitude of the two potential interactions and the viscous wake interaction for increasing rotor-stator spacing. It can be seen that the viscous wake interaction is not only dominant, but decreases at a slower rate with increasing rotor-stator spacing. At about one rotor-tip-chord spacing, the potential interaction noise is essentially zero. Spacing increases produce significant noise reduction up to about 2.0 rotor chords. Further reduction is possible with further spacing increases[10]; however, the results are seldom justified in view of the overall weight penalties.

It has been shown theoretically[11] that the effect of spacing on blade passing frequency noise is difficult for different aerodynamic designs. To establish the spacing-versus-noise trends for lift fans, tests were conducted at spacings of 0.15, 1, and 2 chords using 45 vanes and 90 vanes. The 0.15-chord spacing is typical of a conventional fan design where low noise is not an objective. The 1-chord spacing represents a moderate spacing design. The widest spacing used was two rotor tip chords. As pointed out previously, the 1- and 2-chord spacings essentially eliminate potential interaction as a pure-tone noise-generating mechanism.

Figures 45 through 48 present the three 45-vane test results at 100% speed. It can be seen that there has been a substantial decrease in noise in going from the 0.15-chord spacing to the 1- or 2-chord spacings. However, the 2-chord spacing decreased the noise below that measured at 1 chord only between 70 and 110 degrees, as can be seen in Figures 45 and 46. Figure 47 is a plot of blade row spacing versus the fundamental and second harmonic aft quadrant power levels and the maximum 150-foot arc PNL. Each curve shows a sharp drop when spacing is increased from 0.15- to 1-chord spacing with a decreased slope from 1- to 2-chord spacing. The arc PNL, shown in Figure 48, shows a large decrease in going from 0.15- to 1-chord spacing, with a reduction of peak noise of 5.8 PNdB. The increase in spacing to 2 chords is seen to reduce the noise an additional 0.6 PNdB for a total reduction due to spacing of 6.4 PNdB on the 150-foot arc.

Figures 49 through 53 are narrowband overlays of the 0.15- and 2-chord spacing configurations. As noted previously, the tone reduction has been accompanied by an appreciable broadband decrease. This broadband reduction is very large and is most likely due to the reduction in the strength of the random inlet turbulence to the stator. The random turbulence in the rotor wakes impinging on the stator results in a random lift fluctuation which in turn manifests itself in broadband noise[9]. The initial increase in spacing most probably gives this random turbulence a chance to dissipate to such a point that other sources of broadband noise are dominant.

Figures 54 through 59 show some results from spacing variations using 90 leaned vanes. Figure 54 shows no consistent trend for noise at the blade passing frequency; however, comparison with radial vanes in Figure 45 shows the fundamental to be reduced 6 dB at the 0.15-chord spacing. Also, Figure 55 for the second harmonic shows the 2-chord spacing to have produced a significant noise reduction over the 0.15- and 1-chord spacing.

Figures 56 through 58 are narrowband comparisons of the three spacings. The second harmonic reduction is clearly seen. In addition, the broadband noise has been reduced. This broadband reduction is also seen where there is no appreciable blade passing frequency tone reduction.

Figure 59 is the resulting 150-foot arc PNL. With leaned vanes, 2-chord spacing reduced PNL by 2.5 PNdB, as compared with 6.7 PNdB for 45 radial vanes; but, the PNL with 2-chord spacing was about the same. Thus, the change in vane number and the addition of lean reduced noise about 4 PNdB at the 0.15-chord spacing.

Without lean, increasing spacing from 0.15 to 1 chord resulted in significant noise reduction. With and without lean, increasing spacing from 1 to 2 chords reduced noise, but not as dramatically.

Acoustic Treatment

Treatment of the fan flowpath hub and tip walls, shown in Figure 60, consisted of single-degree-of-freedom resonators made of $\frac{1}{2}$"-thick honeycomb having $\frac{1}{2}$" cells. The face plates were 0.030" thick, perforated with 0.0625"-diameter holes to give a 10% porosity. (Porosity is the ratio of total hole area to the area of an unperforated sheet.)

The acoustic splitter (Figure 61) had two-degree-of-freedom resonators 0.3" thick, covered by face plates with the same hole size and porosity as used on the flowpath wall treatment. The splitter was treated on one side only, on the surface facing the tip wall. The flowpath walls could not be opened up enough to use a thicker splitter treated on both sides, although this would have been preferred. Figure 62 shows the fan during assembly, with the wall treatment and splitter installed. Removable solid covers were made for the walls and splitter, so that the 2-chord spacing configuration could be run with or without treatment.

Figures 63 and 64 are comparisons between treated and untreated flowpaths for the blade passing frequency and the second harmonic. As might be expected, the aft quadrant noise has decreased. There are also some decreases in the extreme (less than 40°) front quadrant angles. These noise reductions can be seen in the probe data in Figures 65 through 68. In particular, it should be noted that there is an inlet noise reduction even though the treatment is all aft of the rotor. It may, therefore, be speculated that some of the tone energy is being radiated forward from the stator and passes over the treatment while traveling in the upstream direction. Figures 66 and 68 show that the most significant exhaust suppression has occurred outboard of the splitter. This is to be expected, since the relatively small distance between the two treated surfaces (splitter and tip wall) makes an efficient trap for acoustic energy.

Figure 69 shows the 150-foot arc PNL. It can be seen that not only has the aft quadrant noise decreased but an appreciable front quadrant reduction is observed as well. The peak PNL has been reduced about 4 PNdB. Some insight into these reductions can be obtained from the narrowband filter

comparisons of Figures 70 through 73. Each of the angles shown indicates a considerable broadband noise decrease. Of particular interest are Figures 72 and 73 for 160° and 60°, respectively. At these angles, even though there has been no blade passing frequency reduction, the broadband noise decrease has resulted in the PNL reductions shown in Figure 69.

Figures 74 through 79 show data for the treated and untreated configurations at 80% fan speed. The spectral details (Figures 72 through 79) show characteristics similar to those observed at 95% speed. The maximum arc PNL has been reduced about 2.8 PNdB as seen in Figure 76.

Although in some instances the acoustic treatment did not reduce the blade passing frequency tones, considerable noise reduction did result, verifying that treated walls plus splitter(s) will provide effective noise reduction in lift fans. The amount of treatment and the treatment geometry used in these LF336 tests were limited to practical modifications of existing hardware. A fan design incorporating acoustic treatment from the start could not only have additional splitters but could have treatment tuned to the most effective maximum suppression frequency.

Acoustic Exit Louvers

Lift-fan-powered aircraft utilize louvers at the exit of the fan to obtain thrust vectoring for transition between vertical and horizontal flight. The position of these louvers, directly across the exhaust stream, makes them ideally suited for inclusion in the fan suppressor system.

The acoustically-treated louvers are shown in Figure 80. The louver cascade consisted of eight airfoils, each 0.58" thick with a 7.9" chord. The airfoils were treated on both sides with 2-degree-of-freedom resonators. The louvers were tested with and without end plates. The end plates were steel plates attached to the octagonal louver frame shown in Figure 80, to enclose the fan discharge within the acoustic louver cascade. The end plates were provided to determine if any appreciable acoustic energy radiated from the open ends of the louver cascade.

The tests were run using the 90-leaned-vane stator at two-chord spacing with wall and splitter acoustic treatment. Thus, these results represent the lowest noise levels measured during the test program. Figures 81 through 86 present some results of the louver tests without end plates. The fundamental and second harmonic levels shown in Figures 81 and 82 for 95% fan speed are rather disappointing. The data with louvers show no improvement, and even show increases in many of the rear angles. The aft quadrant PWL's of each tone also indicate a slight increase. The 80% fan speed data in Figures 83 through 86, however, show much more favorable results. Figures 83 and 84 for the pure tones show reductions at all aft quadrant angles, with a particularly large decrease in the fundamental. The resulting PNL distribution is shown in Figure 85. The maximum-arc PNL has decreased 2 PNdB. The narrowband comparison in Figure 86 shows the spectral details at 110°. Although the second harmonic has not been appreciably reduced, there has been some high frequency broadband noise reduction. The reason for the less-than-

desirable results at 95% fan speed is probably twofold. First, at high power settings, the Mach number of the flow over the louvers is quite high, of the order of 0.7. High Mach numbers are known to reduce the effectiveness of resonator treatment. Second, the louvers tend to backpressure the fan slightly at high power settings, which in turn may increase the noise generated due to the higher aerodynamic loading. At 80% fan speed, however, both of these phenomena are reduced in importance. The reduced treatment effectiveness can be largely overcome by redesigning the treatment for these high Mach numbers; however, this may require compromises in treatment design.

Figures 87 through 91 present a comparison of data at 80% fan speed taken with and without end plates. The fundamental blade passing frequency tone has, in general, increased with the addition of end plates while the second harmonic level shows only small changes. The resulting PNL (Figure 89) indicates almost no difference in the aft quadrant with or without the end plates. The narrowband comparisons of Figures 90 and 91 show that even though the blade passing frequency tone has increased with end plates, there has been a reduction in broadband noise at frequencies above and below the fundamental up to the second harmonic. The high frequency noise increase with end plates does not have a significant effect on PNL due to low annoyance weighting at these frequencies.

Figures 92 through 96 contain data with the louvers set at 0° (not turning the flow) and at a 30° vector angle. For these tests, additional microphones were placed beyond the normal 160° aft quadrant angle. These microphones were located at 170°, 190°, 200°, and 210° with respect to the fan inlet axis, in order to gain information on the acoustic directivity asymmetry caused by the vectored louvers. Figures 92 through 94 clearly show for the fundamental, second harmonic, and arc PNL, the directivity shift at 80% fan rpm when the louvers are turned 30°. Similar effects were observed at higher fan speeds. The peak fundamental and second harmonic levels are in the front quadrant, although the vectored configuration shows a higher level. The minimum in the directivity is at 150°, 30° from the unvectored jet axis. The tone level also increased in the inlet quadrant when the louvers were deflected. The arc PNL in Figure 94 shows the same trends as seen for the tones. However, the PNL at 200° has increased with the vectored louvers to the point where it equals the peak at 70°. Figures 95 and 96 are the spectral details at 190° and 200°. At both angles the noise level has increased at all frequencies. Further investigation will be necessary to find the cause of this phenomenon.

In summary, the louvers have reduced noise at 80% fan speed but will require careful design to make them effective at high fan speeds and high flow Mach numbers.

Some Overall Comparisons

The test program on the LF336 lift fan began with a conventionally-designed single-stage fan and proceeded through various practical design modifications with the primary intention of reducing noise while maintaining aerodynamic and mechanical performance. Figures 97 through 104 show some of the noise reductions obtained.

At 95% fan speed, Figures 97 through 100 show, respectively, the fundamental, second harmonic, arc PNL, and 200-foot sideline PNL reductions for 90 leaned vanes at 0.15-chord spacing and at 2-chord spacing with frame treatment. The aft quadrant fundamental power has been reduced 11.8 dB, while the second harmonic power is down 13.0 dB. The peak PNL on the 200-foot sideline is down 8 PNdB. It is also interesting to note that at 0.15-chord spacing, the change in the design of the stator from 45 radial vanes to 90 leaned vanes has resulted in a 4 PNdB peak sideline noise reduction.

Figures 101 through 104 show the noise reductions for the fan at 80% rpm with 90 leaned vanes, two-chord spacing, with frame acoustic treatment, and acoustically-treated louvers. The fundamental and second harmonic aft quadrant power levels have decreased 19.6 and 10.7 dB, respectively. The arc peak PNL reduction was 13.5 PNdB, and the 200-foot sideline reduction was 11.5 PNdB.

Comparisons With Predictions

Prior to the conduct of the tests, estimates of the reductions in the 500-foot sideline maximum PNL were calculated for some of the configurations to be tested. Existing analytical techniques were used to calculate estimated effects of spacing, vane number, acoustic treatment, and acoustic louvers. No analytical techniques for vane lean acoustic calculations were available at that time.

Spacing - Figure 105 shows the prediction and resultant data for the 45-vane configuration at three spacings. In general, the comparison is good. The data scatter at 0.15-chord spacing is typical of scatter of tone controlled spectra.

Vane Number - Changing from 45 vanes to 90 vanes lowered the 150-foot arc PNL between 1 and 4 PNdB for all but the most forward angles (Figure 17). Extrapolating these results to the 500-foot sideline, the peak PNL reduction was about 1 PNdB compared to a predicted reduction of 1.9 PNdB.

Treatment - The addition of acoustic treatment lowered the 150-foot arc peak PNL about 4 PNdB (Figure 69). Extrapolating these results to the 500-foot sideline, the peak PNL was reduced 2.8 PNdB compared to a predicted value of 4.5 PNdB.

Treated Louvers - Acoustically-treated exit louvers reduced the 150-foot arc PNL as shown in Figure 85. Extrapolating these results to the 500-foot sideline, the peak PNL was reduced about 2 PNdB compared to a predicted value of 2.3 PNdB.

Sideline Extrapolations

Table IV shows the projected 500- and 1000-foot sideline maximum PNL for four of the configurations tested. These extrapolations are based on spherical divergence and standard day air attenuation[12].

In the LF336/C tests, the fan was mounted on a ground pad with the fan axis parallel to the ground. In Figure 106, the fan is considered mounted in a wing of a vertically-rising VTOL aircraft. The 150'-arc data from the 90 leaned, two-chord spacing, treated frame test were extrapolated using spherical divergence and air attenuation corrections (no ground plane attenuation was included). From these extrapolations, the PNL versus altitude curves of Figures 107 and 108 for 80% and 95% fan speed were obtained.

The salient feature of these figures is the point of maximum PNL at each sideline distance. In Figure 108, an observer at a 200-foot sideline experiences an increase in PNL until the fan reaches an altitude of about 80 feet. Beyond this point, PNL decreases continually as the fan rises. At 80% speed the point of maximum PNL is at a lower altitude. At the 2000-foot sideline, the maximum PNL occurred at a 575-foot altitude for 95% and at a 510-foot altitude for 80%.

CONCLUSIONS

It has been shown that substantial noise reductions can be obtained by proper selection of fan geometries and treatments. It is expected that advanced lift fan designs can be within the noise level objectives expected for commercial V/STOL applications. The significant conclusions that can be drawn from this test program are:

1. A vane/blade ratio greater than two can significantly reduce noise in a short duct lift fan.

2. The split vane row, which had 90 vanes in the annulus tip region and 45 vanes in the annulus hub region, has been shown to be a poor acoustic simulation of a high vane/blade ratio design. The split vane row did not reduce fan noise.

3. Vane lean (nonradial vanes) has been shown to provide a substantial reduction in lift fan noise.

4. Changing the rotor-stator spacing of the 45-vane configuration from 0.15 chord to 1 chord significantly reduced fan noise. Increasing the spacing to two chords provided an additional smaller noise reduction. Using 90 leaned vanes, noise reductions were obtained up to a 2-chord spacing.

5. The use of acoustic treatment on the fan flowpath walls and on the circular splitter was very effective in reducing fan noise.

6. Acoustically-treated exit louvers reduced aft radiated noise. Shielding the axial gap between the vanes and the louvers had no significant effect on the noise measurements.

7. The quietest configuration tested was with 90 leaned vanes at 2-chord spacing with flowpath and louver treatment. This configuration reduced the fundamental tone PWL by 19.6 dB, the second harmonic tone PWL by 10.7 dB, and the 150-foot-arc PNL by 13.5 dB.

APPENDIX A

EFFECTS OF CONFIGURATION CHANGES ON PERFORMANCE

Sources of Performance Effects

The new vane rows have some exit swirl. This swirl is not inherent to the configuration changes but, rather, was caused by varying the vane orientation angles linearly with radius to simplify stator manufacture and assembly. The new vane rows have higher inlet flow Mach numbers because of the reduced stator inlet area caused by the added vanes, vane stiffening rings, and acoustic splitter. This effect is not inherent to the configuration changes but, rather, is due to the limitations of wall curvature modifications to the existing LF336/A hardware. Vane stiffening rings (see Figure 12) are required in short-chord vane rows for mechanical reasons. There is a performance loss caused by vane and ring interaction. The acoustic splitter was truncated at the base (see Figure 61) to maximize treatment length, which increases base drag loss.

Measured Effects on Performance

Table V summarizes the measured thrust performance for the LF336/C tests. The thrust load cell was calibrated to measure thrust forces within 1/2 of 1%. Performance measurements of Table V are within 1% to 2%, due to measurement accuracy of thrust, fan speed, ambient conditions for performance corrections, transient wind effects, and data plotting accuracy.

Spacing - The LF336/A and LF336/B tests showed that, with the 45-vane stator, there is no measurable performance loss due to increased spacing.

Split Vane Row - LF336/C Tests 2, 6, and 7 (see Table V) showed that the 90/45-vane row reduced fan thrust about 2.5% below the 45-vane LF336/C Test 1 base case. This vane row was tested with and without the acoustic splitter (Tests 2 and 7); there was no measurable effect on performance. With the splitter installed, the split vane row was tested with and without acoustic treatment (Tests 2 and 6); there was no measurable effect on performance.

90 Radial Vanes - The 90-vane row with no splitter (Test 9) reduced fan thrust 3.7%, about 1% more than did the 90/45-vane row. With the splitter installed (Test 3), the 90-vane row thrust was down 5.7%. The addition of the splitter in this vane row, therefore, caused an additional 2% loss.

90 Leaned Vanes - Tests 5, 8, 10, and 11 were compared. At 1-chord spacing without a splitter (Test 8), the thrust loss was 4.6%, about 1% more than for Test 9 with 90 radial vanes. At 0.15-chord spacing without a splitter (Test 10), an additional 2% loss was observed, indicating that the close spacing increased the flow blockage. At 2-chord spacing with the acoustic splitter (Tests 5 and 11), thrust was down 8.5 to 9.8% from the 45-vane base case. The addition of the splitter quite obviously caused severe flow blockage, more severe than was the effect of close spacing observed in Test 10.

Acoustic Exit Louvers - Comparing Tests 11 and 12, the addition of exit louvers had, within measurement accuracy, no effect on performance.

Effects of Acoustic Features on Advanced Fan Designs

An increase in spacing is expected to have no significant effect on fan performance in advanced fan designs. The increase in surface area increases skin friction, but this increase is very small. An increase in the number of vanes will affect performance only if vane mechanical stiffening rings are required. The vane-ring interaction is expected to cause between a 1 and 2% performance loss. Vane lean is expected to have a small effect on performance, about 1%, due to the radial flow component introduced by the lean angle. Acoustic splitters will affect performance due to increased skin friction (very small effect), and by base drag loss (about 1%), if splitters are truncated at their bases. These estimated effects on advanced fan designs are in some cases less than those measured in the LF336/C tests because of the limitations of modifications to the existing LF336 fan.

REFERENCES

1. McCann, E.O.: LF336/A and LF336/B Acoustic Tests Data Report. General Electric Company TM 69-200, April 21, 1969.

2. Kazin, S.B.: Results and Analysis of LF336/A Acoustic Test Data. General Electric Company TM 69-223, April 30, 1969.

3. Kazin, S.B.: Results and Analysis of LF336/B Acoustic Test Data, With Comparison to the LF336/A. General Electric Company TM 69-243, May 12, 1969.

4. McCann, E.O.; Volk, L.J.: LF336/C Modification and Acoustic Test Program Data Report (three volumes). General Electric Company TM 70-729, September, 1970.

5. Tyler, J.M.; Sofrin, T.G.: Axial Flow Compressor Noise Studies. 1961 SAE Aeronautic Meeting, 345D.

6. Benzakein, M.J.; Kazin, S.B.: Fan Compressor Noise Reduction. ASME Paper 69-GT-9, March, 1969.

7. Nemec, J.: Noise of Axial Fans and Compressors: Study of Its Radiation and Reduction. J. Sound Vib., Vol. 6, No. 2, 1967, pp. 230-236.

8. Lowson, M.: Theoretical Studies of Compressor Noise. NASA CR 1287, March, 1969.

9. Sharland, I.J.: Sources of Noise in Axial Flow Fans. J. Sound Vib., Vol. 1, No. 3, 1964, pp. 302-322.

10. Copeland, W.L.; Crigler, J.L.; Dibble, A.C.: Contribution of Downstream Stator to the Interaction Noise of a Single-Stage Axial-Flow Compressor. NASA TN D-3892, April, 1967.

11. Benzakein, M.J.; Kazin, S.B.: A Theoretical Prediction of Aerodynamically Generated Noise in Fans and Compressors. Paper presented at the ASA Conference in Cleveland, Ohio, November, 1968.

12. Standard Values of Atmospheric Absorption as a Function of Temperature and Humidity for Use in Evaluating Aircraft Flyover Noise. S.A.E. ARP 866, August 31, 1964.

TABLE I. LF336/A LIFT FAN DESCRIPTION.

Fan Pressure Ratio	1.30
Fan Tip Diameter, inches	36
Fan Radius Ratio	0.475
Fan Flow, lbs/sec	218
Bypass Ratio	5.0
Fan Tip Speed, ft/sec	950
RPM	6047
Total Thrust, Unvectored, lbs	5500
Blade Number	42
Vane Number	45
Blade-Vane Axial Spacing, expressed in blade tip chords	.15

TABLE II. TEST LOG

Fan	Test	Date	Vane Row	Spacing, Chords	Acoustic Splitter	Acoustic Treatment	Louvers	Remarks
LF336/A	1	1/69	45	.15	No	No	No	Basepoint Configuration
	2	1/69	45	.15	No	No	Yes	Non-Acoustic Louvers
LF336/B	1	2/69	45	2	No	No	No	
LF336/C	1	12/69	45	1	No	No	No	
	2	1/70	90/45	2	Yes	No	No	
	3	1/70	90	2	Yes	No	No	
	4	2/70	90/45	2	Yes	Yes	No	
	5	2/70	90/L	2	Yes	No	No	
	6	3/70	90/45	2	Yes	Yes	No	Repeat of Test 4
	7	3/70	90/45	1	No	No	No	
	8	3/70	90/L	1	No	No	No	
	9	3/70	90	1	No	No	No	
	10	6/70	90/L	.15	No	No	No	
	11	6/70	90/L	2	Yes	Yes	No	
	12	7/70	90/L	2	Yes	Yes	Yes	Acoustic Louvers

TABLE III.

SPINNING LOBE NUMBERS FOR 45 & 90 VANES WITH 42 BLADES

45 Vanes		90 Vanes	
Integer k	Lobe Number m	Integer k	Lobe Number m
1	-3	0	42
0	42	1	-48
2	-48	-1	132
-1	87	2	-138

TABLE IV. SIDELINE PNL EXTRAPOLATIONS

	500' Sideline				1000' Sideline			
	80% RPM		95% RPM		80% RPM		95% RPM	
	PNL	ANGLE	PNL	ANGLE	PNL	ANGLE	PNL	ANGLE
LF336/A 45 Vanes .15 Chord Spacing No Treatment No Acoustic Louvers	112.6	120°	113.1	110°	103.4	120°	103.4	110°
LF336/C Test 10 90 Leaned Vanes .15 Chord Spacing No Treatment No Acoustic Louvers	107.5	110°	109.0	110°	98.6	110°	99.6	110°
LF336/C Test 11 90 Leaned Vanes 2 Chords Spacing With Treatment No Acoustic Louvers	103.0	110°	104.4	90°	94.3	110°	95.3	90°
LF336/C Test 12 90 Leaned Vanes 2 Chords Spacing With Treatment With Acoustic Louvers	101.6	110°	--	--	93.5	110°	--	--
Extrapolations assume a standard day and no effect of the ground plane.								

TABLE V

LF336/C Performance Summary

LF336/C TEST	VANES	ACOUSTIC SPLITTER	SPACING, CHORDS	ACOUSTIC LOUVERS	THRUST CHANGE *
1	45	No	1	No	0
7	90/45	No	1	No	-2.6%
2		Yes	2		-2.5%
6		Yes	2		-2.7%
9	90	No	1	No	-3.7%
3		Yes	2		-5.7%
10	90/L	No	.15	No	-6.6%
8		No	1		-4.6%
5		Yes	2		-8.5%
11		Yes	2		-9.8%
11	90/L	Yes	2	No	-9.8%
12		Yes	2	Yes	-10.2%

*Percent thrust change at 95% fan RPM from the base case, LF336/C Test 1.

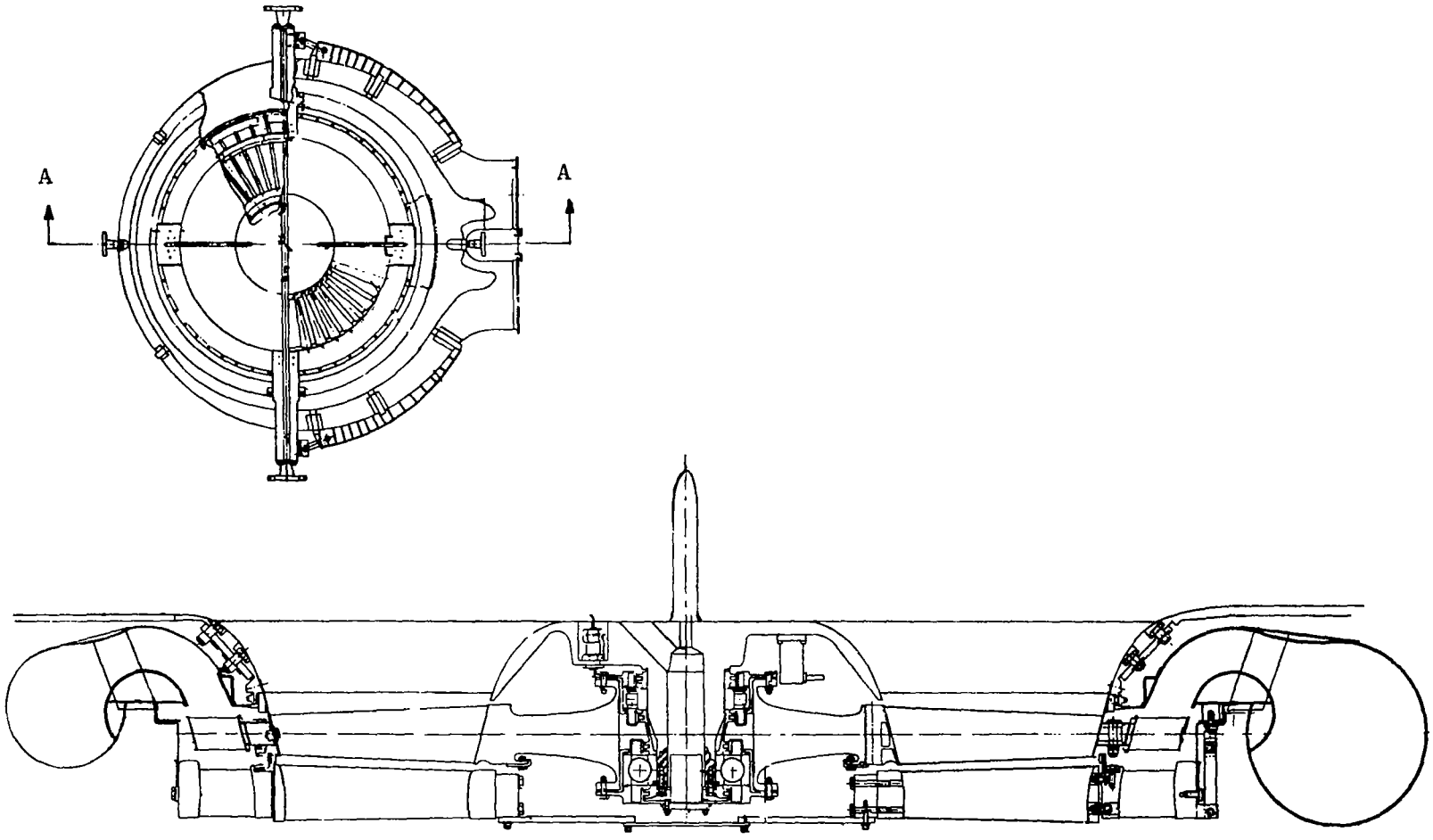

Figure 1. LF336/A Lift Fan

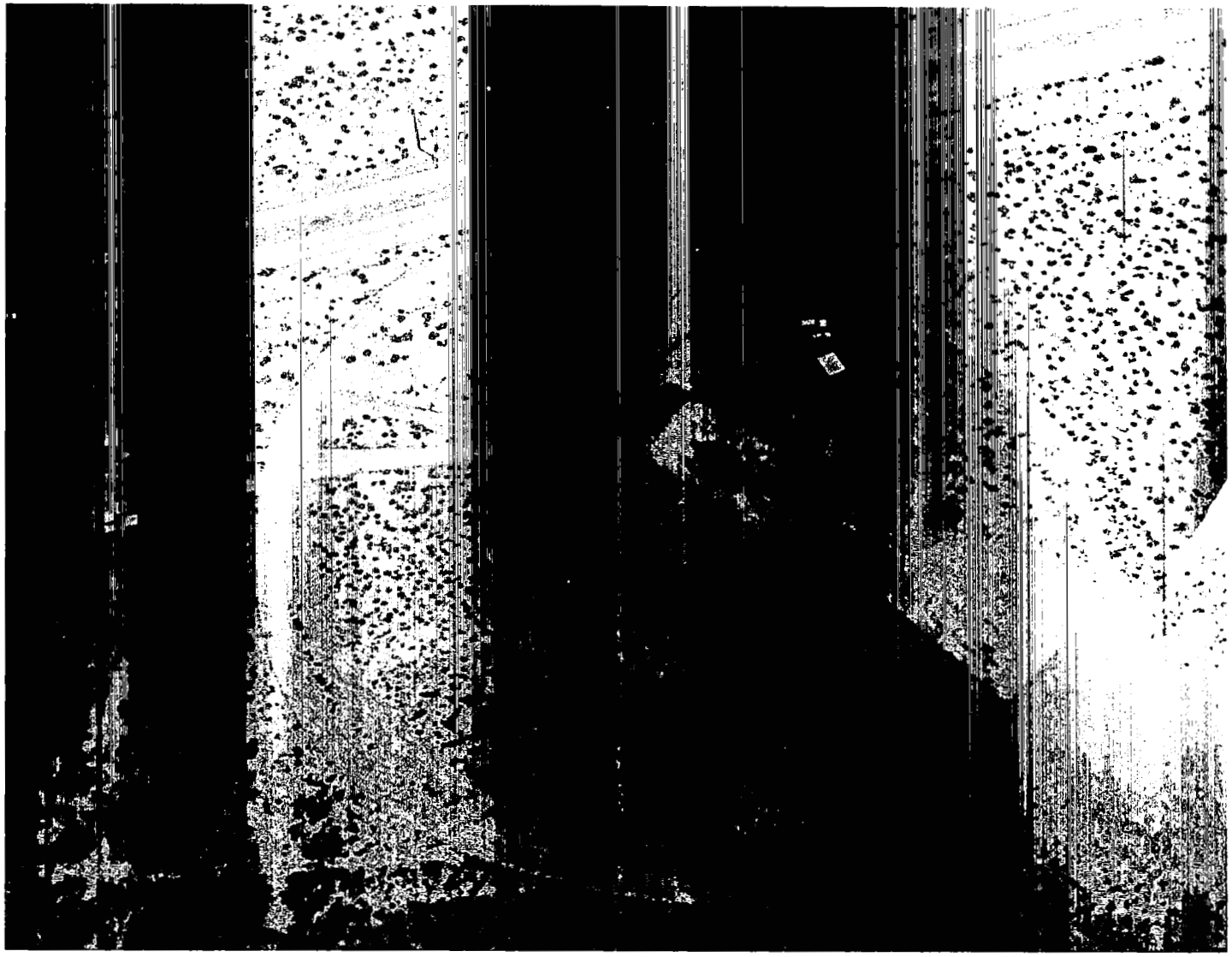

Figure 2. Test Site, Overhead View

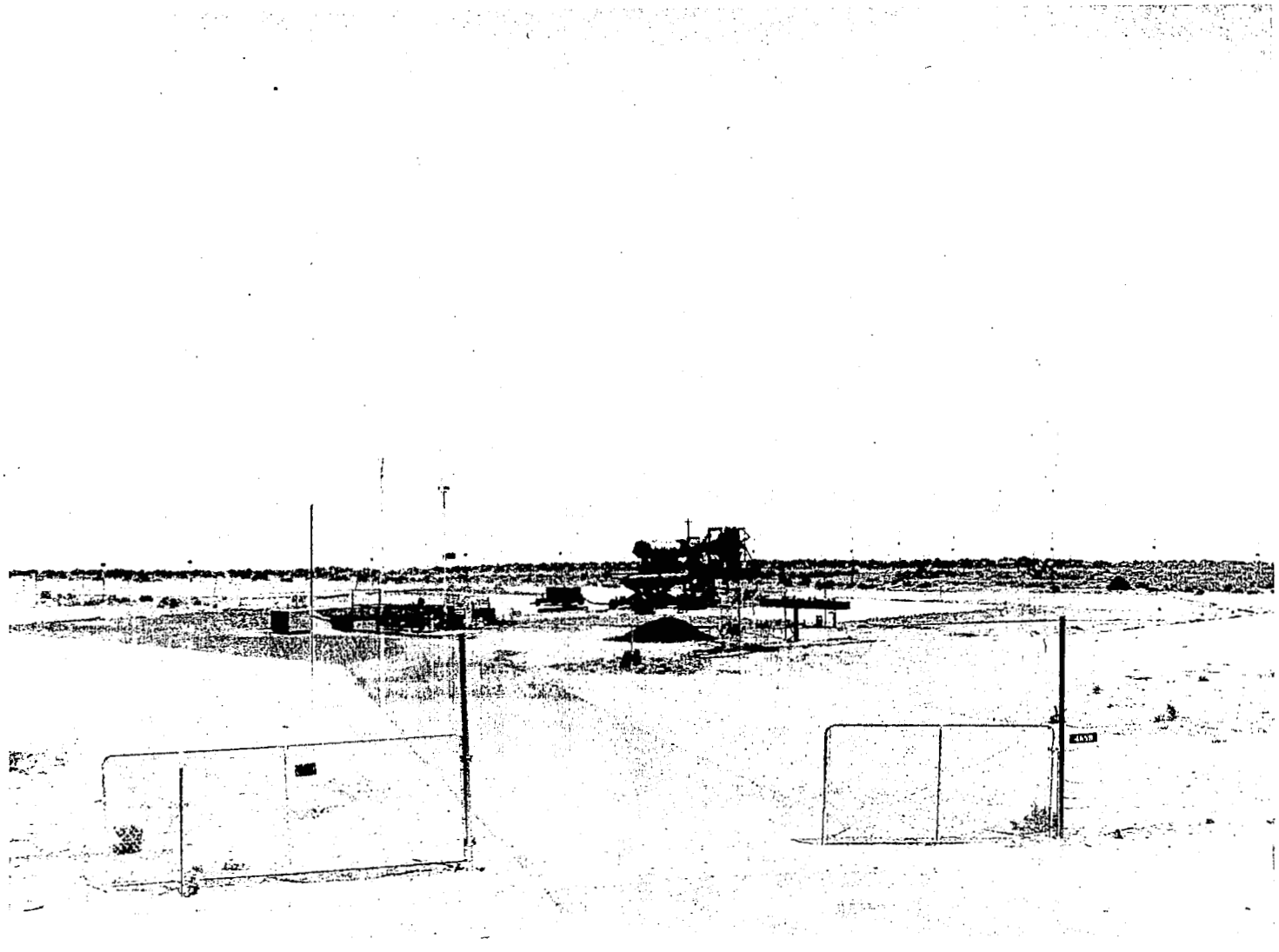

Figure 3. Test Site, Ground Level View 1

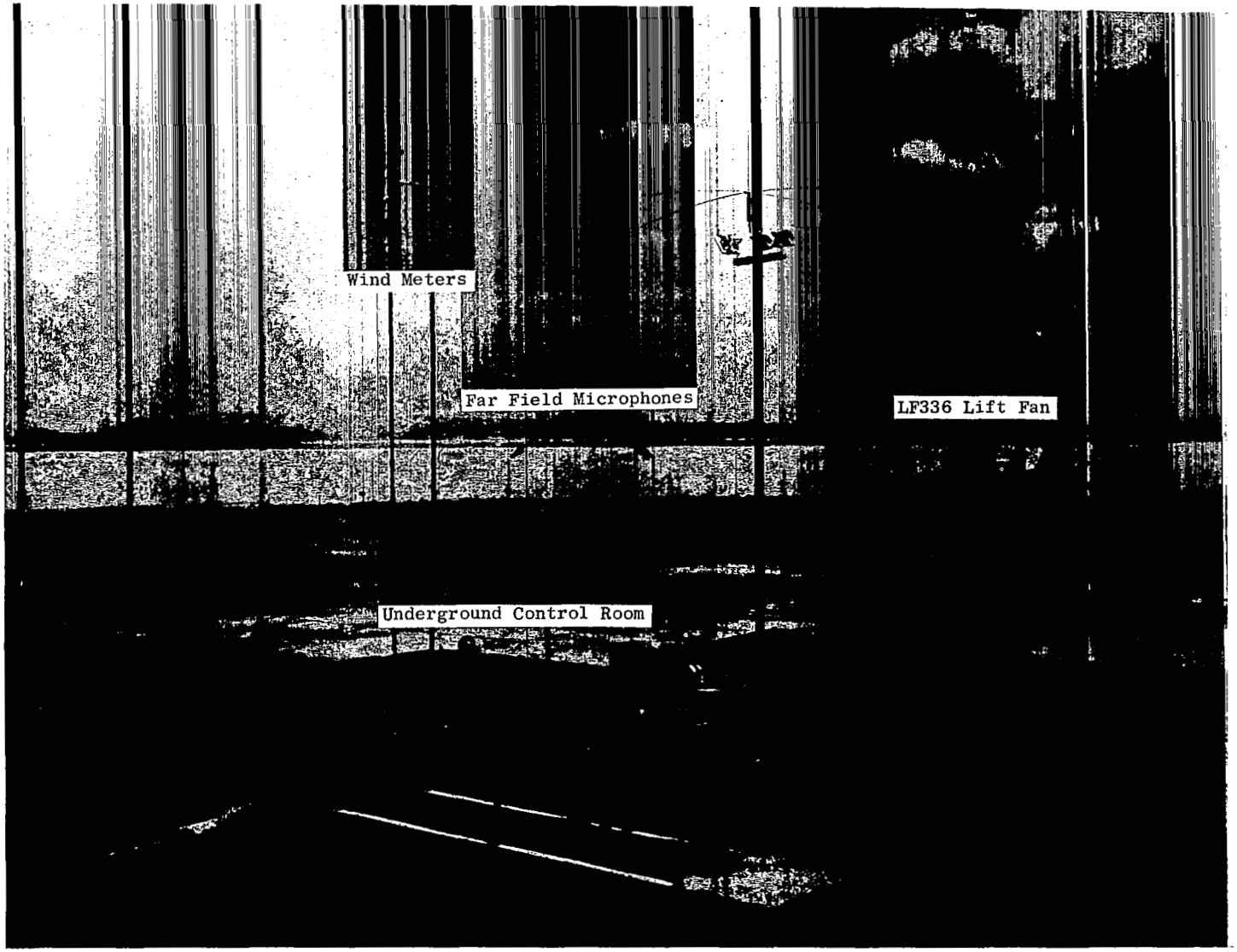

Figure 4. Test Site, Ground Level View 2

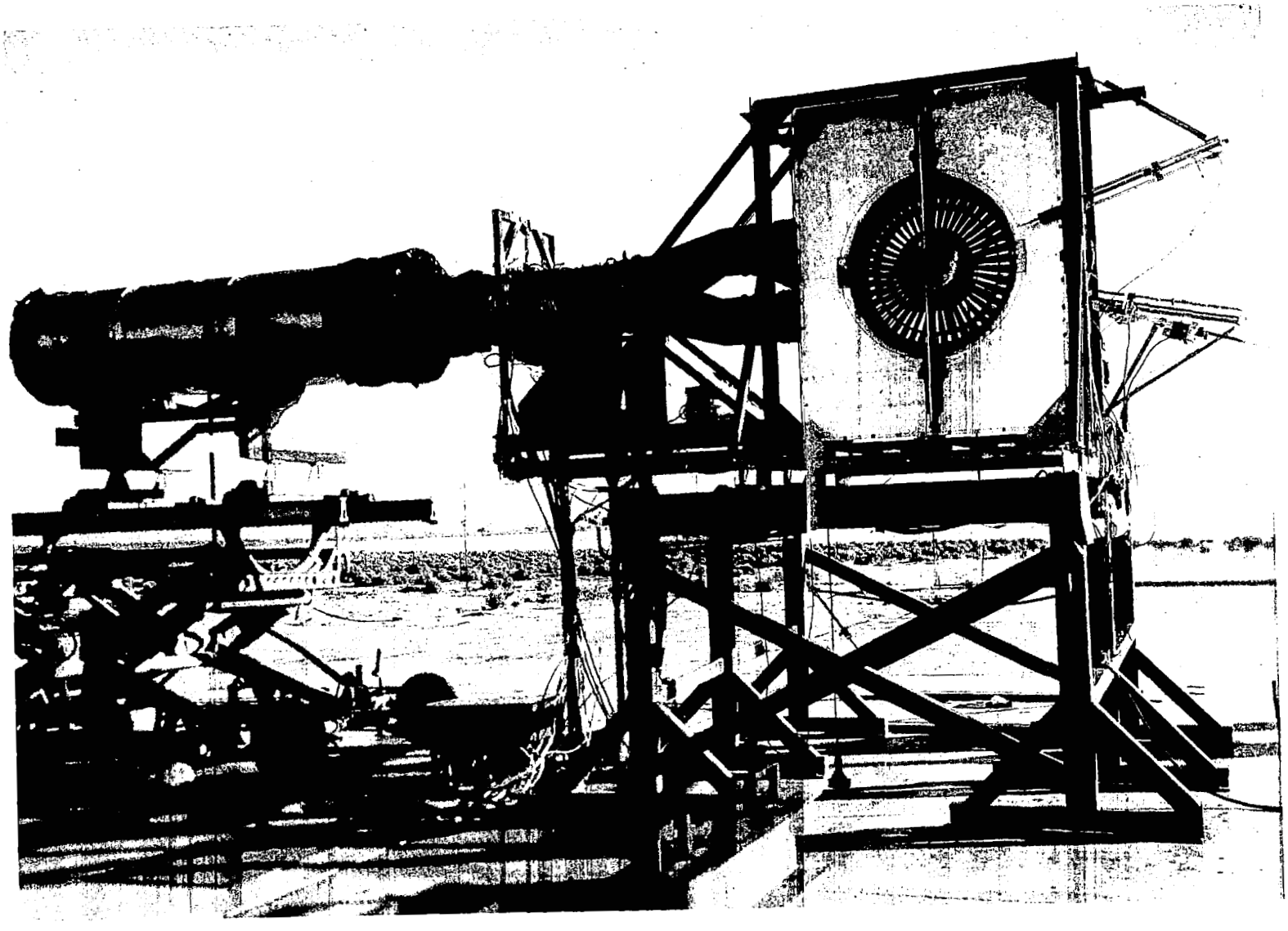

Figure 5. LF336 Tests, Front View

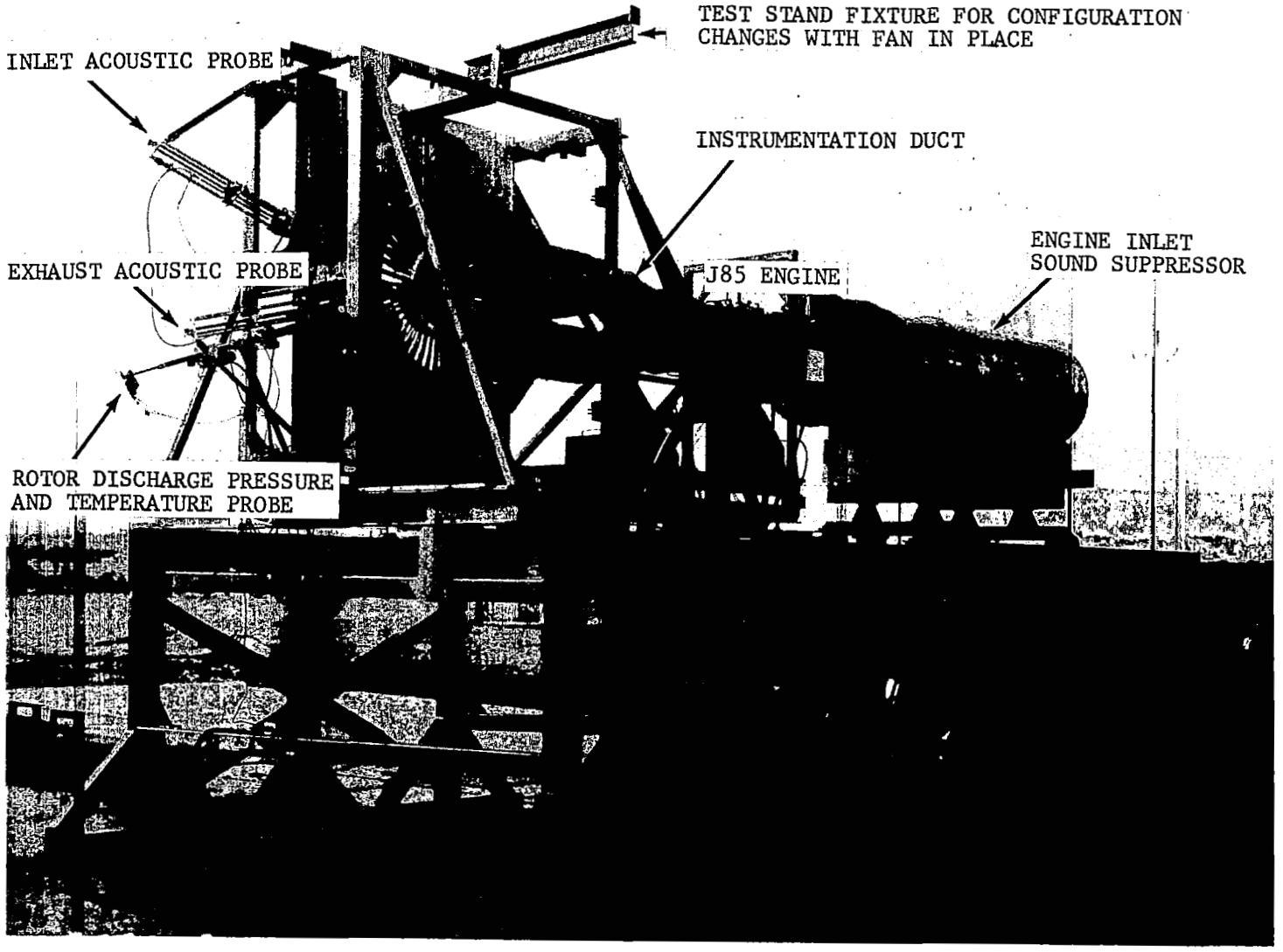

Figure 6. LF336 Tests, Rear View

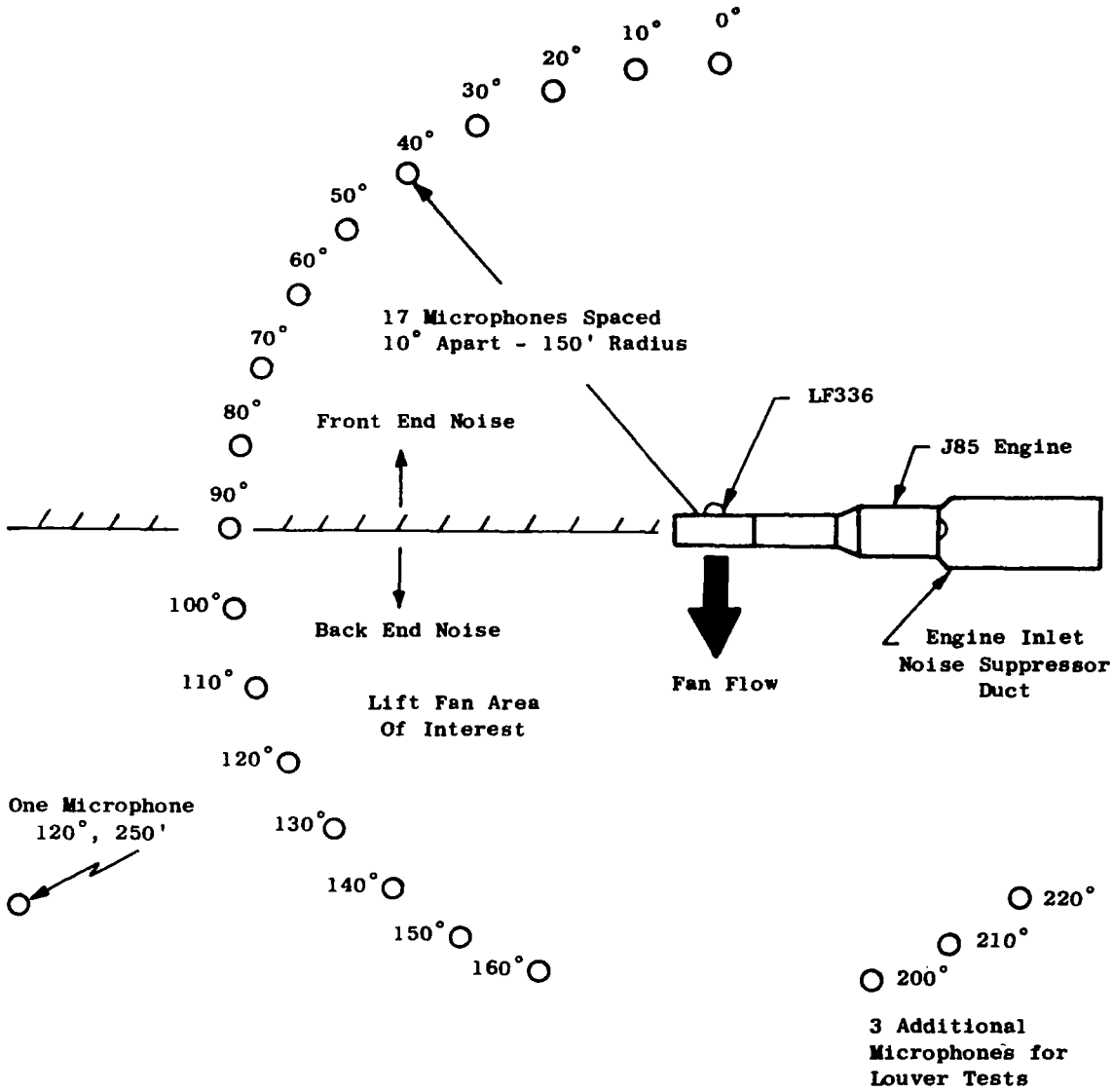

Figure 7. Far-Field Noise Measurements

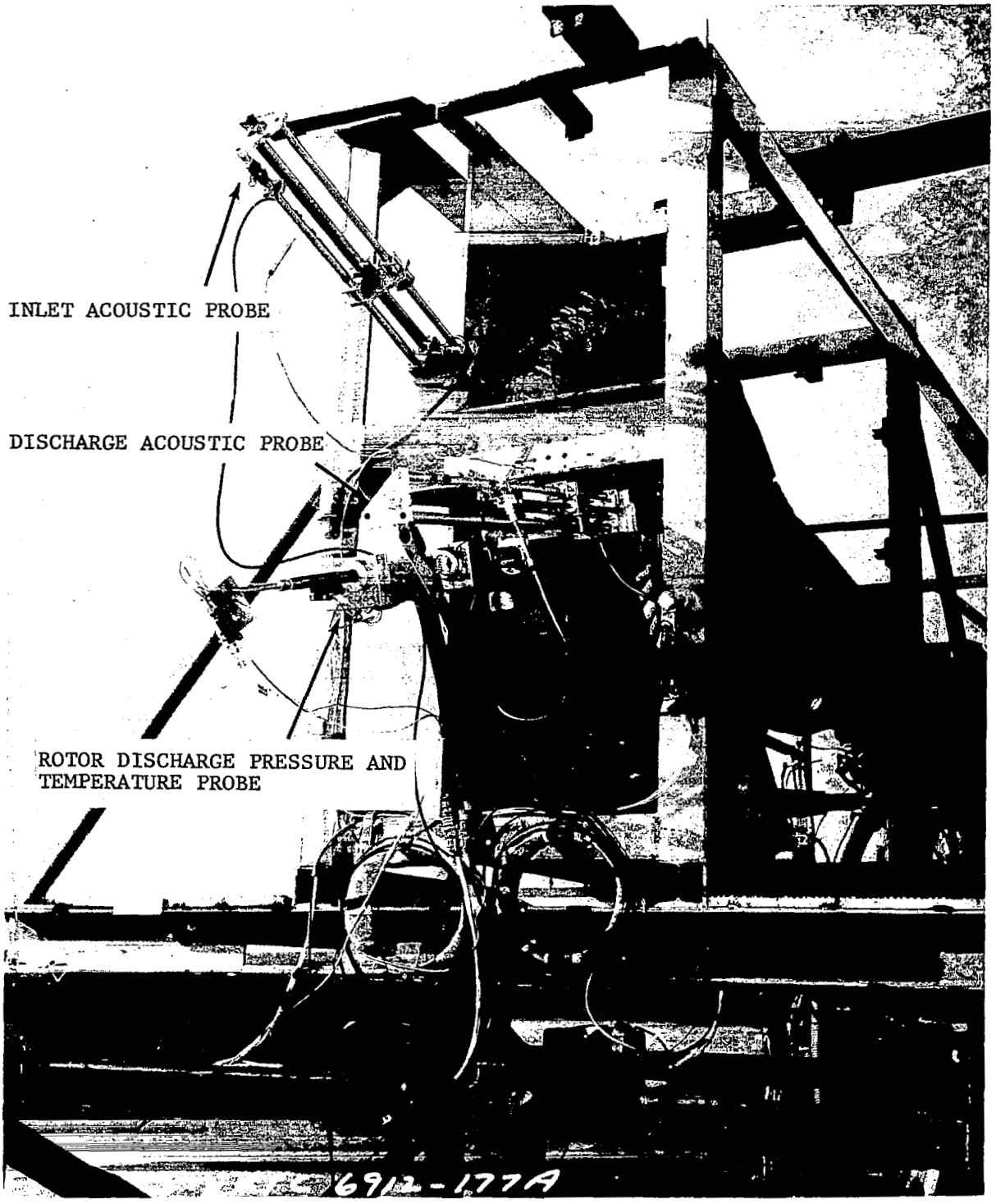

Figure 8. Acoustic Probes

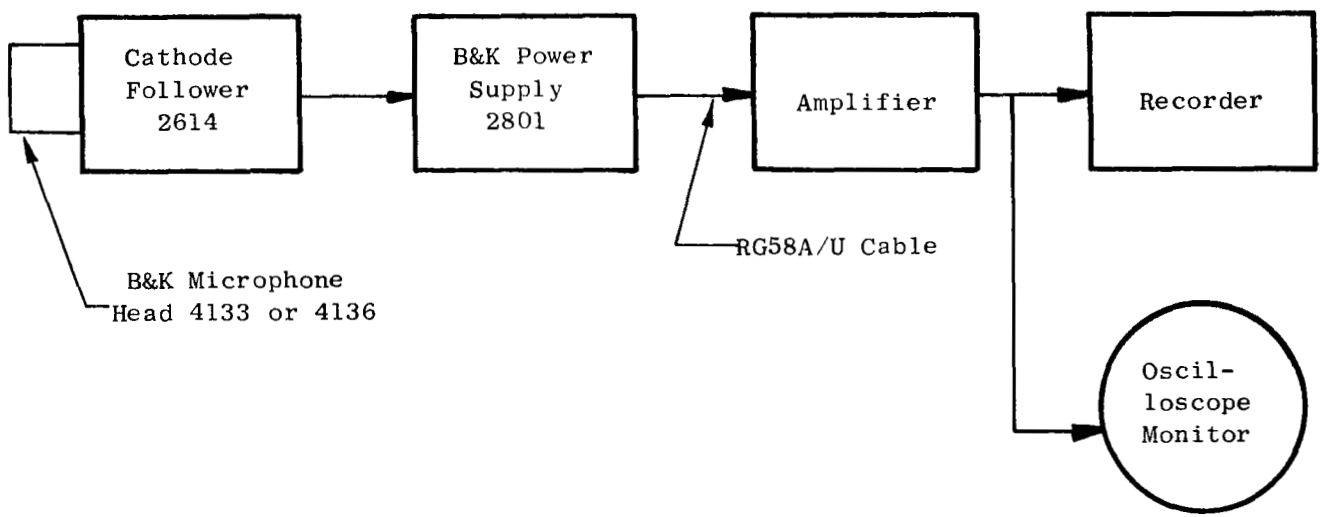

Figure 9. Acoustic Data Instrumentation Schematic

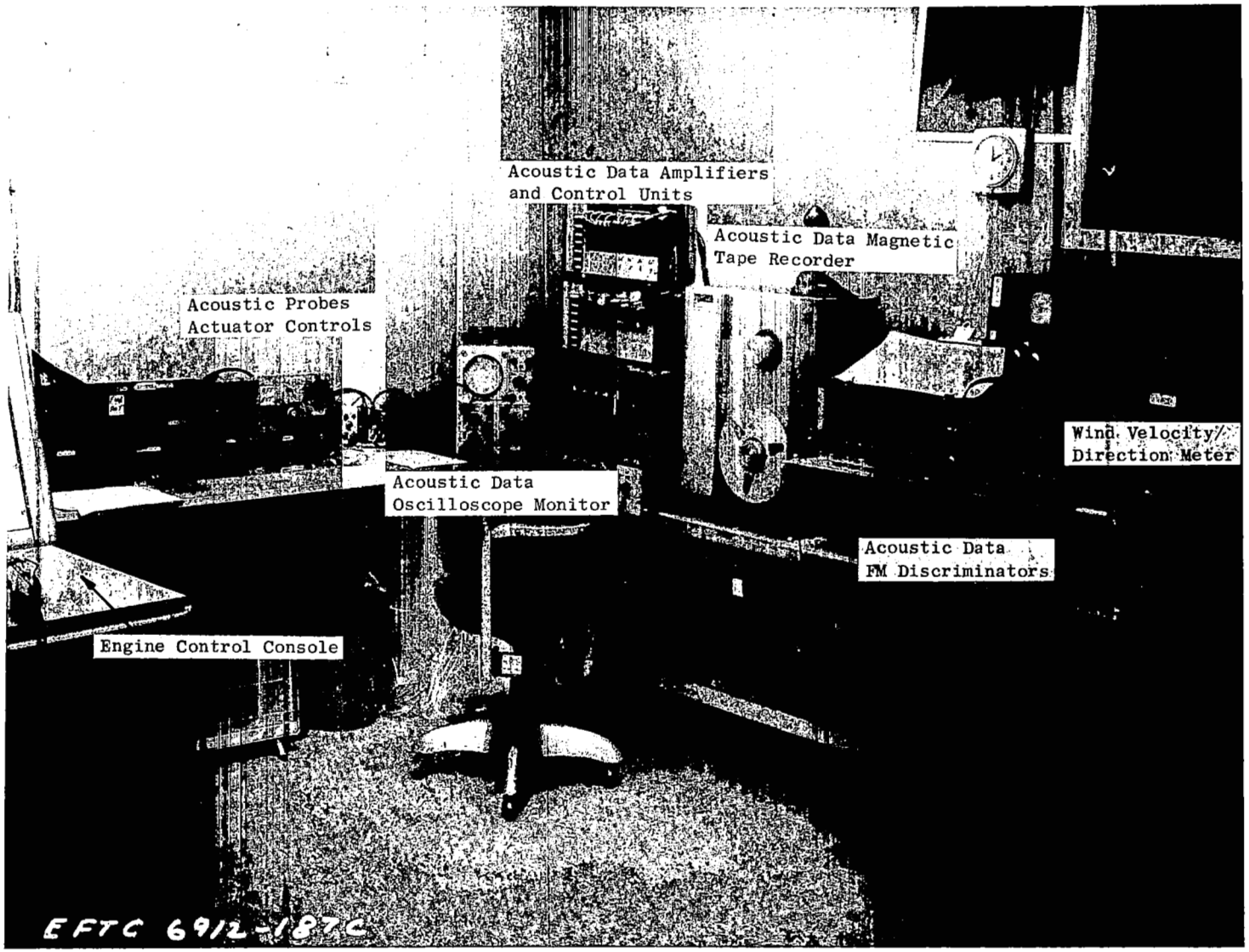

Figure 10. Control Room, View 1

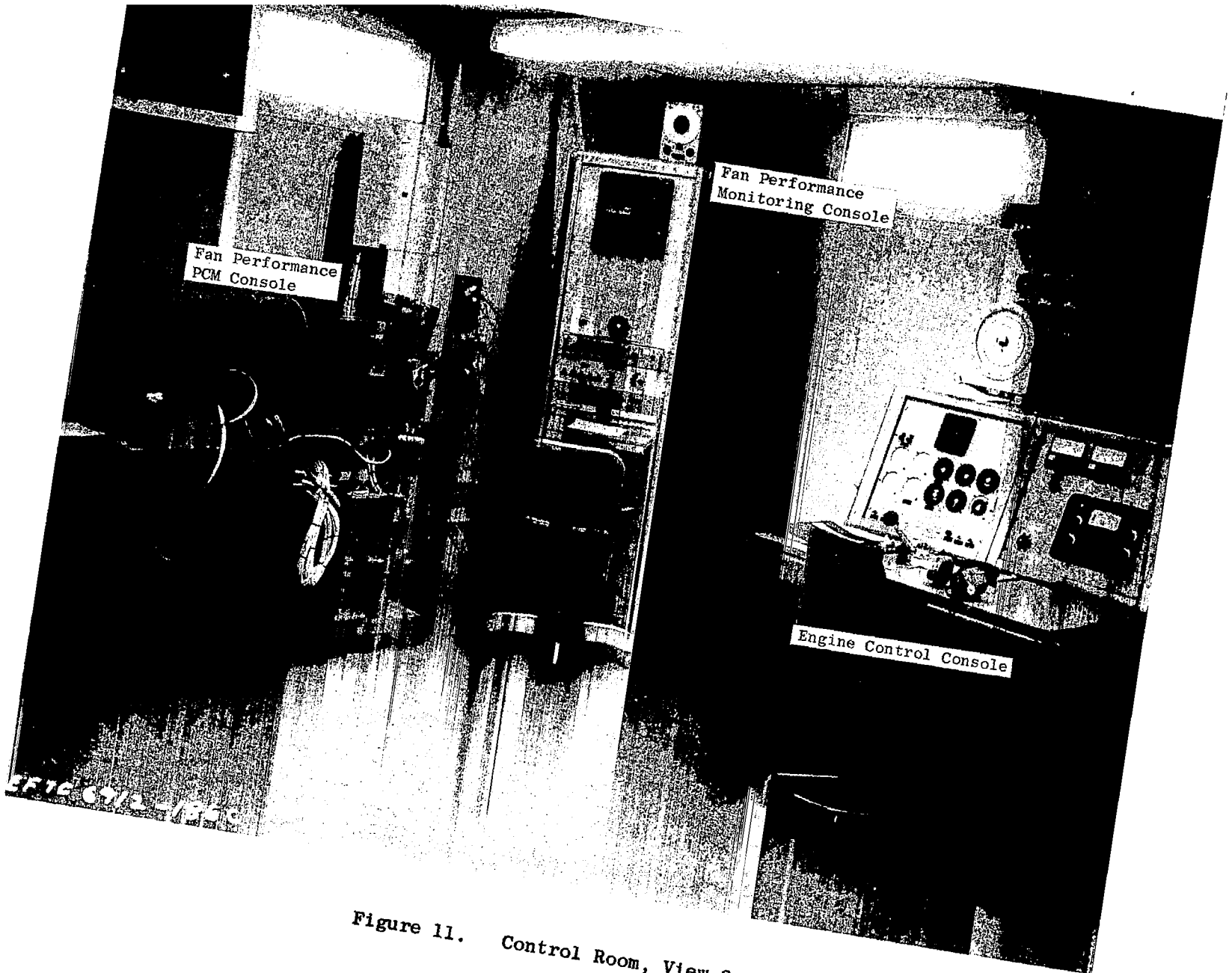

Figure 11. Control Room, View 2

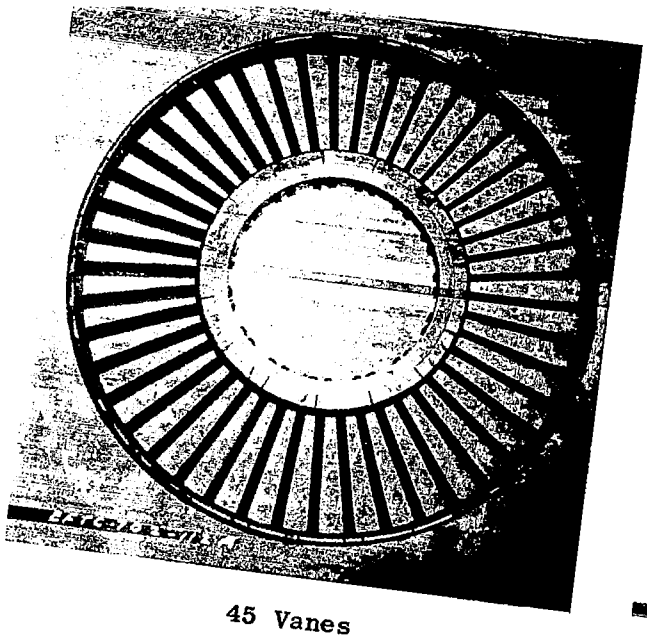

45 Vanes

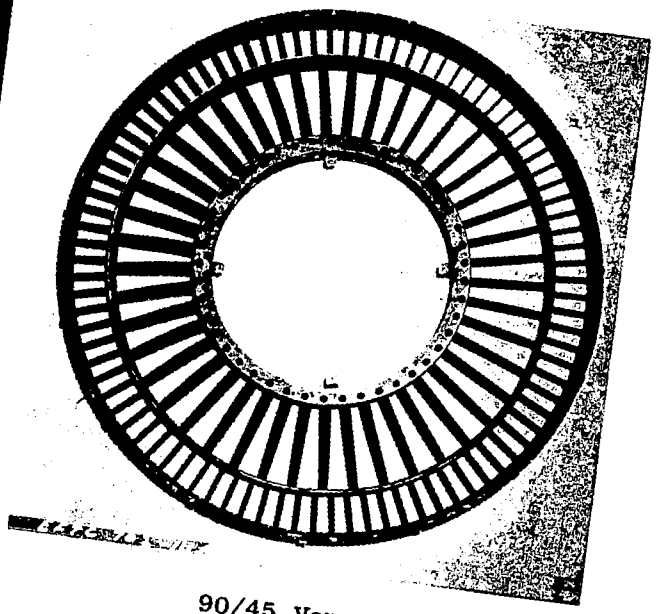

90/45 Vanes

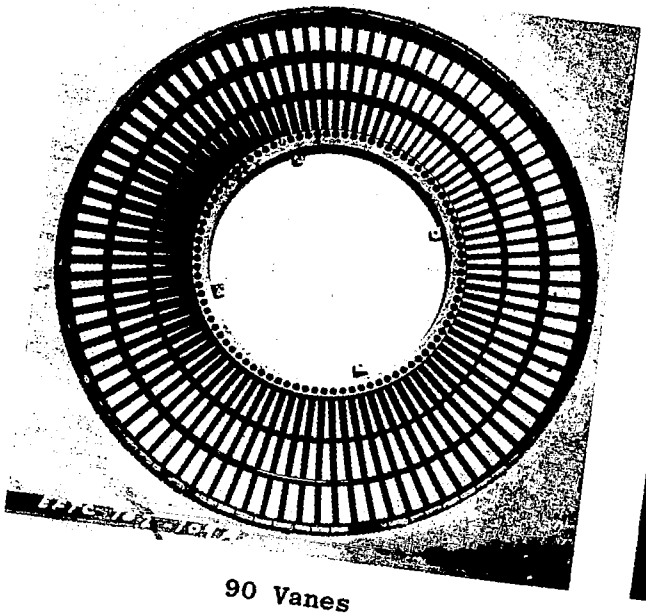

90 Vanes

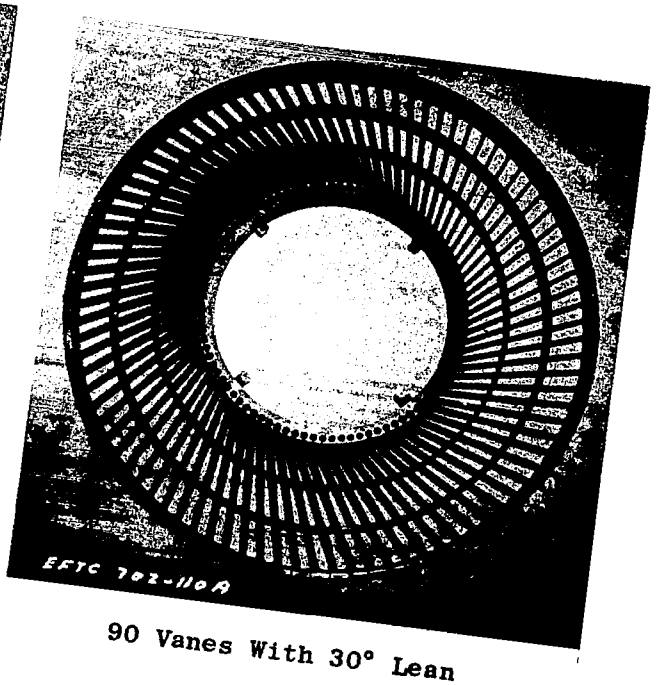

90 Vanes With 30° Lean

Figure 12. Vane Rows

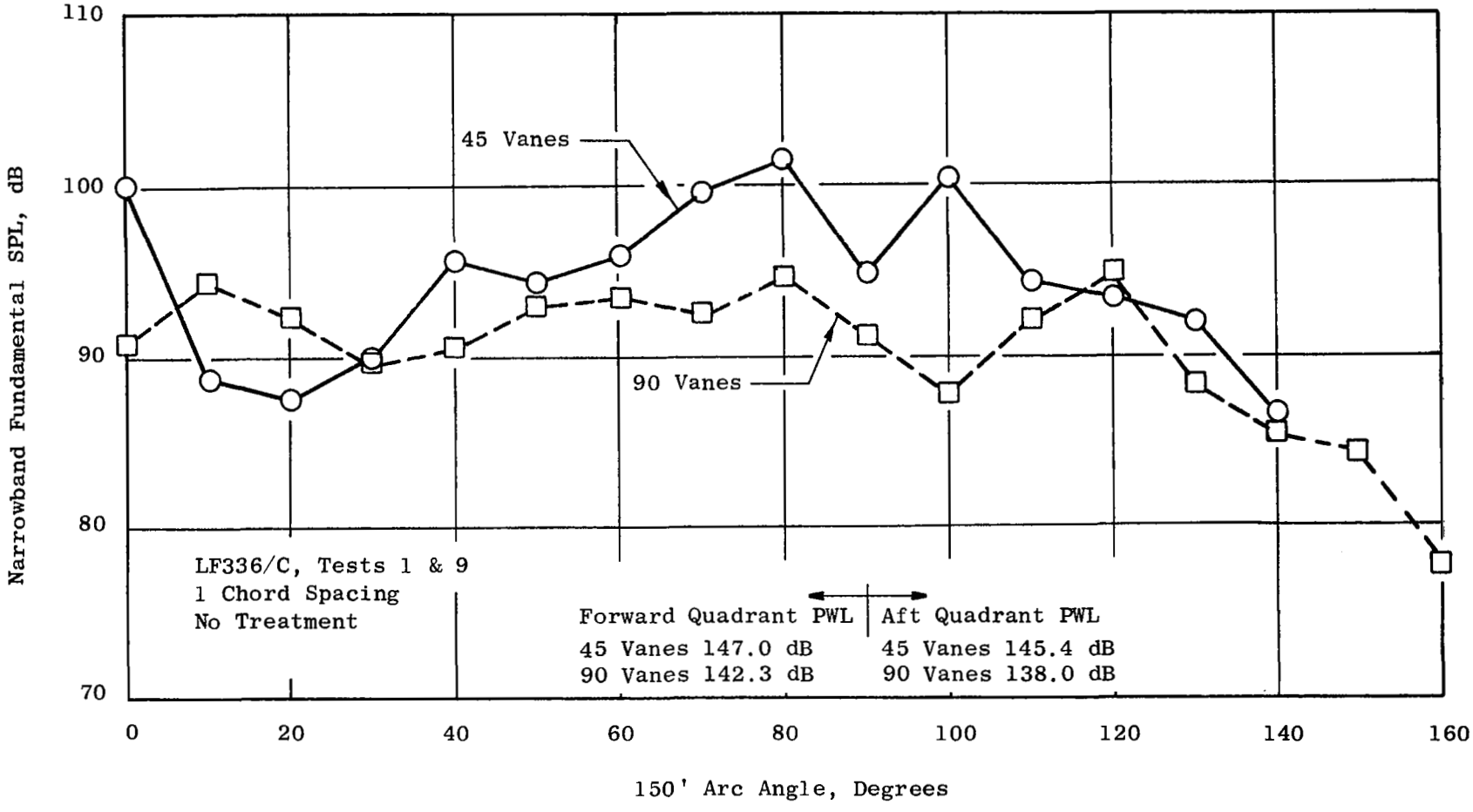

Figure 13. Effect of Vane Number on Arc Fundamental SPL at 95% RPM

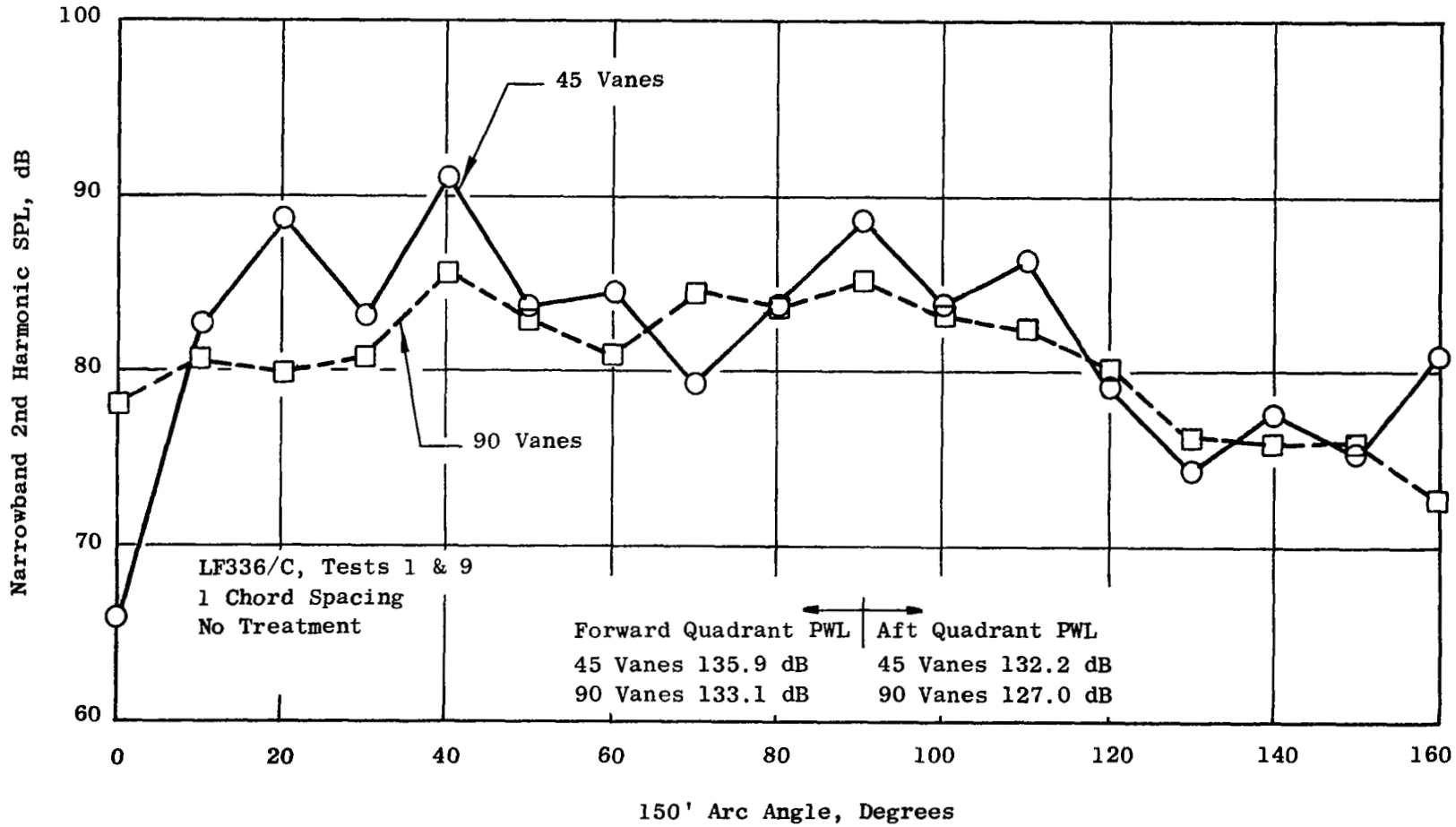

Figure 14. Effect of Vane Number on Arc Second Harmonic SPL at 95% RPM

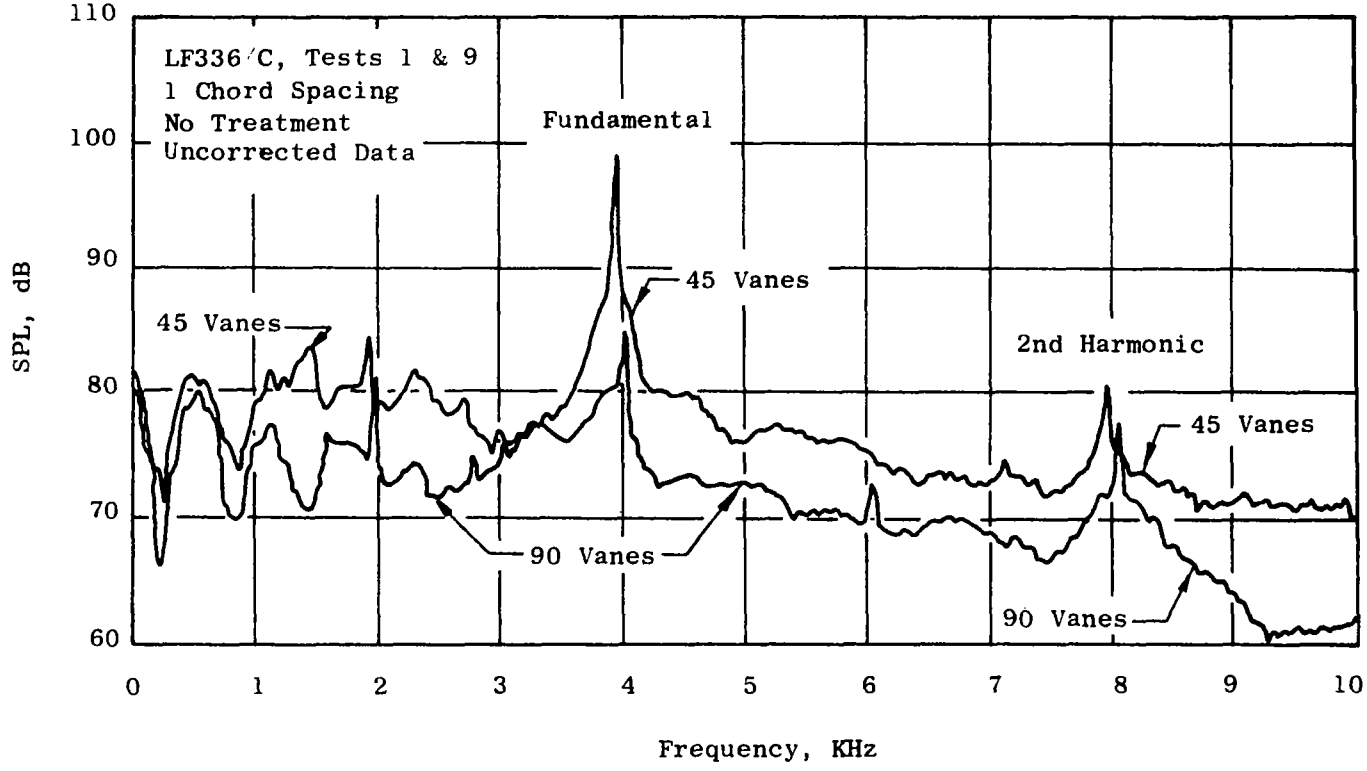

Figure 15. Effect of Vane Number on SPL Spectrum at 100° Arc Angle at 95% RPM

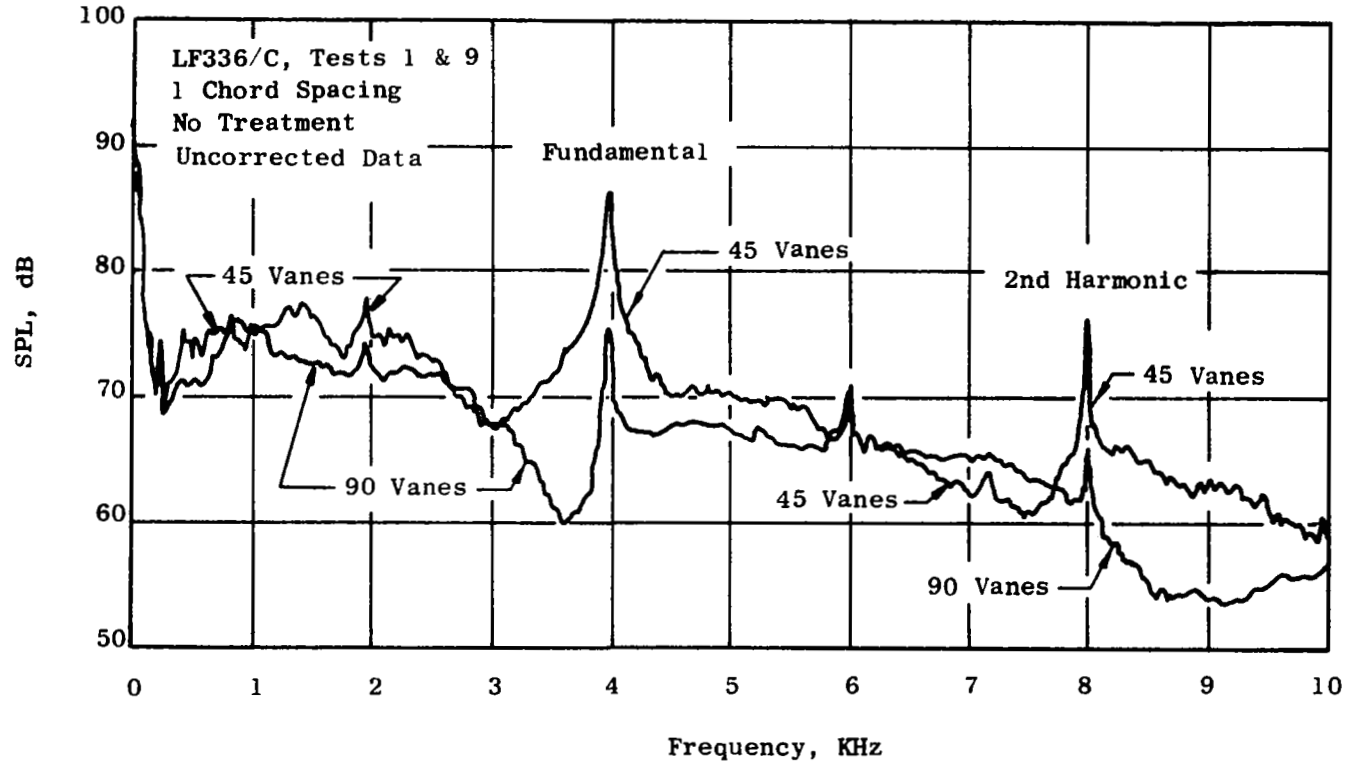

Figure 16. Effect of Vane Number on SPL Spectrum at 160° Arc Angle at 95% RPM

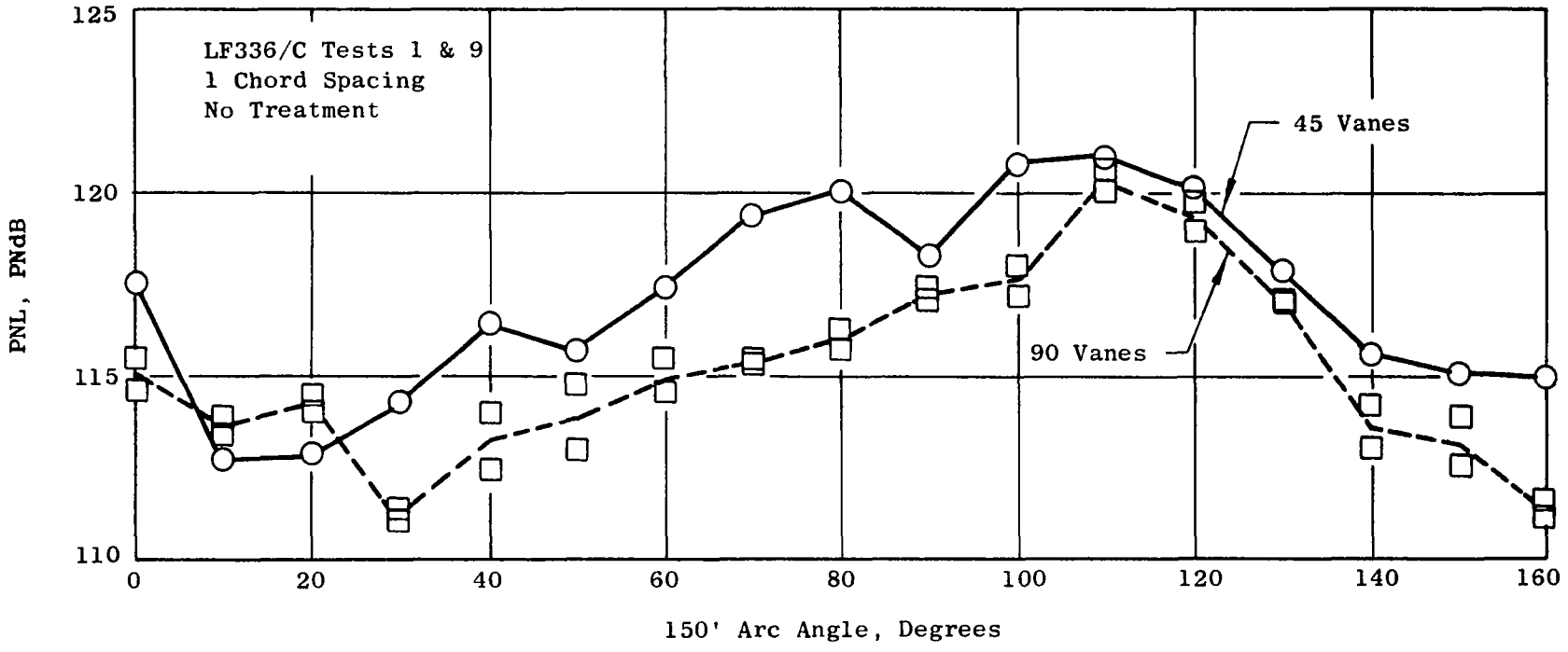

Figure 17. Effect of Vane Number on Arc PNL at 95% RPM

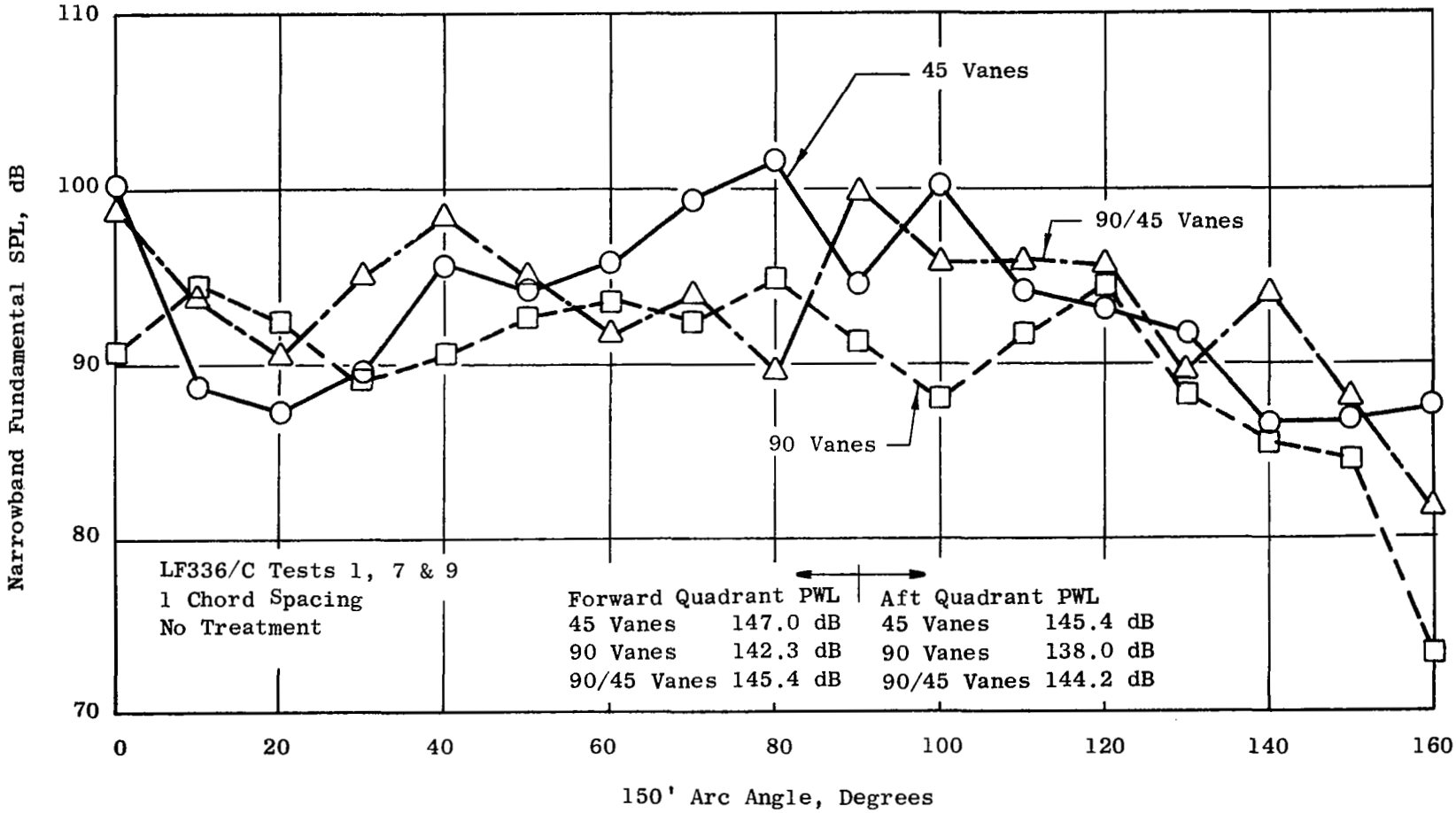

Figure 18. Effect of Split Vane Row on Arc Fundamental SPL at 95% RPM

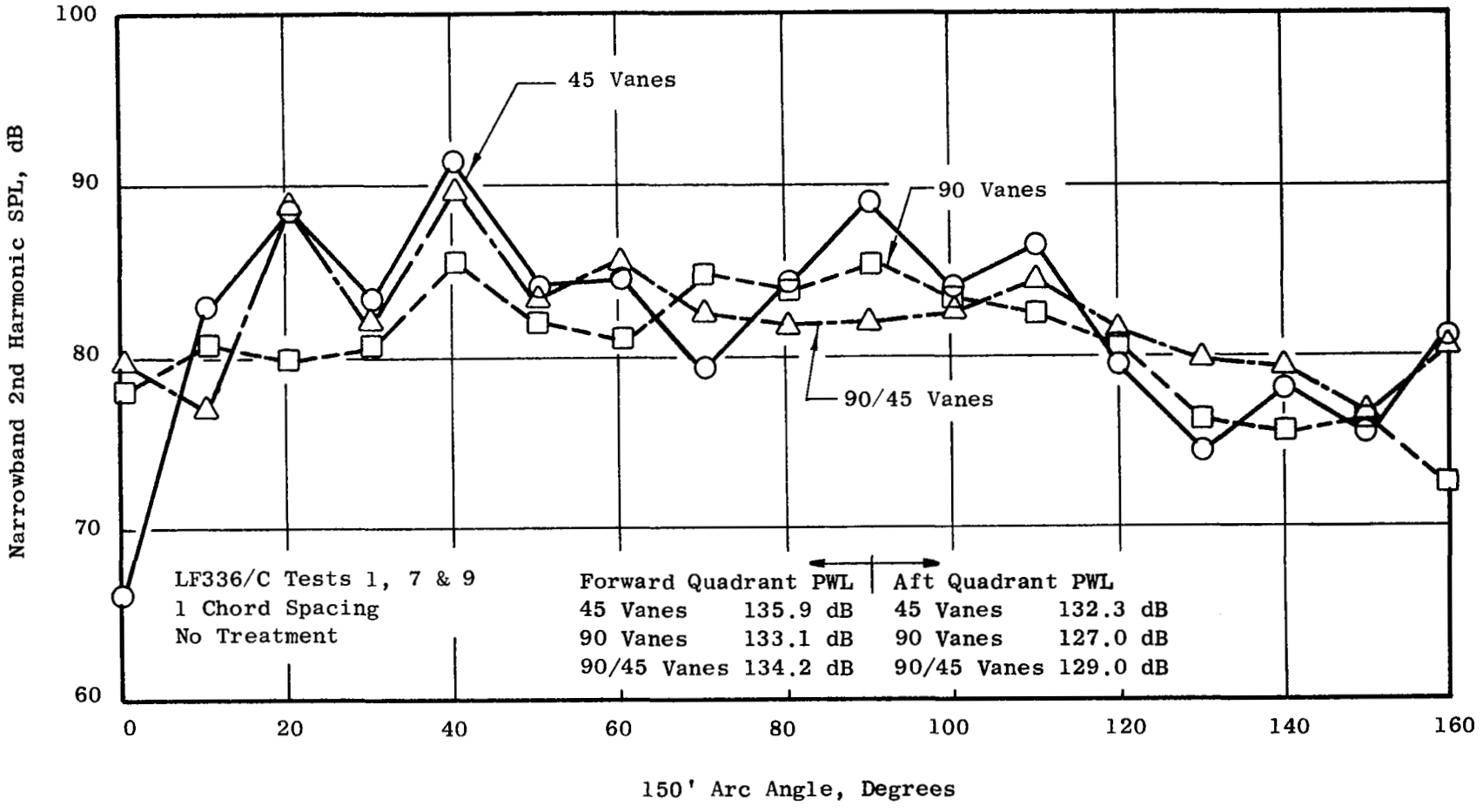

Figure 19. Effect of Split Vane Row on Arc Second Harmonic SPL at 95% RPM

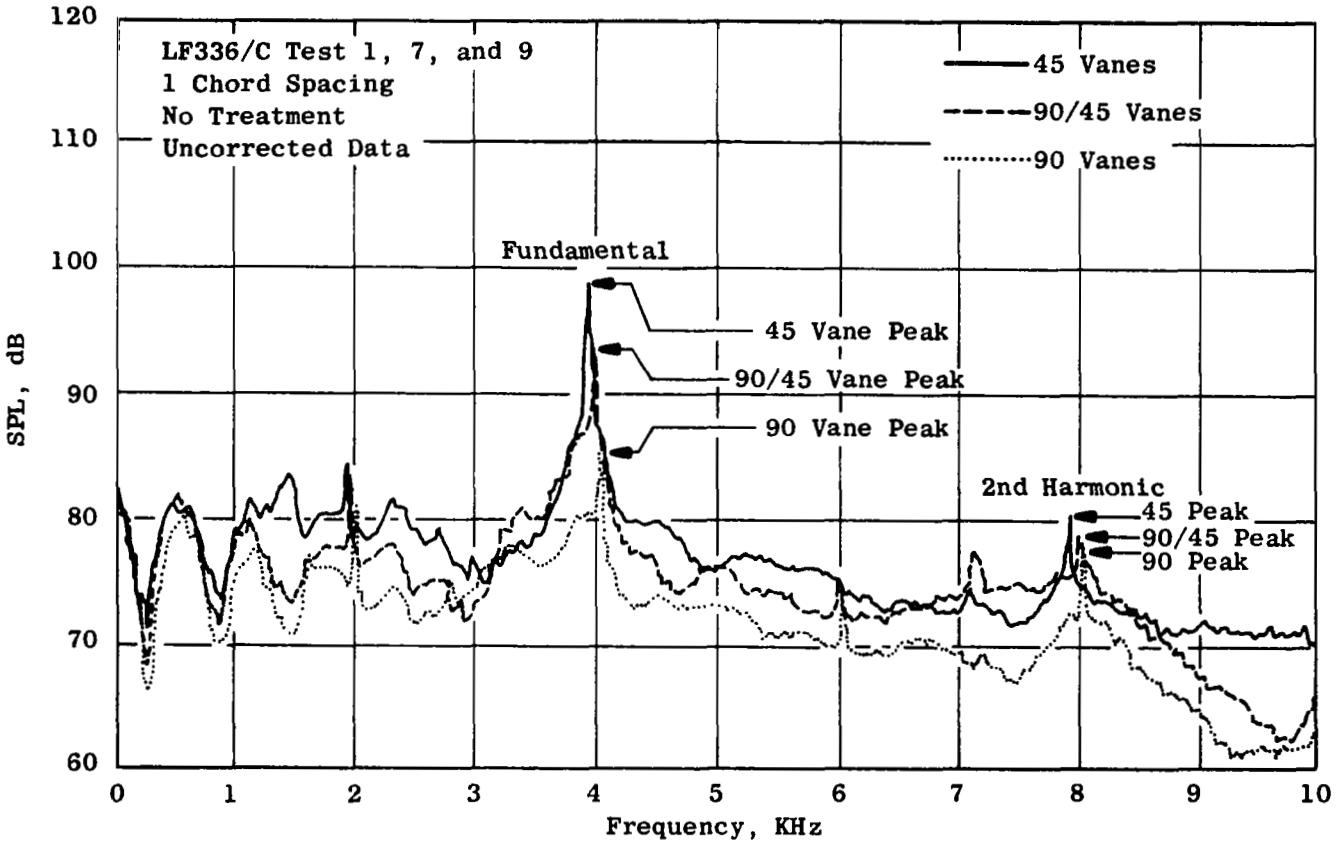

Figure 20. Effect of Split Vane Row on SPL Spectrum at 100° Arc Angle at 95% RPM.

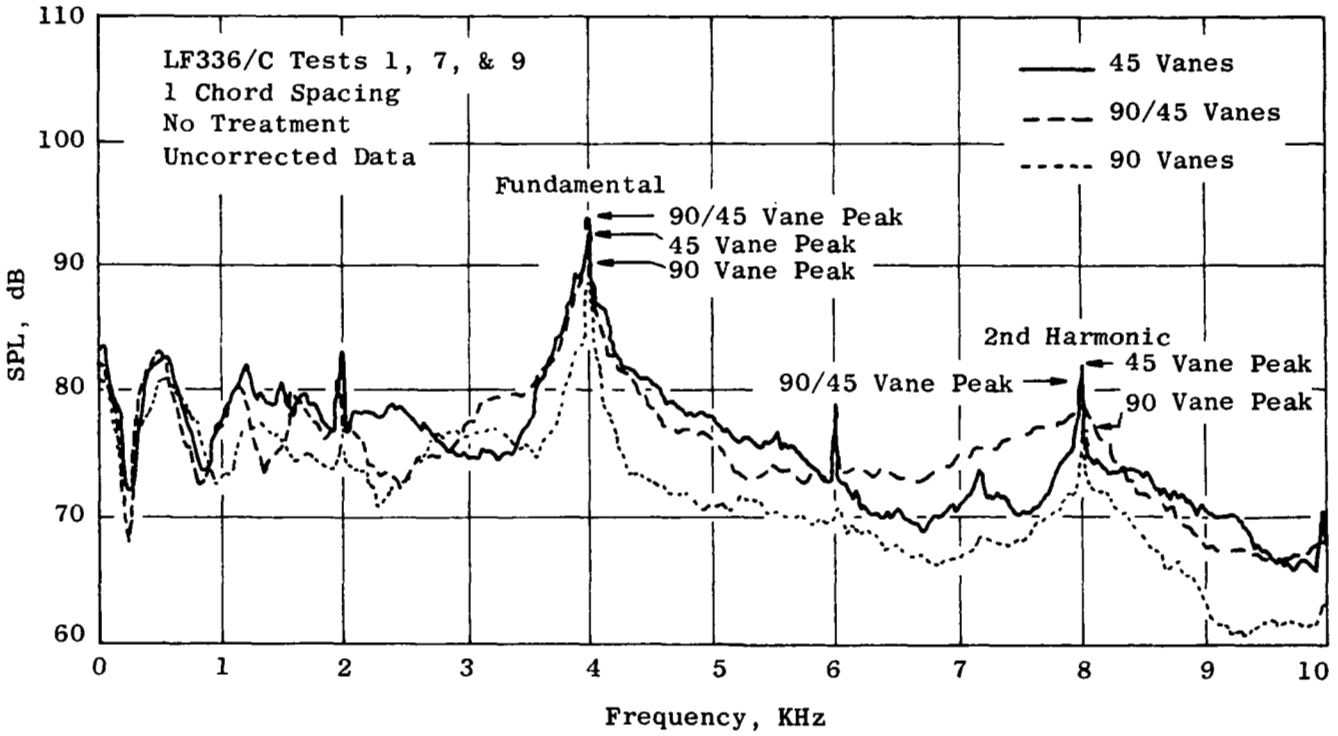

Figure 21. Effect of Split Vane Row on SPL Spectrum at 110° Arc Angle at 95% RPM.

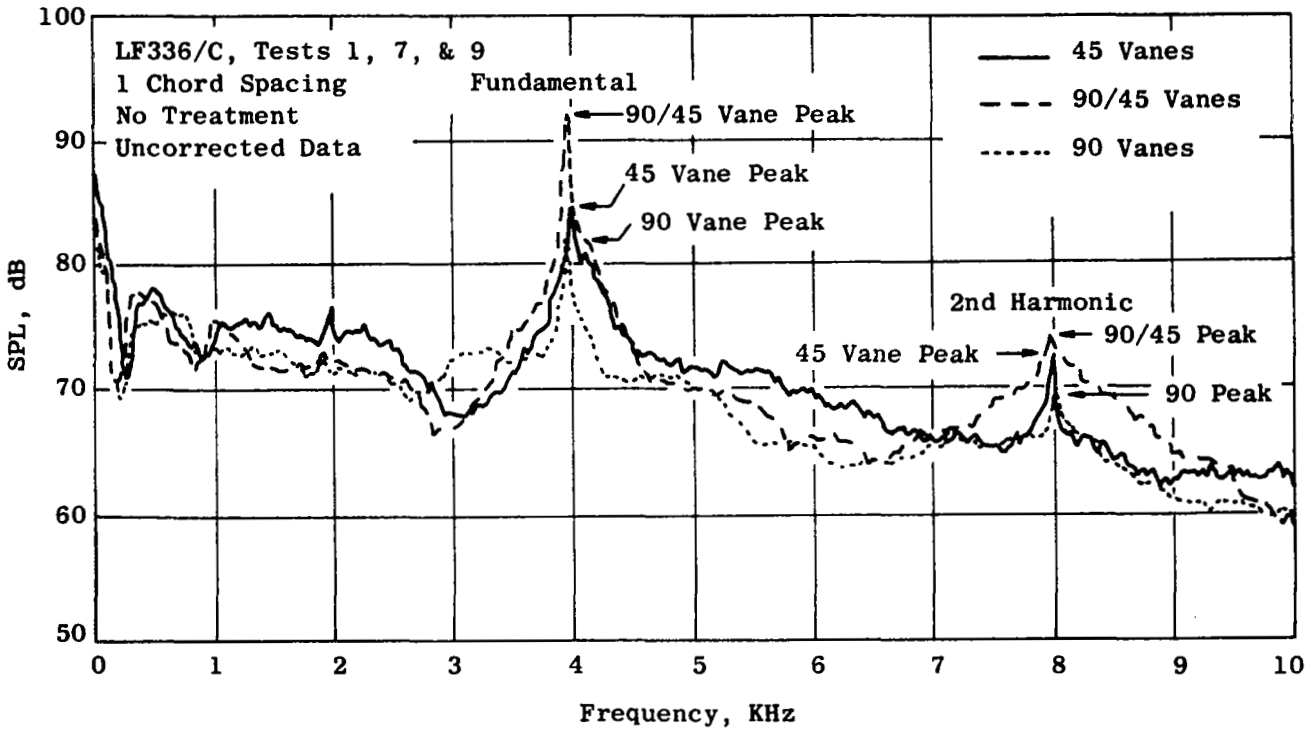

Figure 22. Effect of Split Vane Row on SPL Spectrum at 140° Arc Angle at 95% RPM.

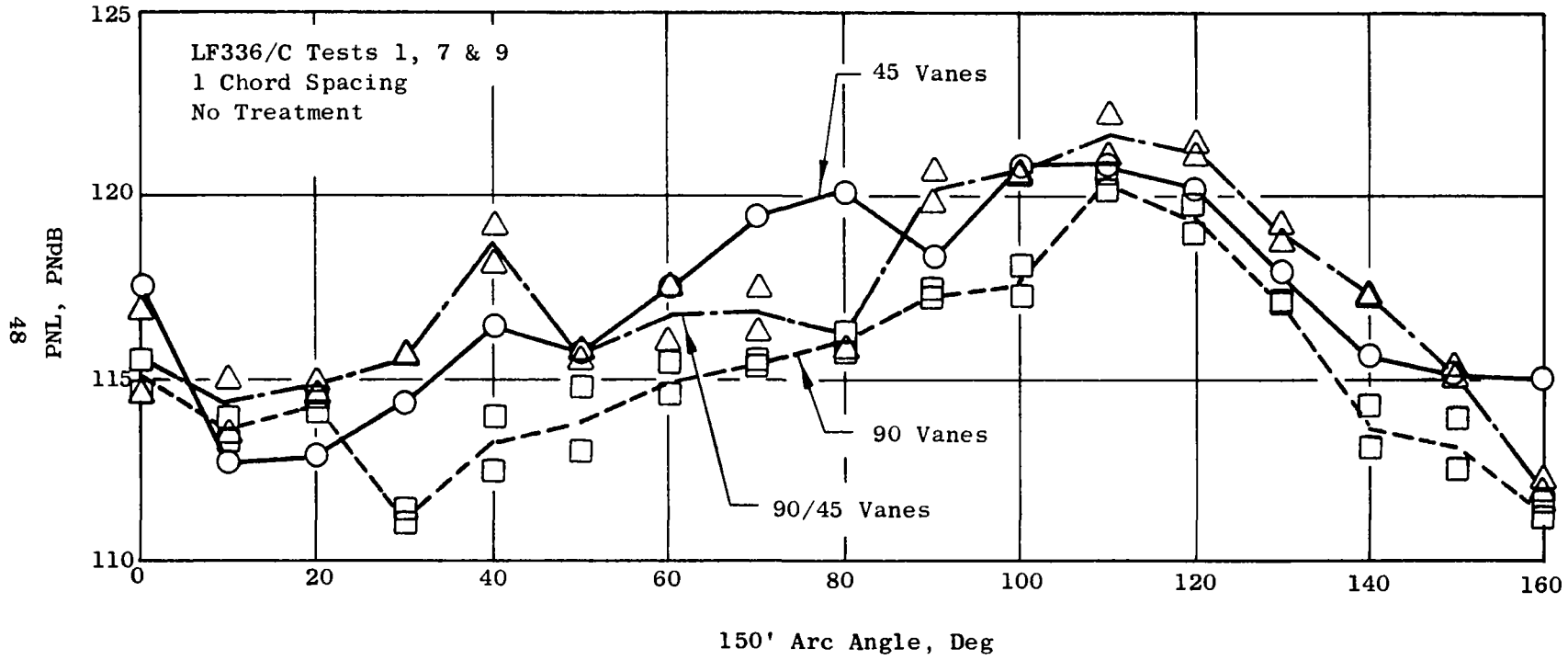

Figure 23. Effect of Split Vane Row on Arc PNL at 95% RPM

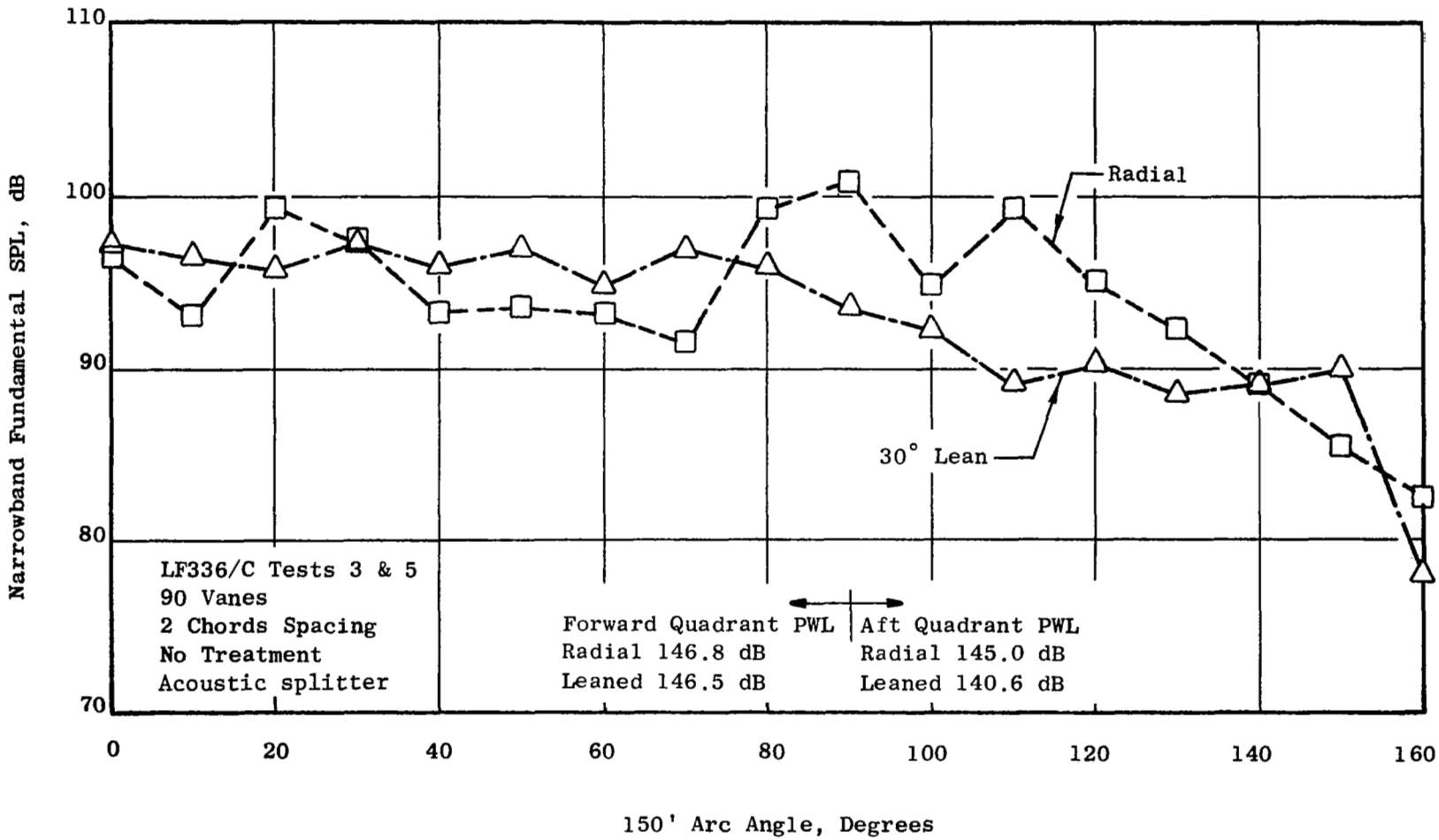

Figure 24. Effect of Vane Lean on Arc Fundamental SPL at 95% RPM

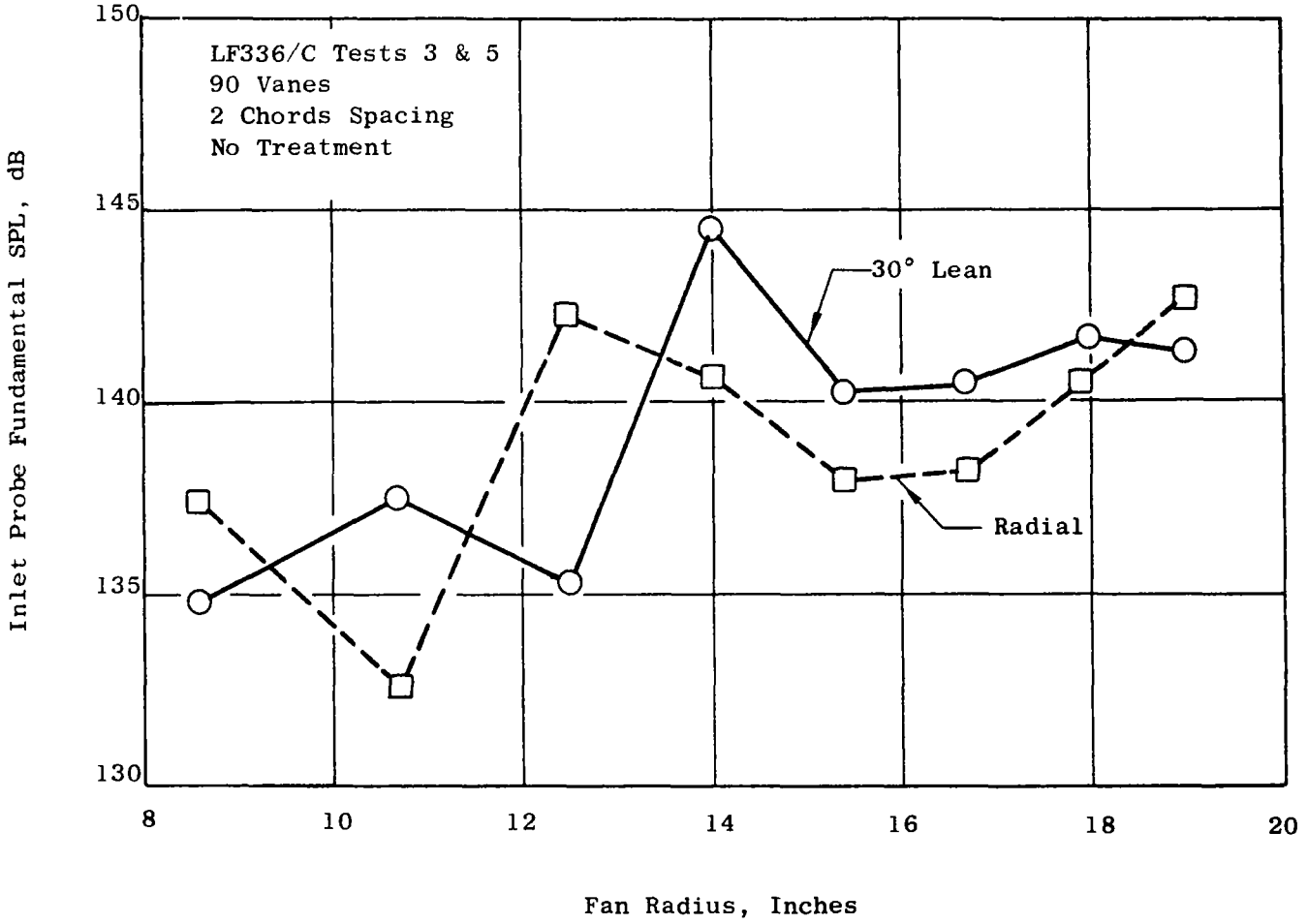

Figure 25. Effect of Vane Lean on Inlet Probe Fundamental SPL at 95% RPM

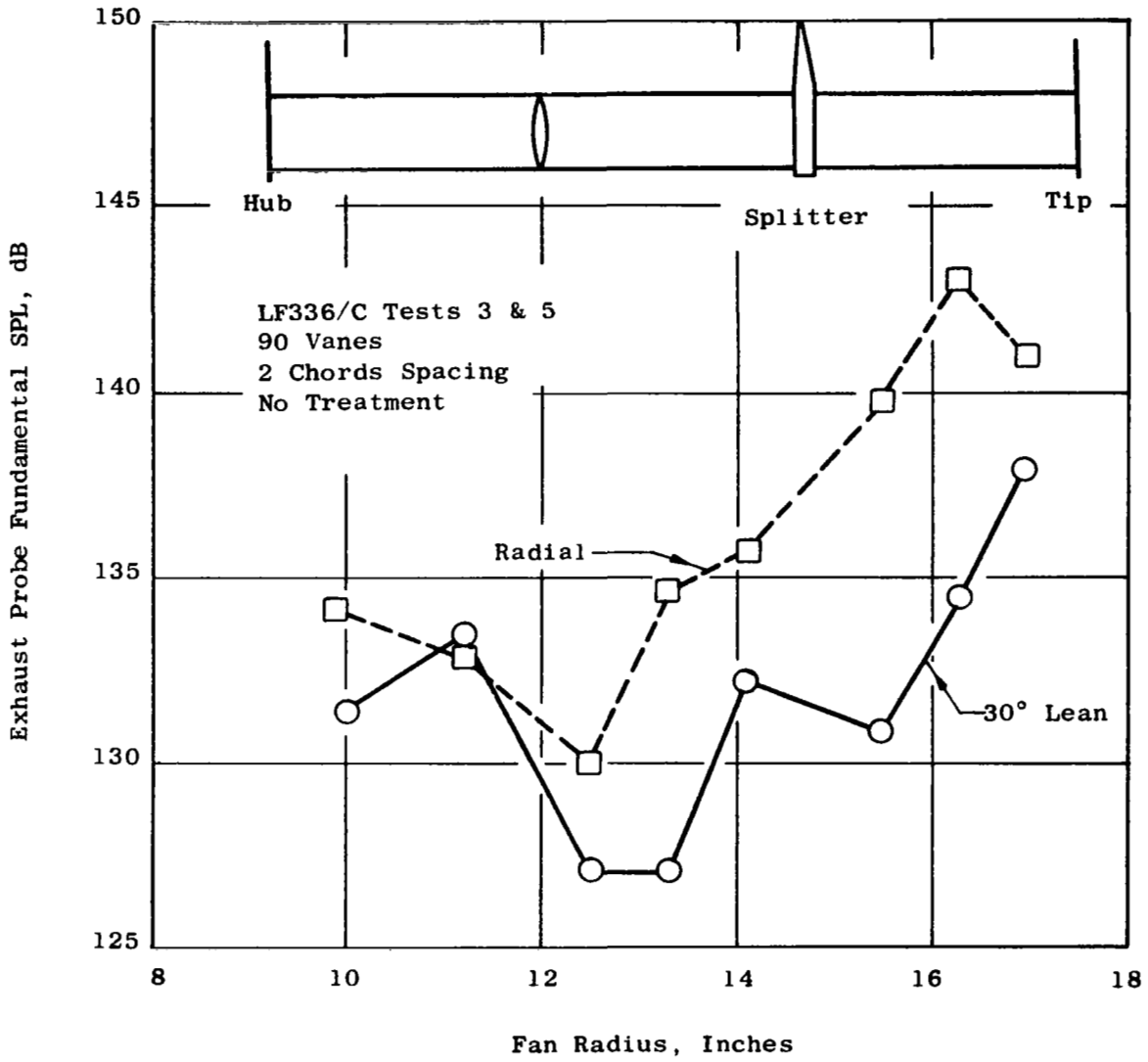

Figure 26. Effect of Vane Lean on Exhaust Probe Fundamental SPL at 95% RPM

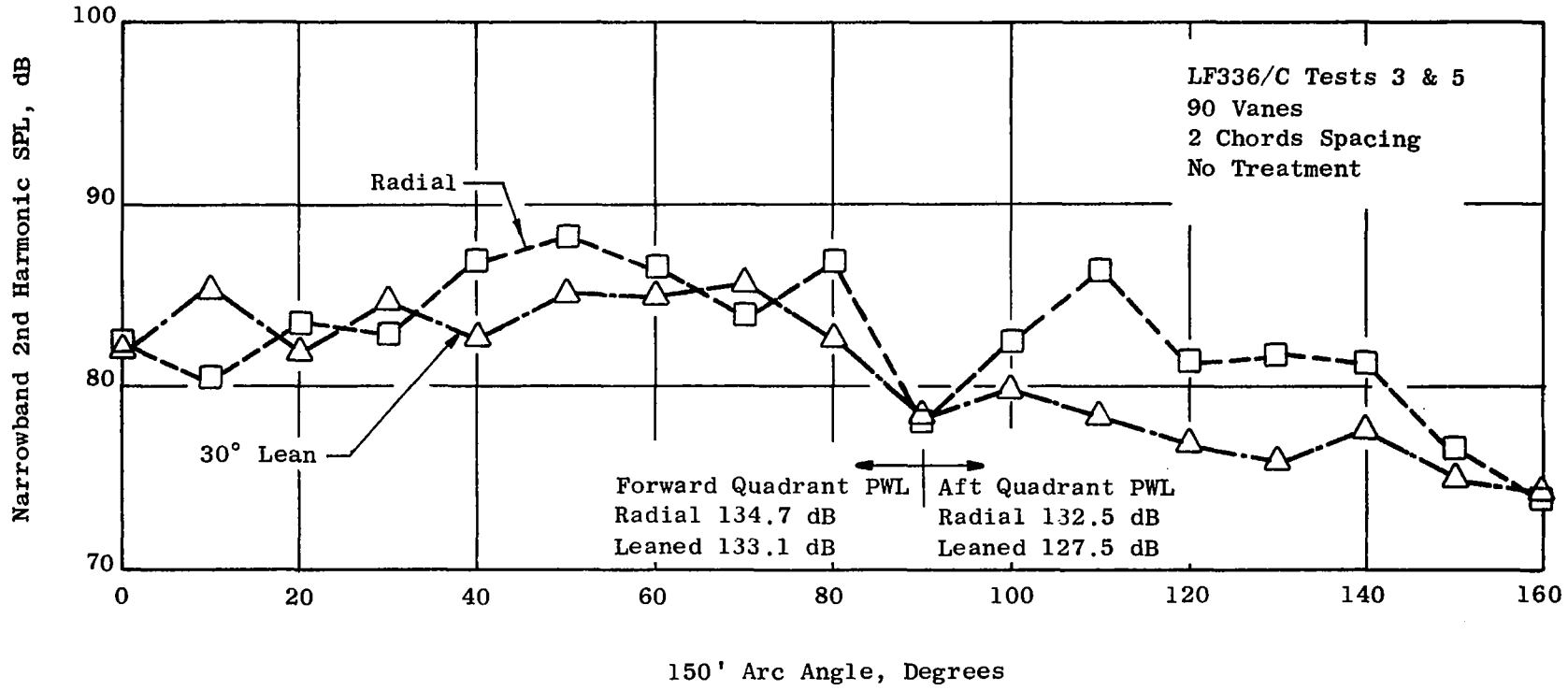

Figure 27. Effect of Vane Lean on Arc Second Harmonic SPL at 95% RPM

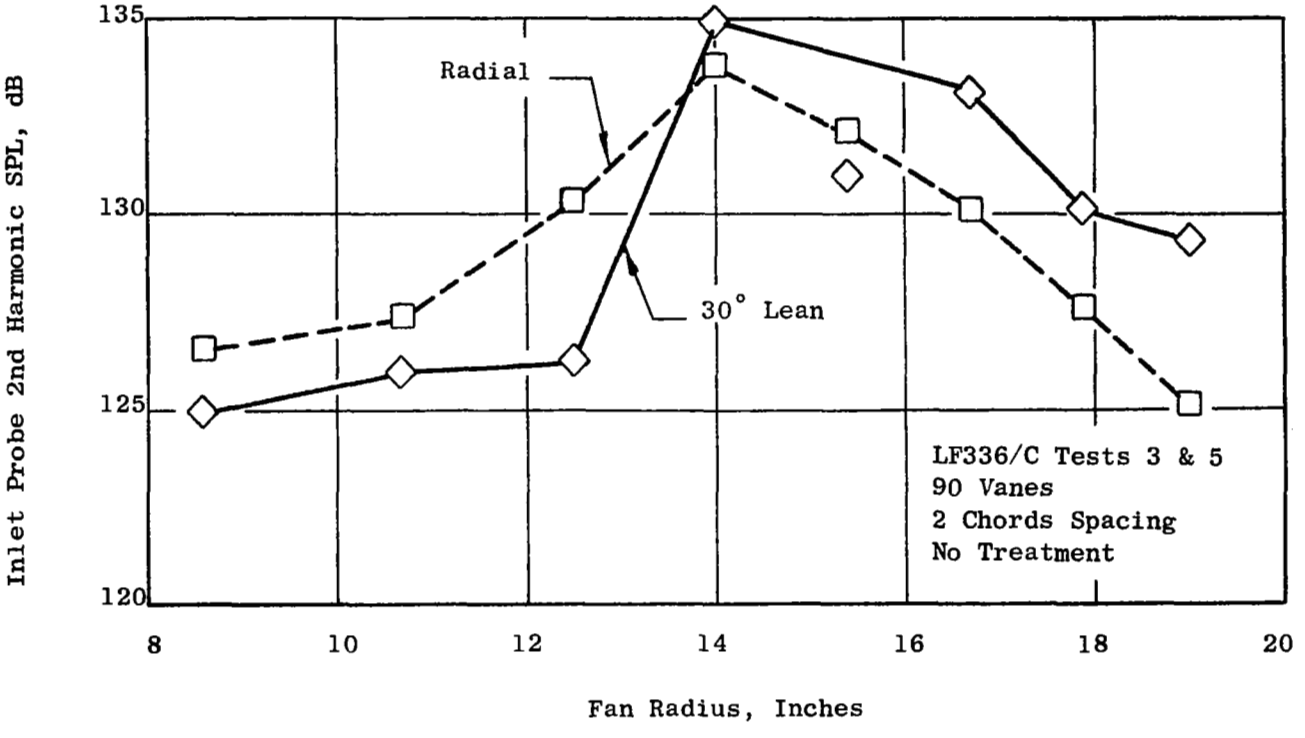

Figure 28. Effect of Vane Lean on Inlet Probe Second Harmonic SPL at 95% RPM

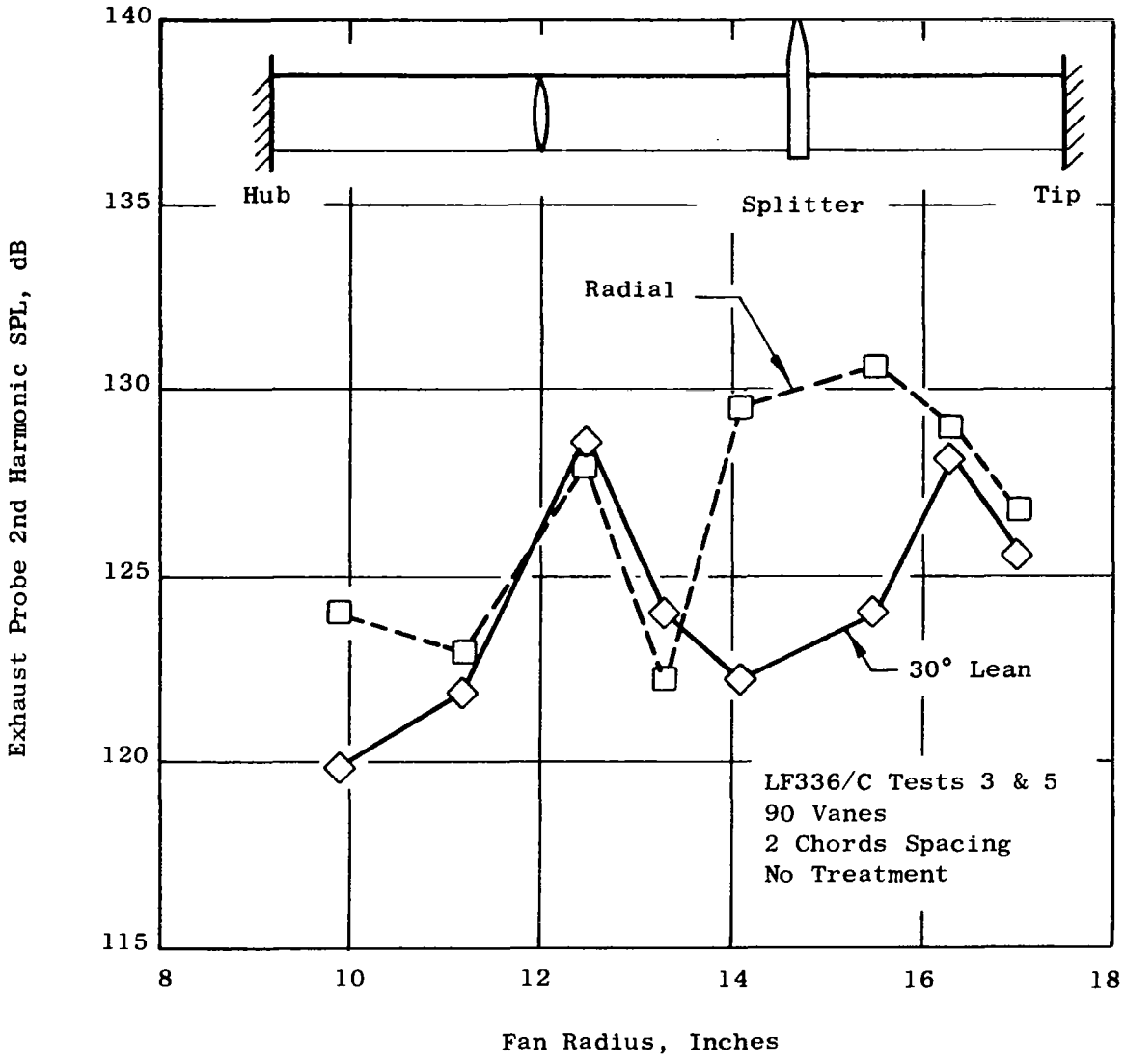

Figure 29. Effect of Vane Lean on Exhaust Probe Second Harmonic SPL at 95% RPM

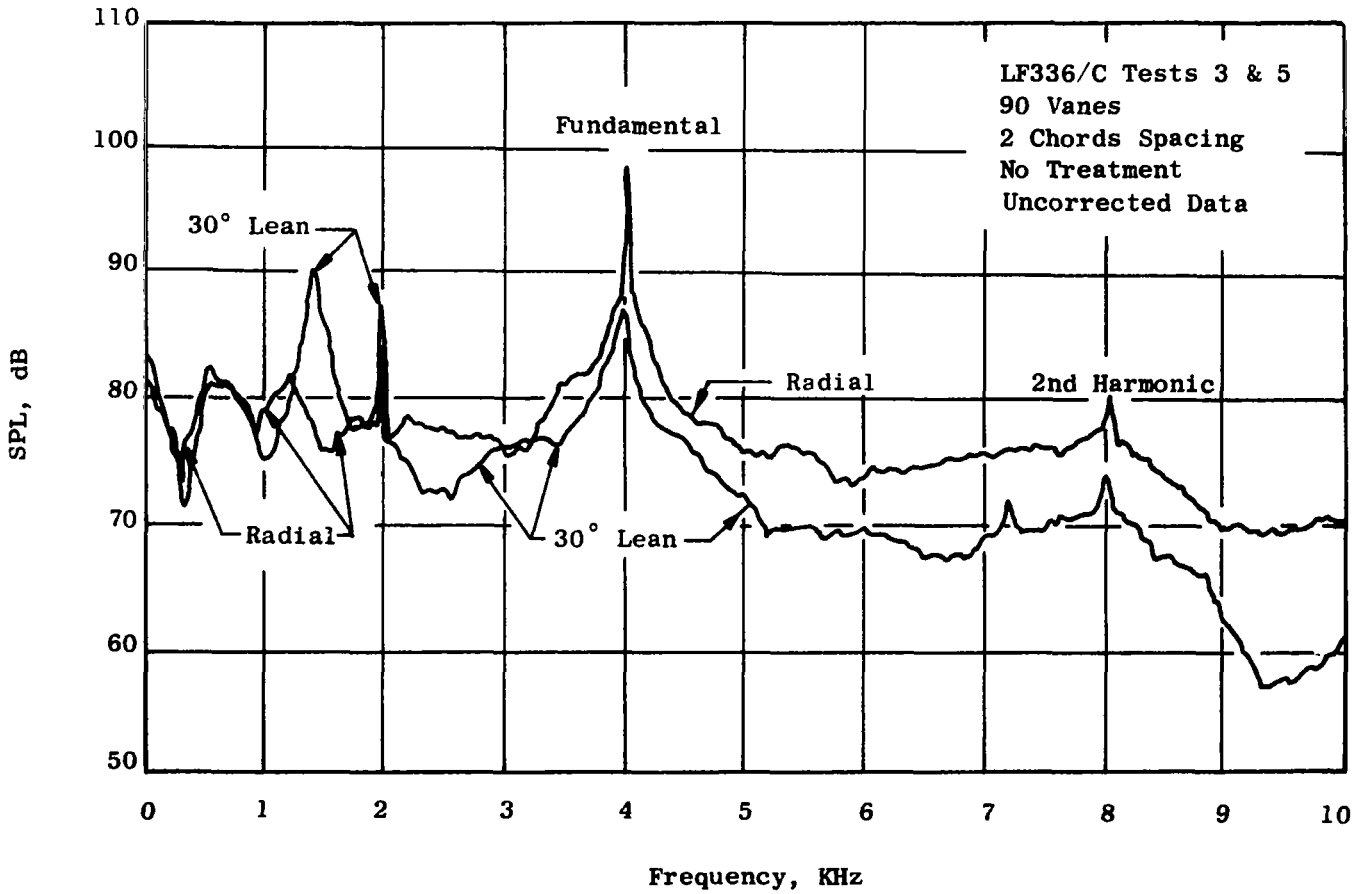

Figure 30. Effect of Vane Lean on SPL Spectrum at 110° Arc Angle at 95% RPM

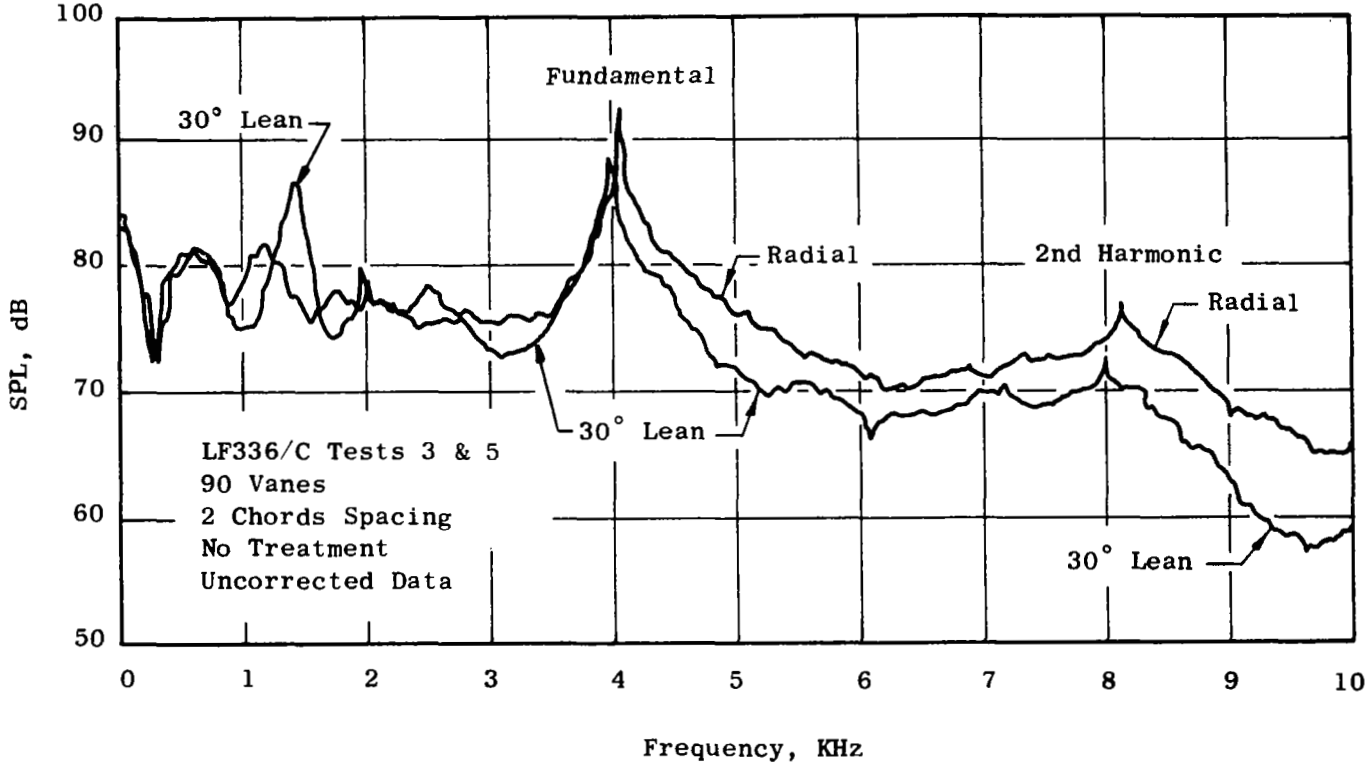

Figure 31. Effect of Vane Lean on SPL Spectrum at 120° Arc Angle at 95% RPM

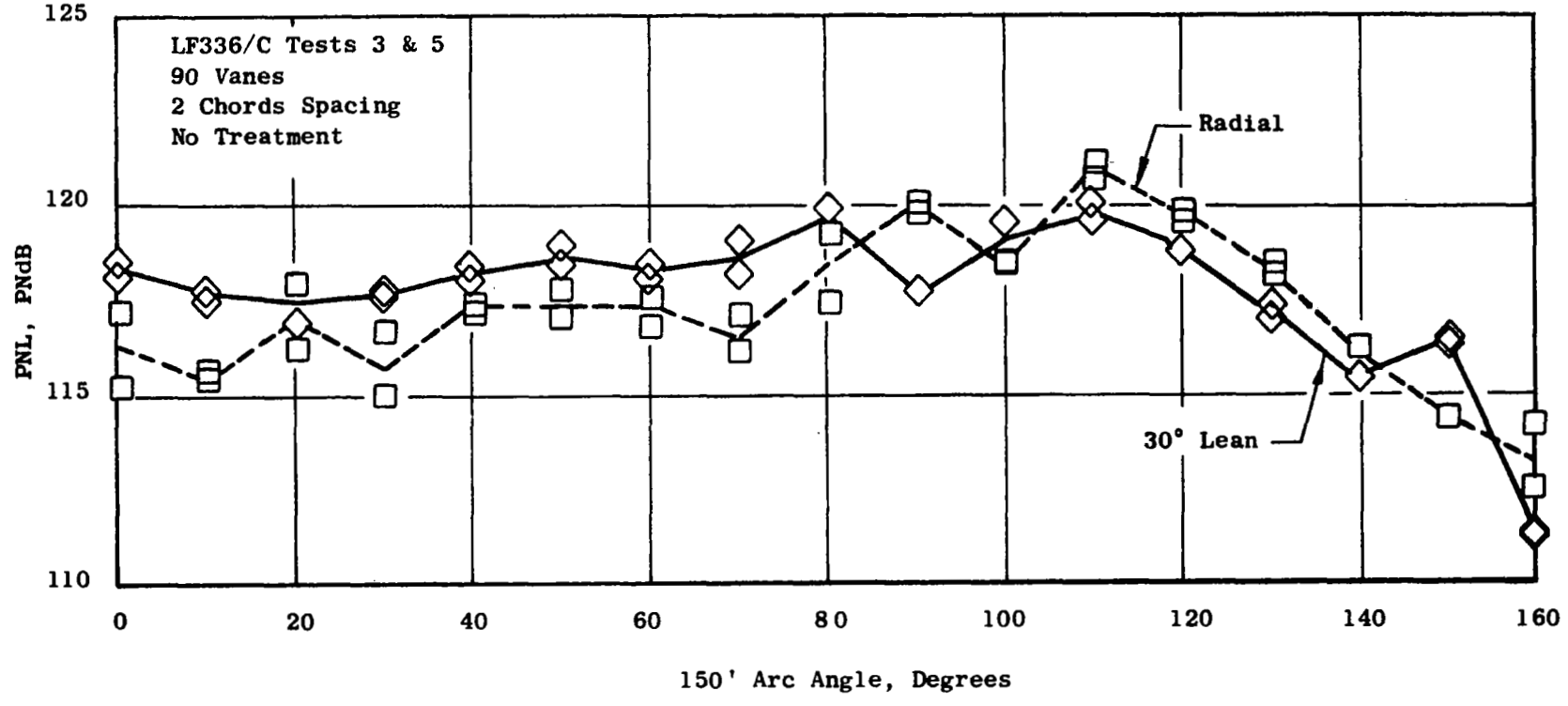

Figure 32. Effect of Vane Lean on Arc PNL at 95% RPM

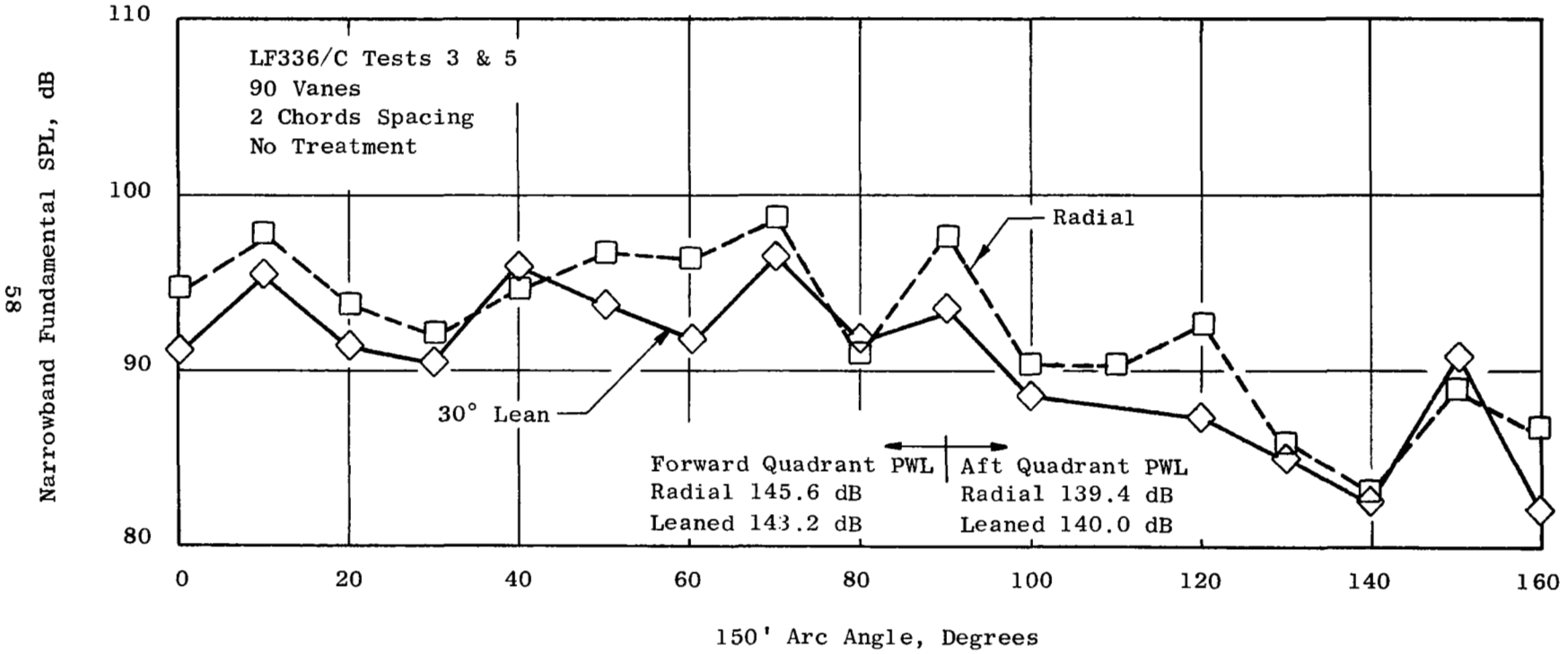

Figure 33. Effect of Vane Lean on Arc Fundamental SPL at 80% RPM

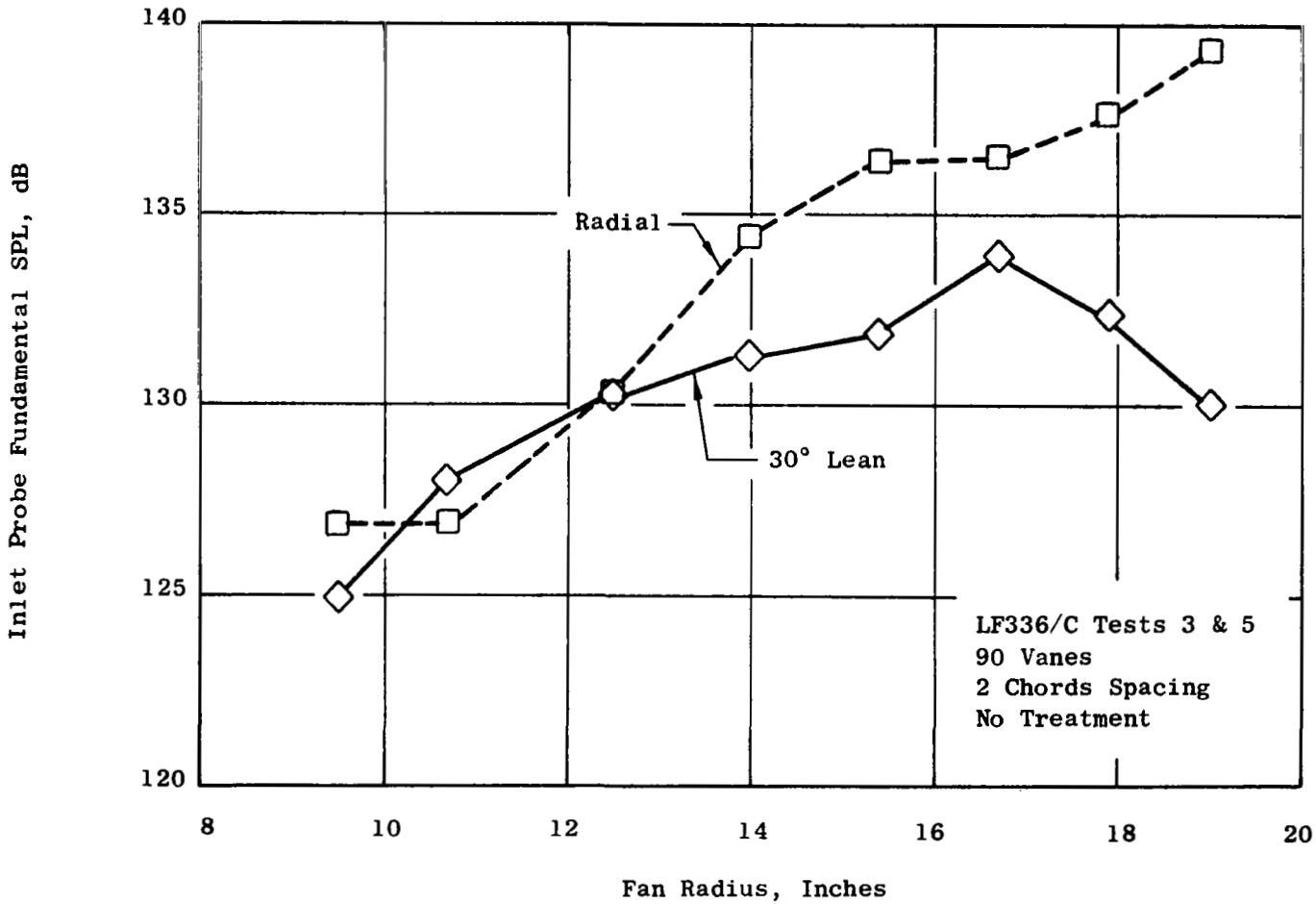

Figure 34. Effect of Vane Lean on Inlet Probe Fundamental SPL at 80% RPM

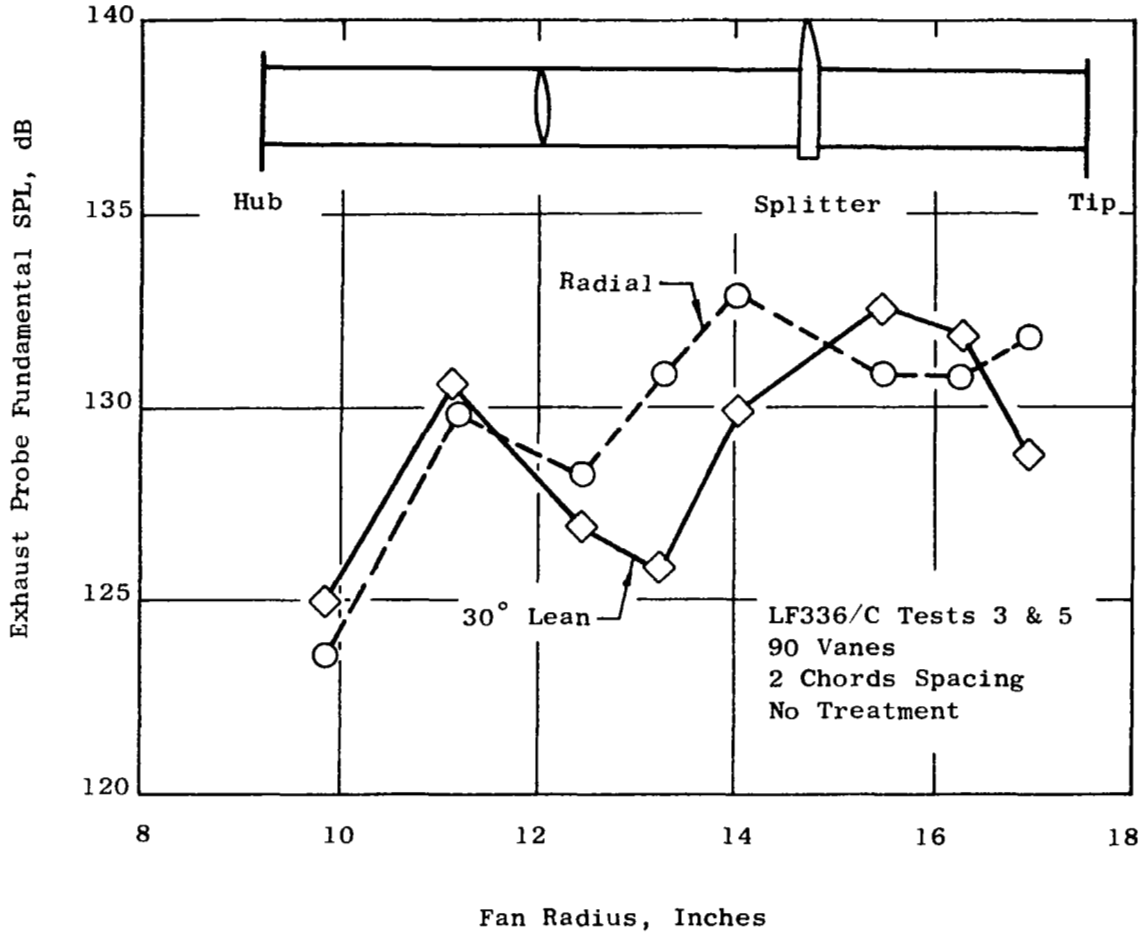

Figure 35. Effect of Vane Lean on Exhaust Probe Fundamental SPL at 80% RPM

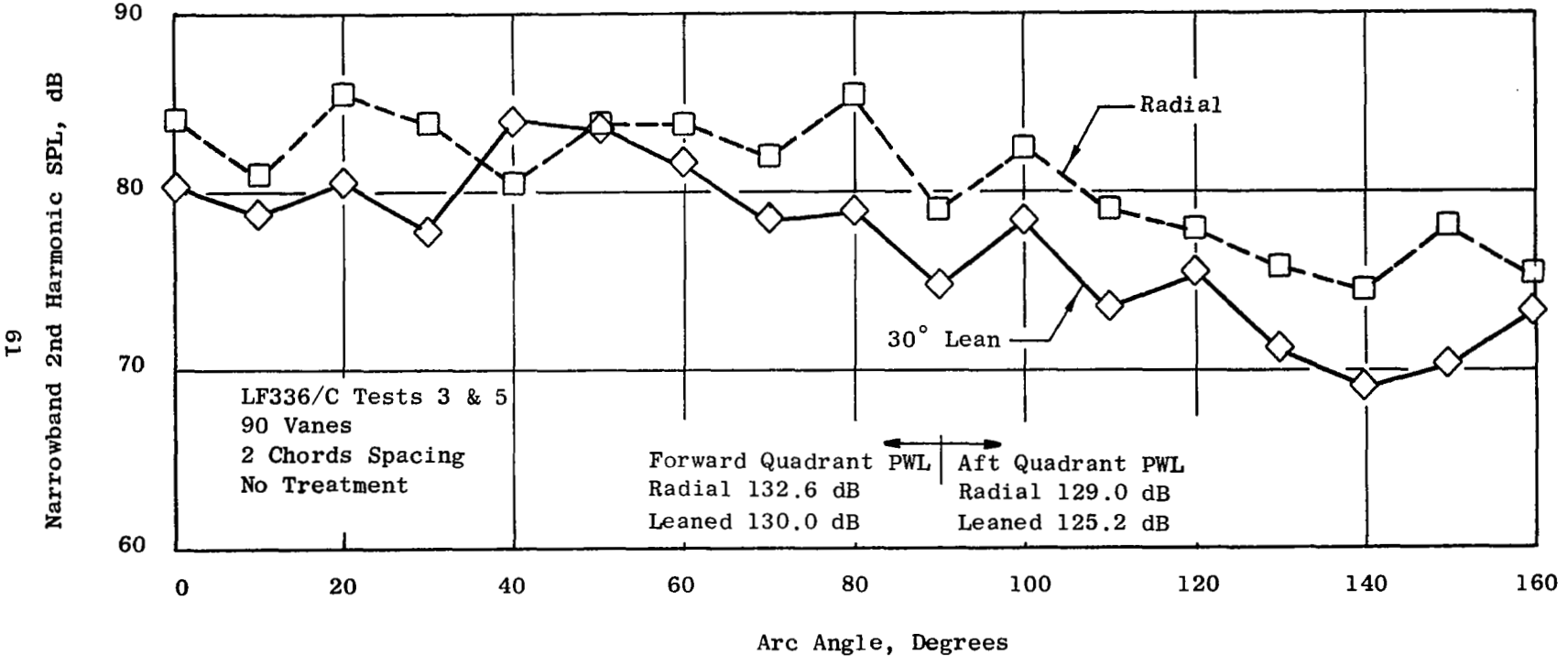

Figure 36. Effect of Vane Lean on Arc Second Harmonic SPL at 80% RPM

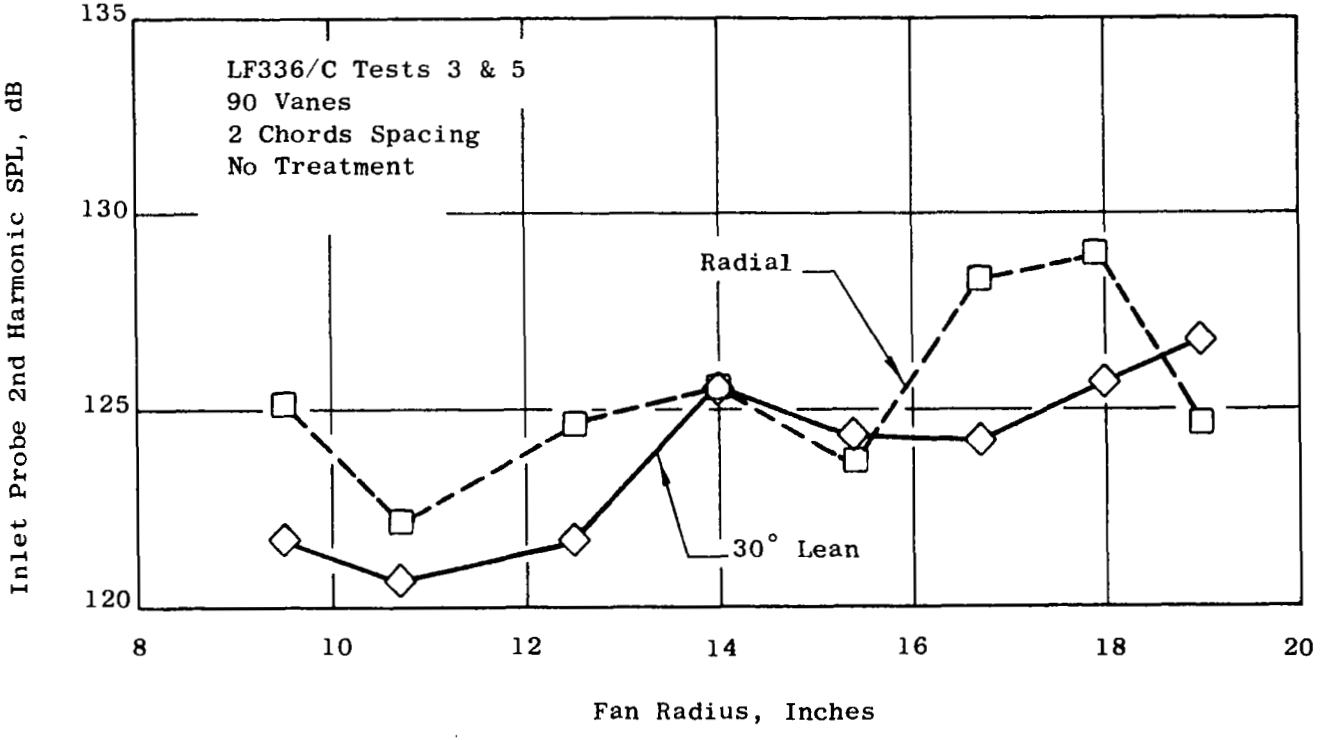

Figure 37. Effect of Vane Lean on Inlet Probe Second Harmonic SPL at 80% RPM

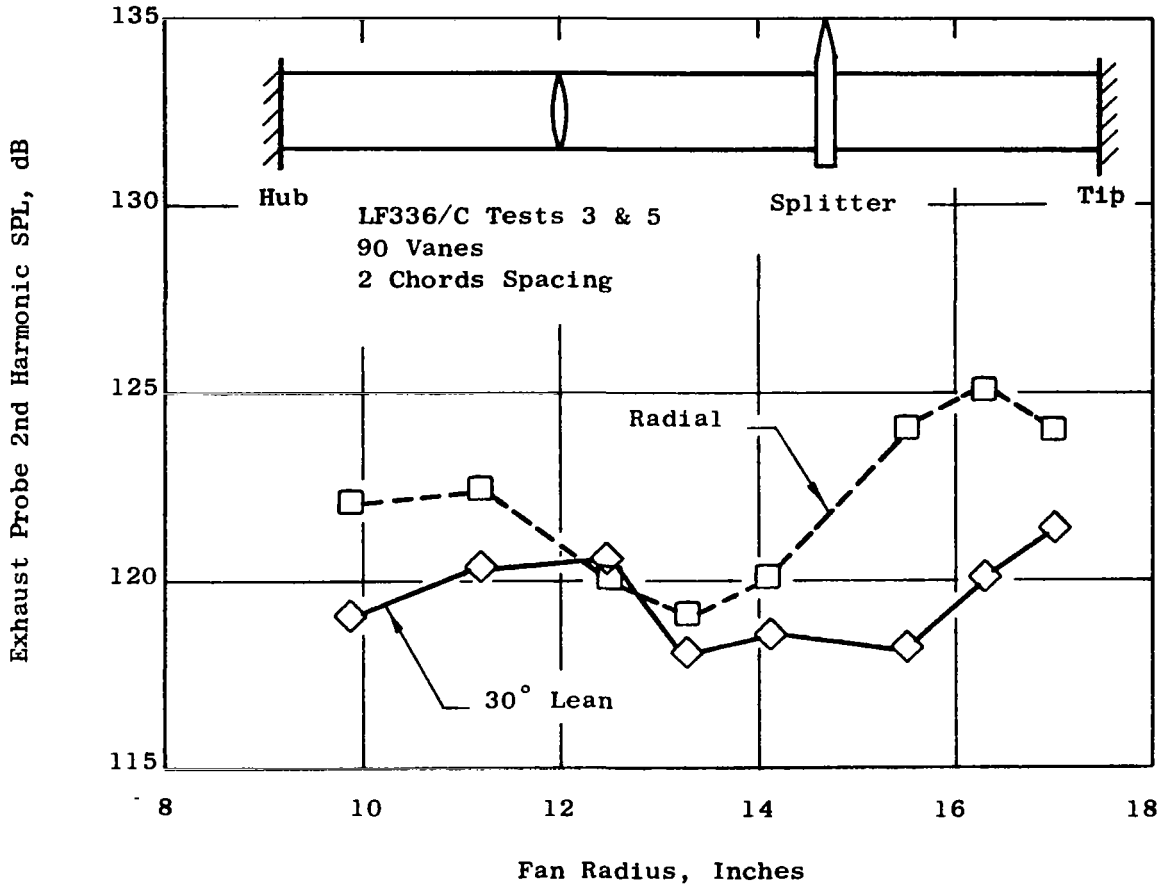

Figure 38. Effect of Vane Lean on Exhaust Probe Second Harmonic SPL at 80% RPM

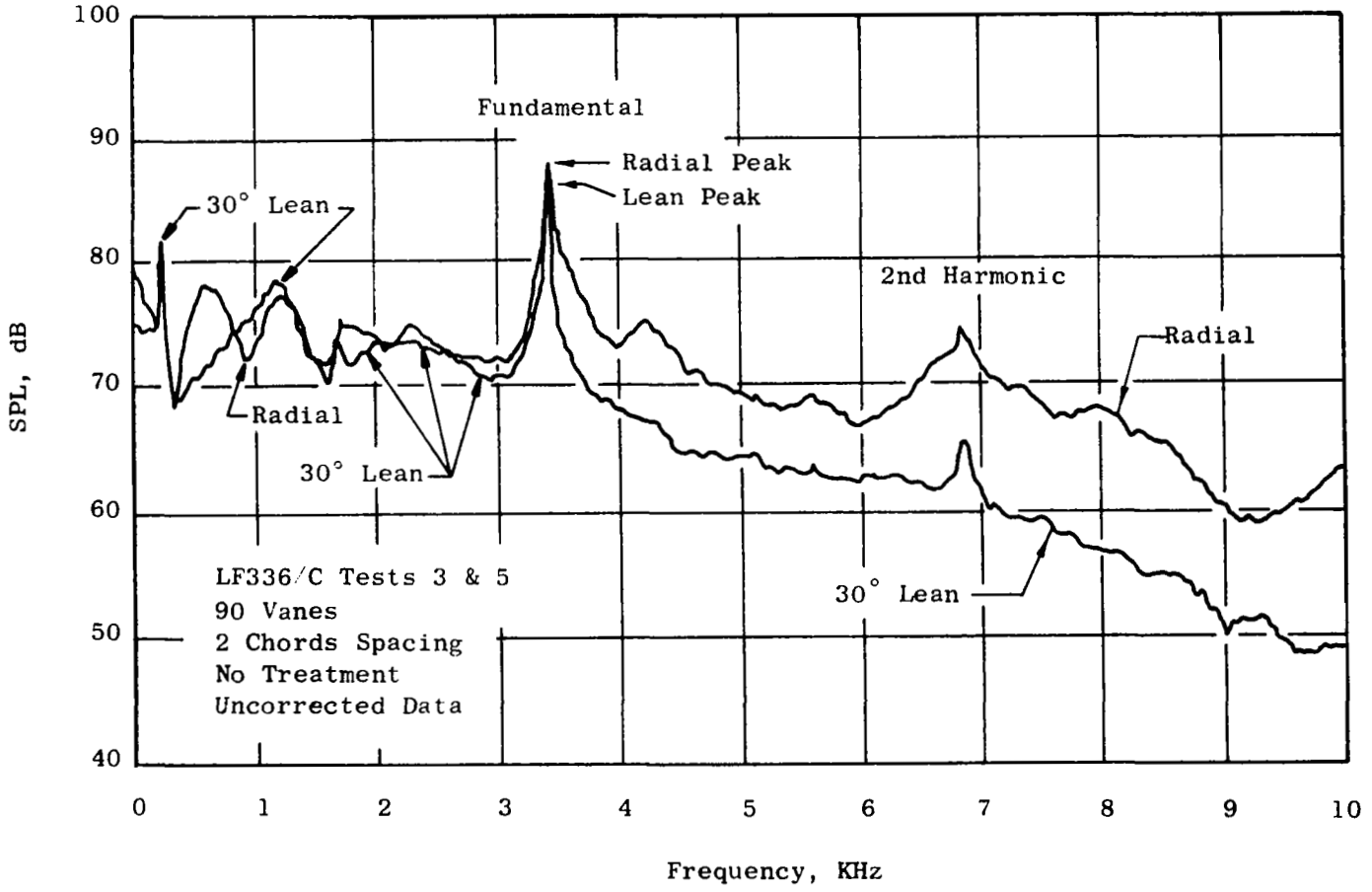

Figure 39. Effect of Vane Lean on SPL Spectrum at 110° Arc Angle at 80% RPM

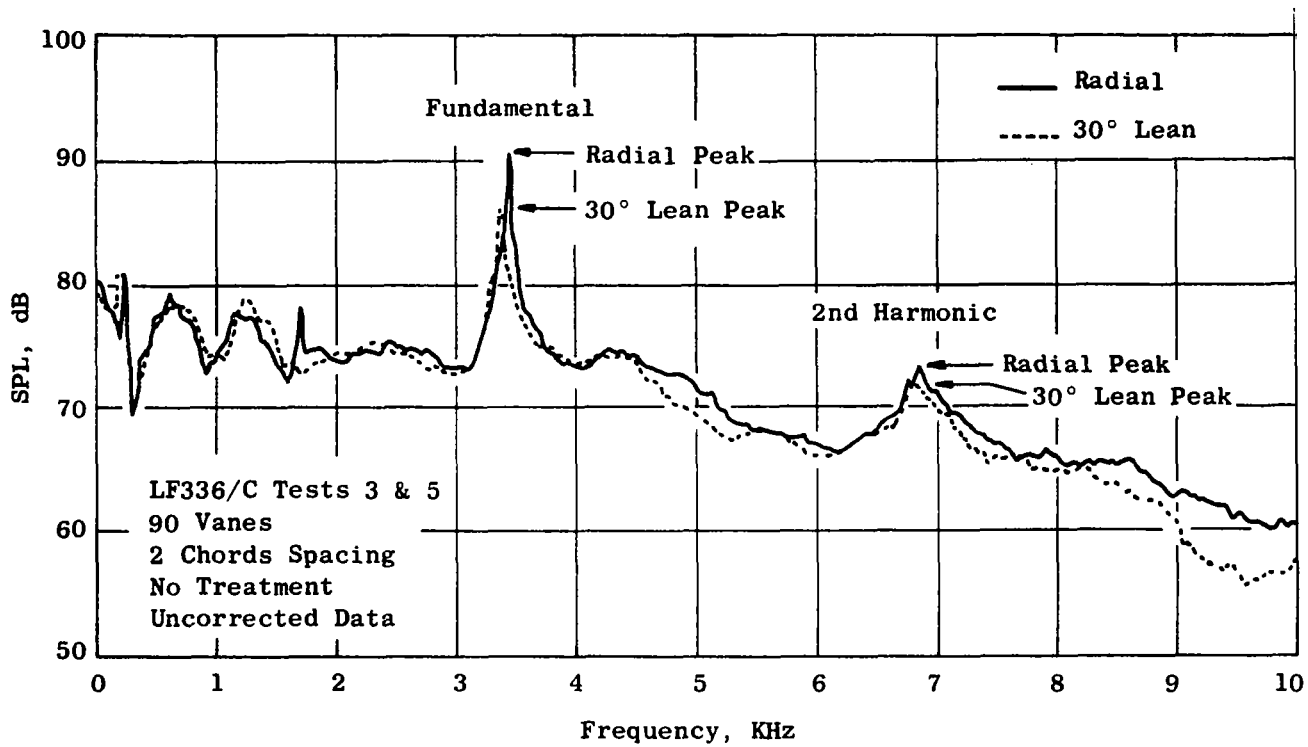

Figure 40. Effect of Vane Lean on SPL Spectrum at 120° Arc Angle at 80% RPM.

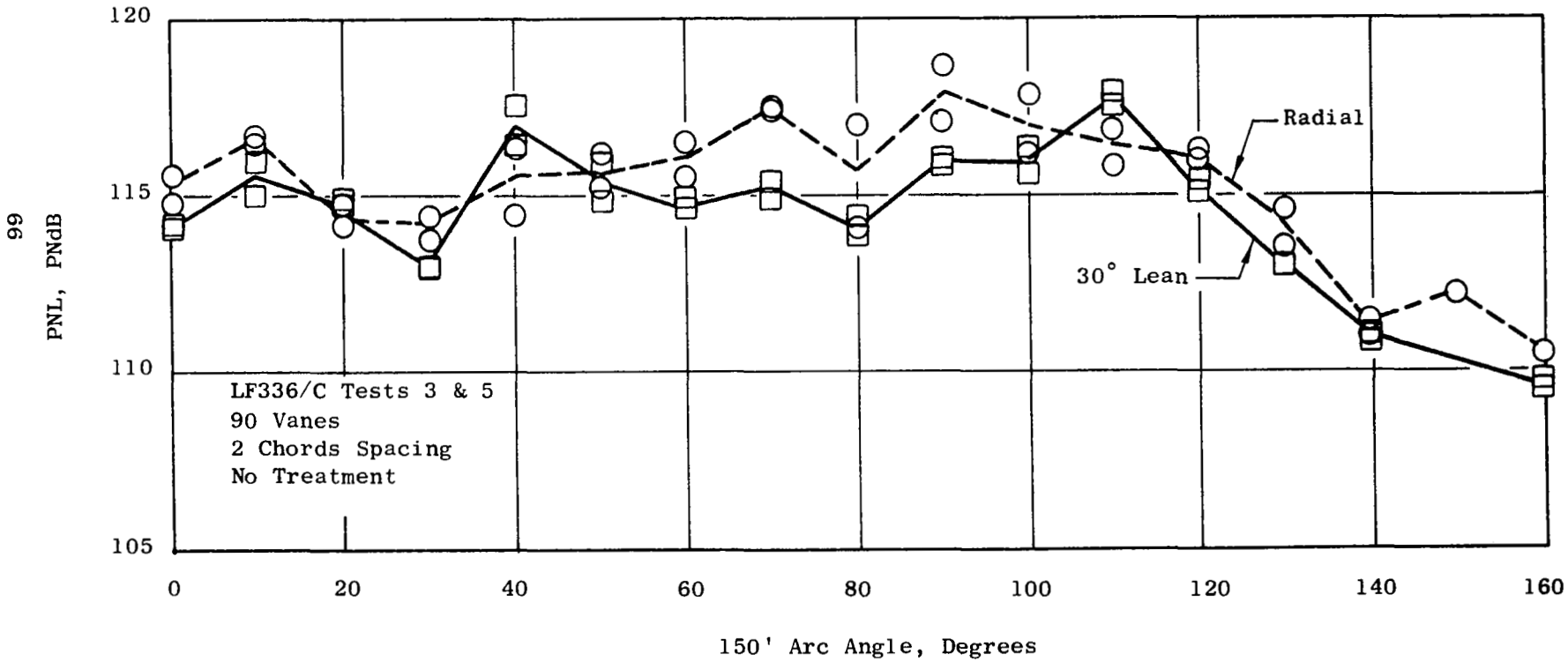

Figure 41. Effect of Vane Lean on Arc PNL at 80% RPM.

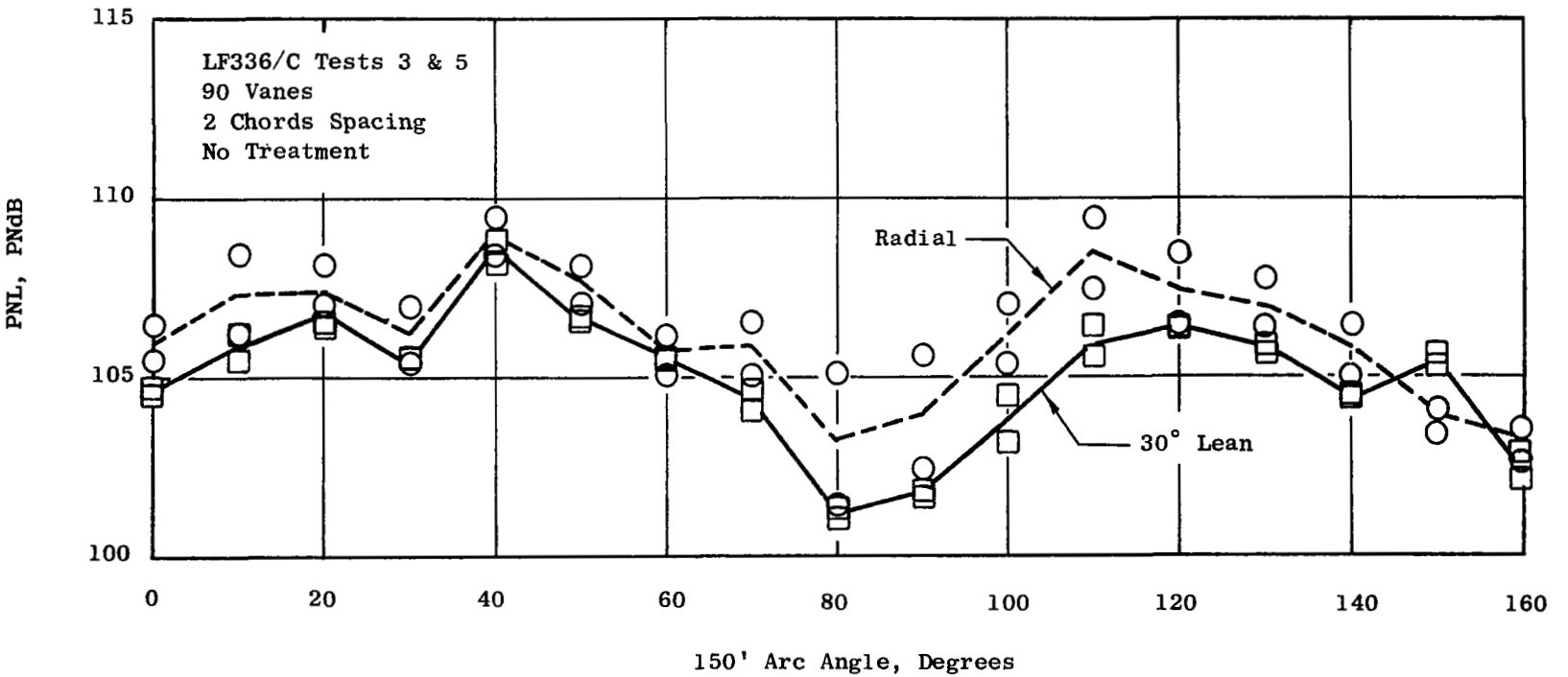

Figure 42. Effect of Vane Lean on Arc PNL at 50% RPM

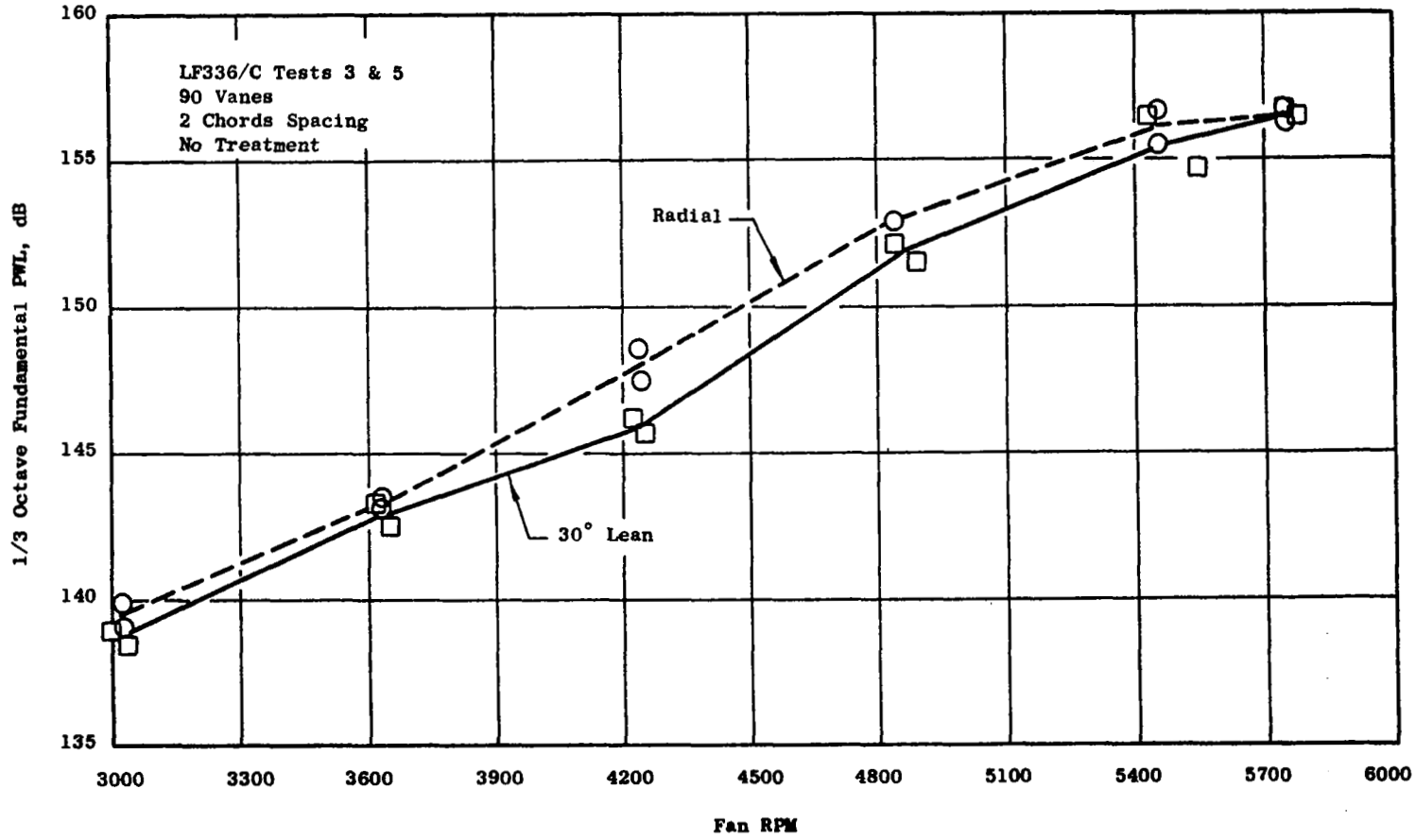

Figure 43. Effect of Vane Lean on Fundamental PWL

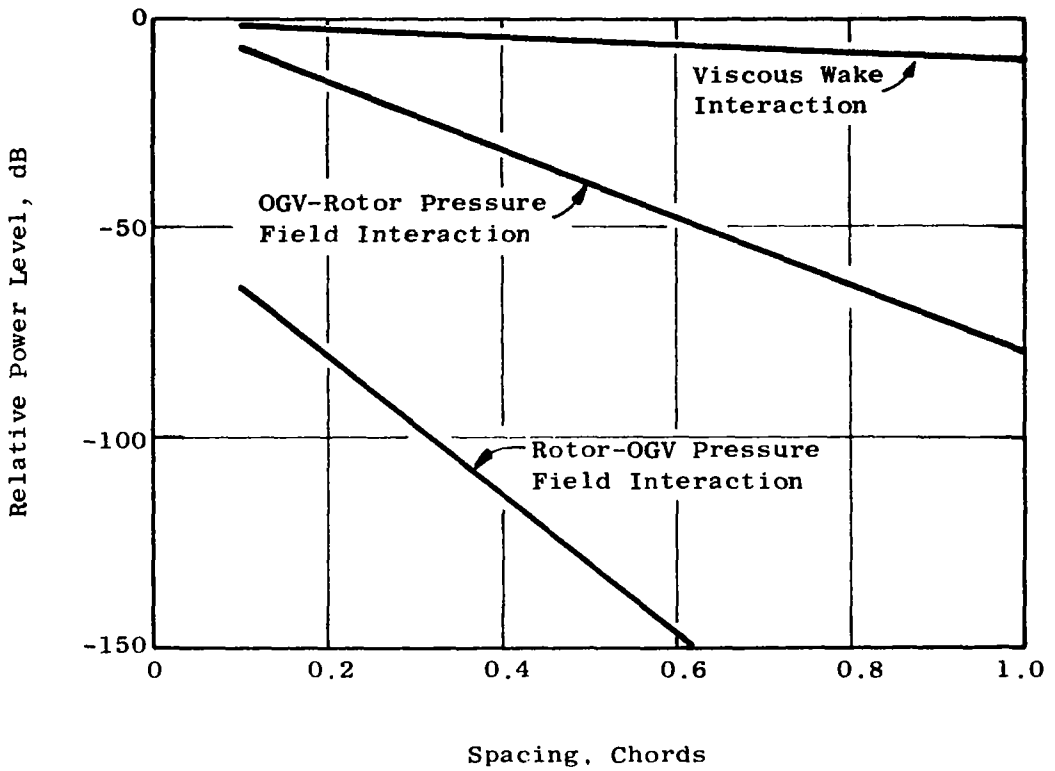

Figure 44. Theoretical Effect of Spacing on Viscous Wake and Potential Interactions

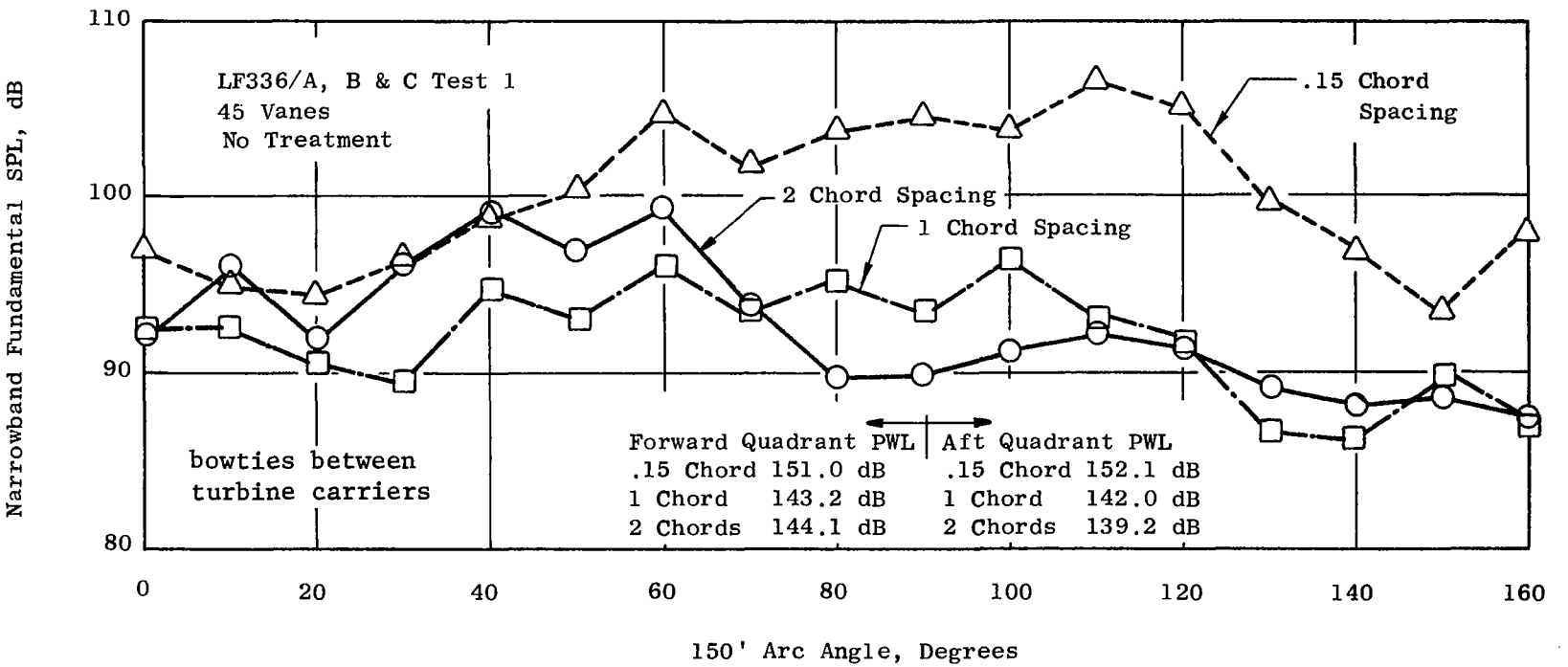

Figure 45. Effect of Spacing on Arc Fundamental SPL at 100% RPM

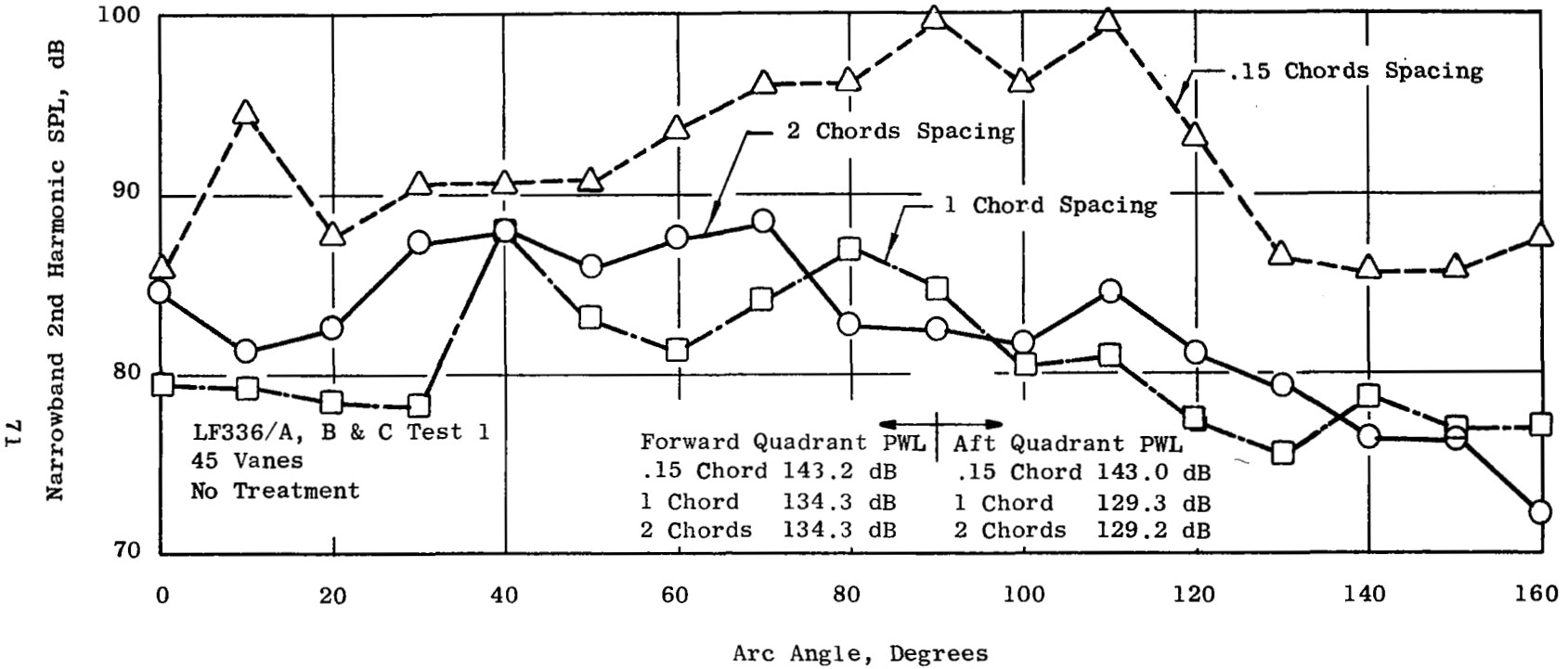

Figure 46. Effect of Spacing on Arc Second Harmonic SPL at 100% RPM

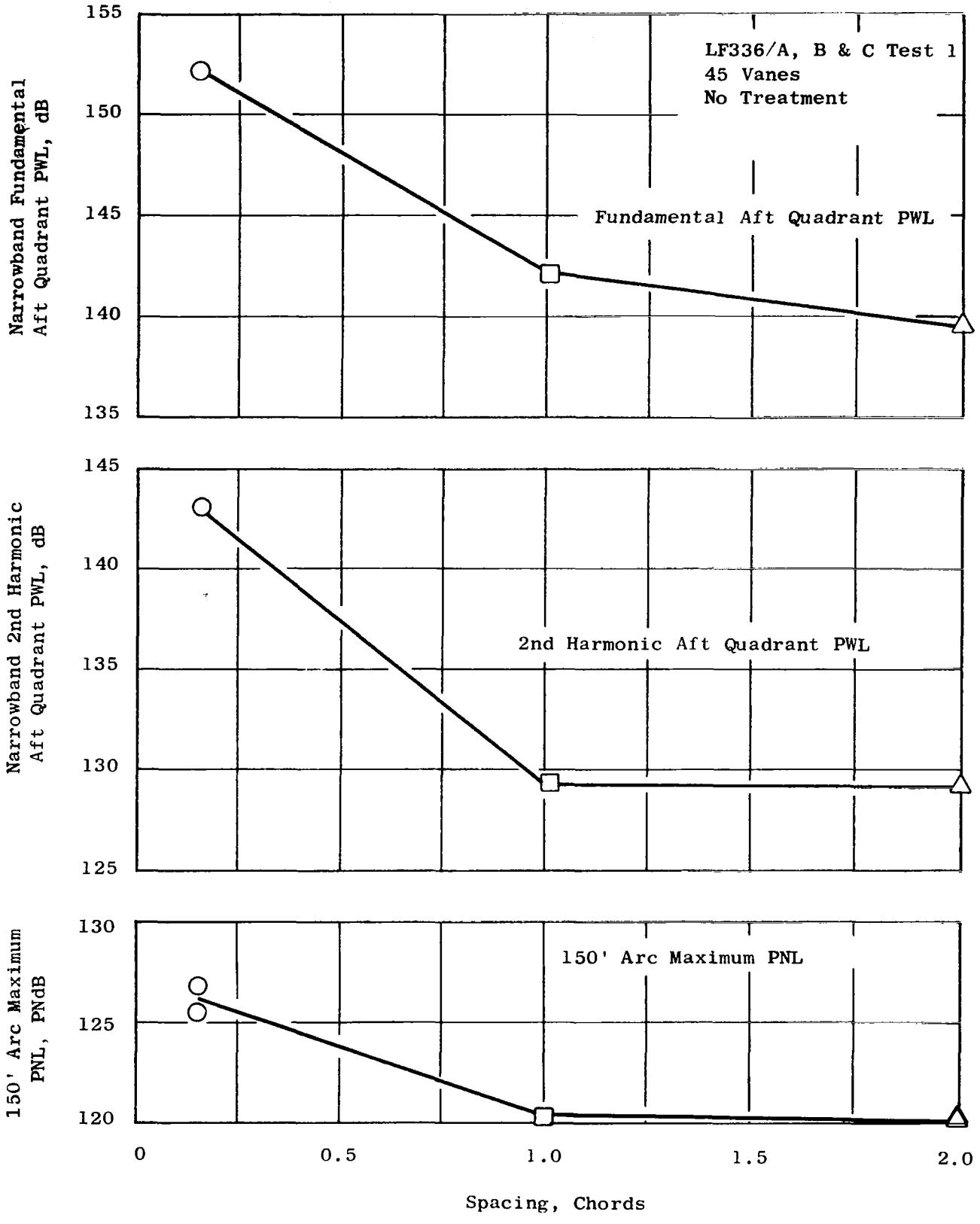

Figure 47. Effect of Spacing on PWL & PNL at 100% RPM

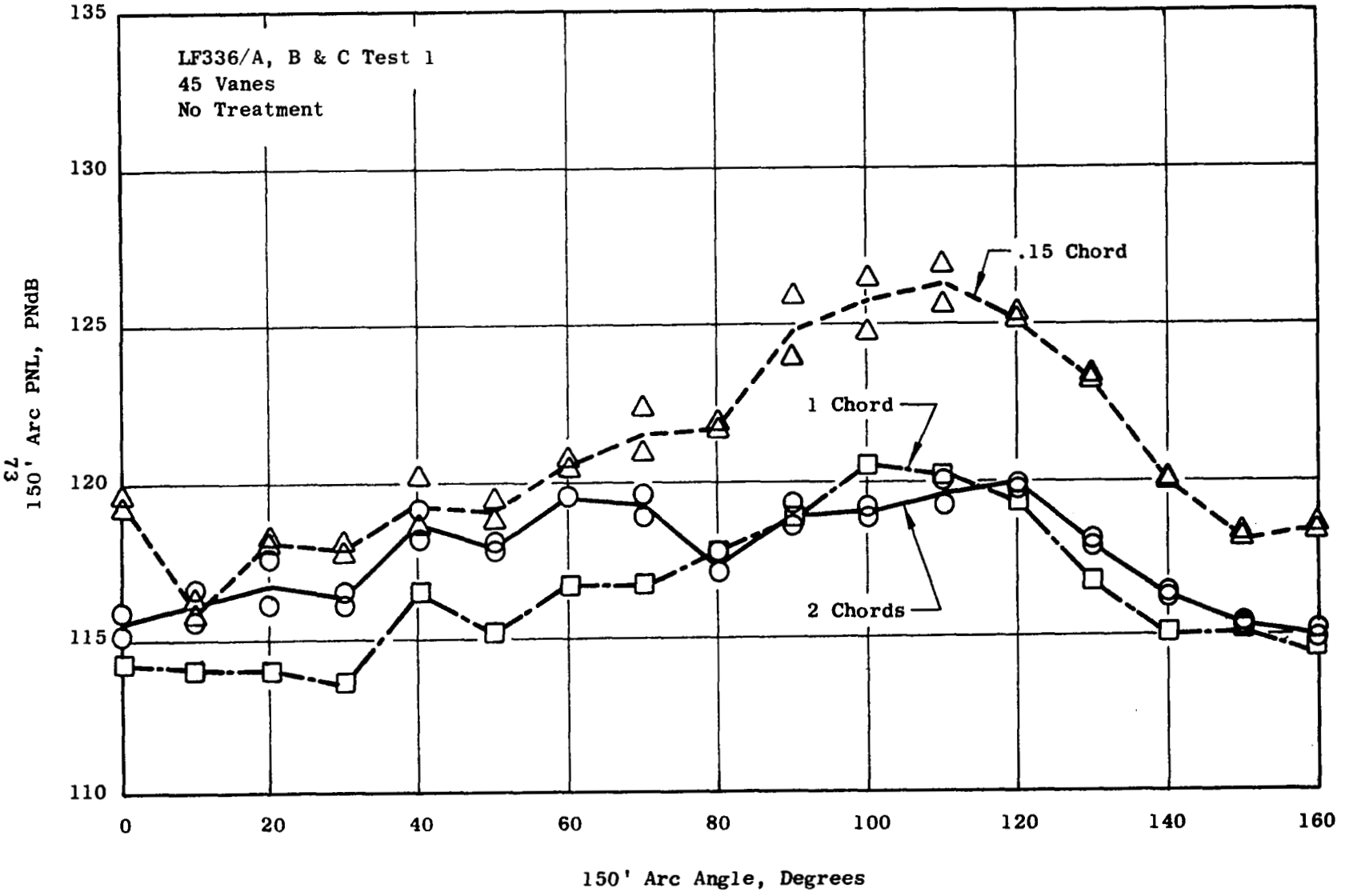

Figure 48. Effect of Spacing on 150' Arc PNL at 100% RPM

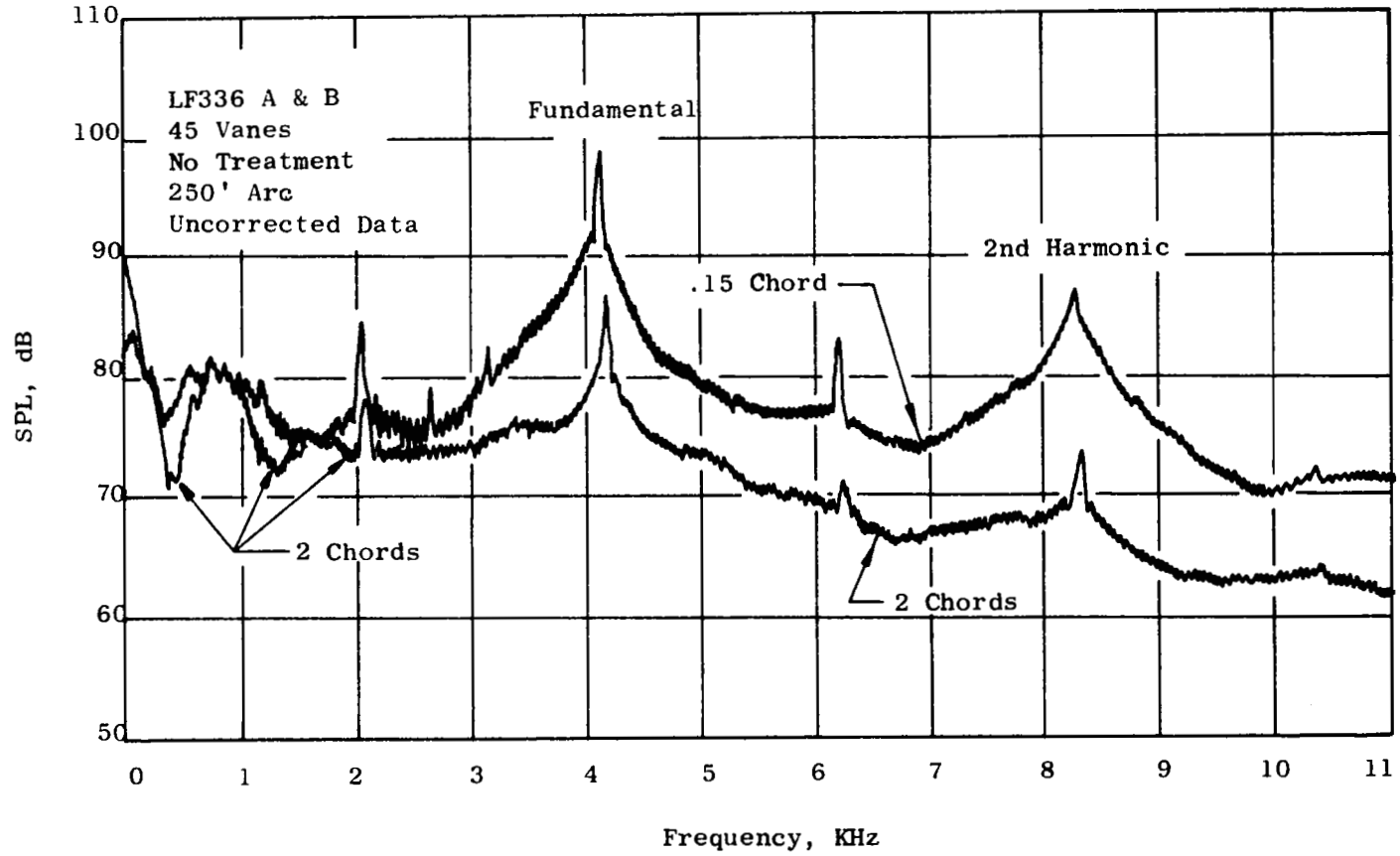

Figure 49. Effect of Spacing on SPL Spectrum at 110° Arc Angle at 100% RPM

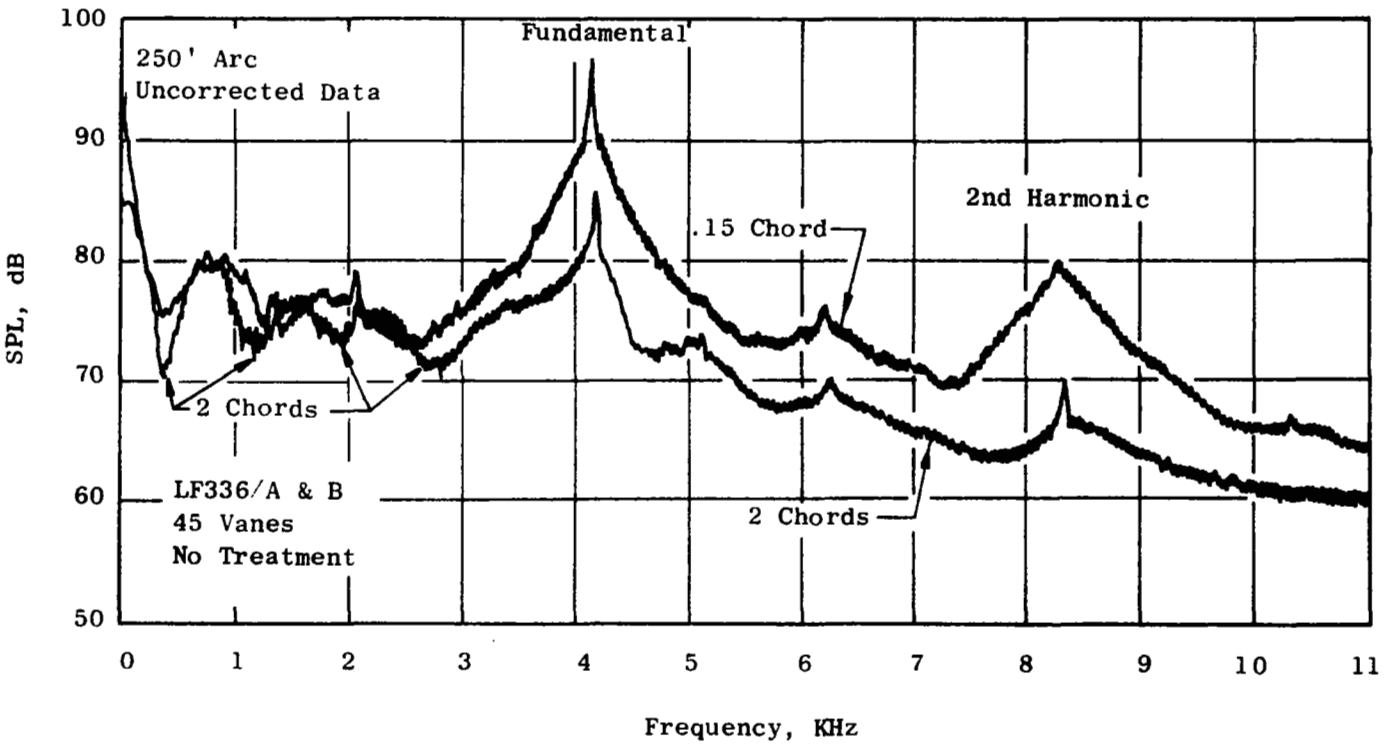

Figure 50. Effect of Spacing on SPL Spectrum at 120° Arc Angle at 100% RPM

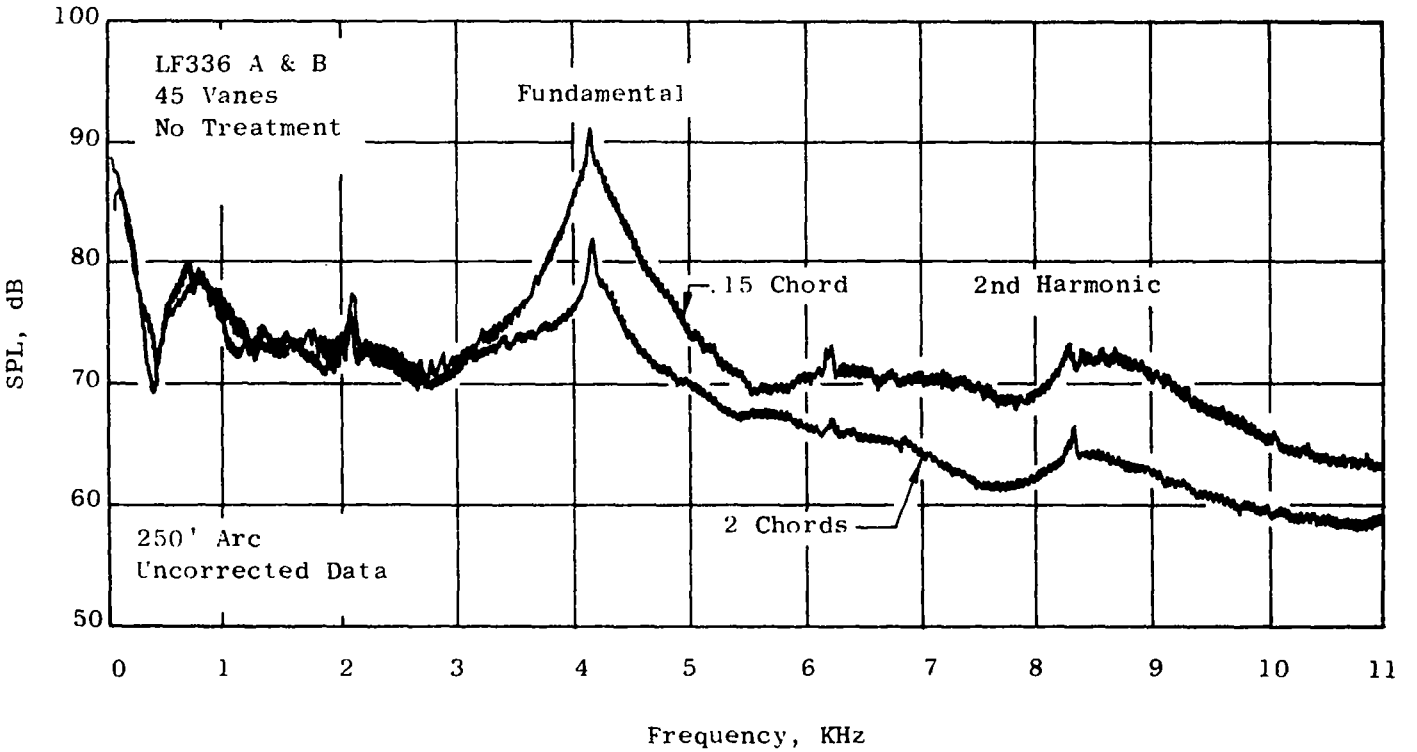

Figure 51. Effect of Spacing on SPL Spectrum at 130° Arc Angle at 100% RPM

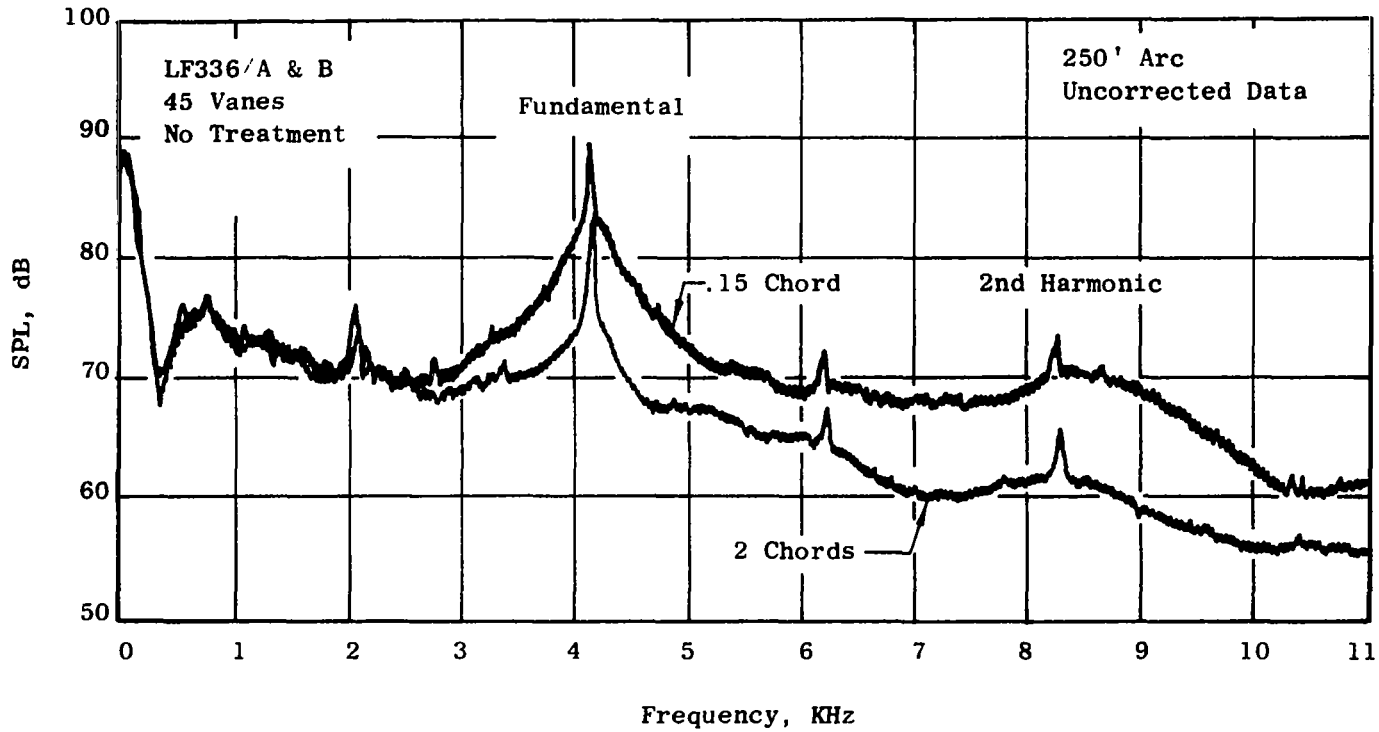

Figure 52. Effect of Spacing on SPL Spectrum at 140° Arc Angle at 100% RPM

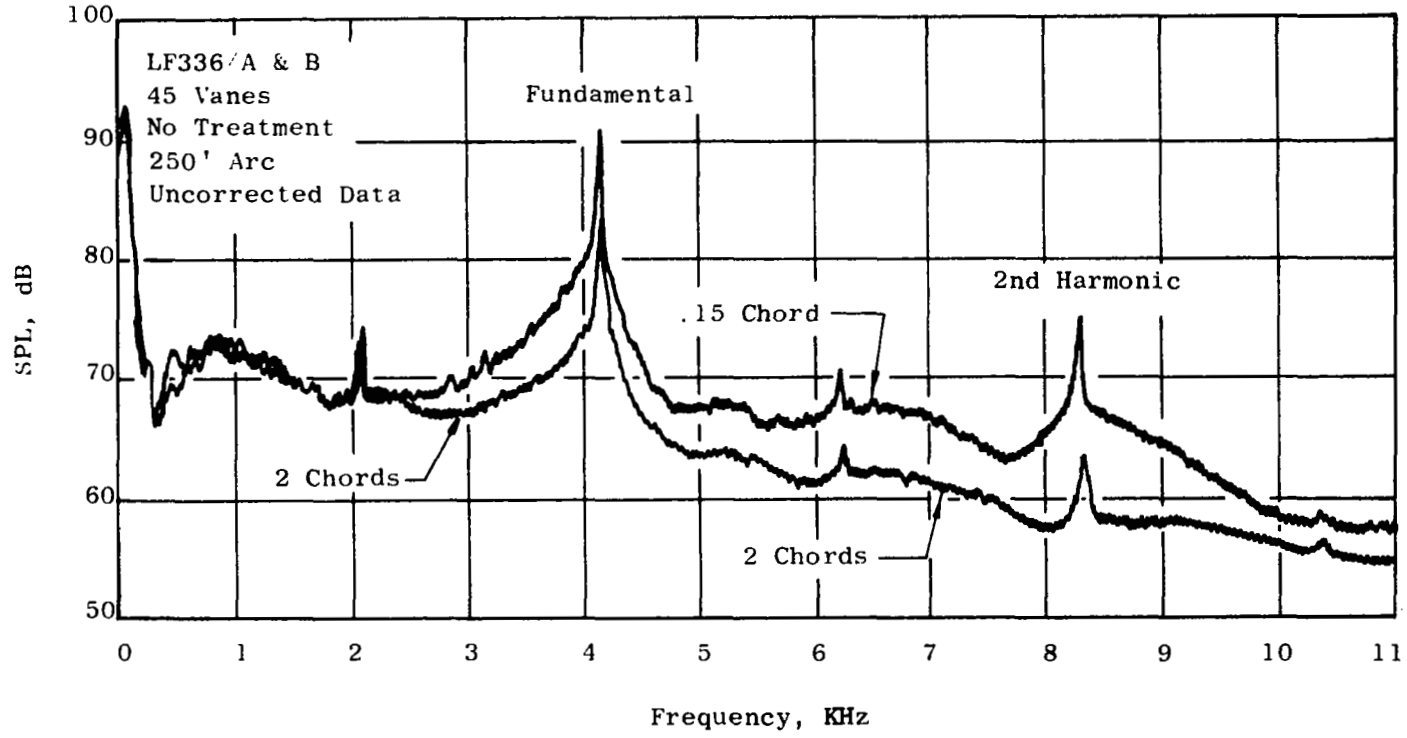

Figure 53. Effect of Spacing on SPL Spectrum at 160° Arc Angle at 100% RPM

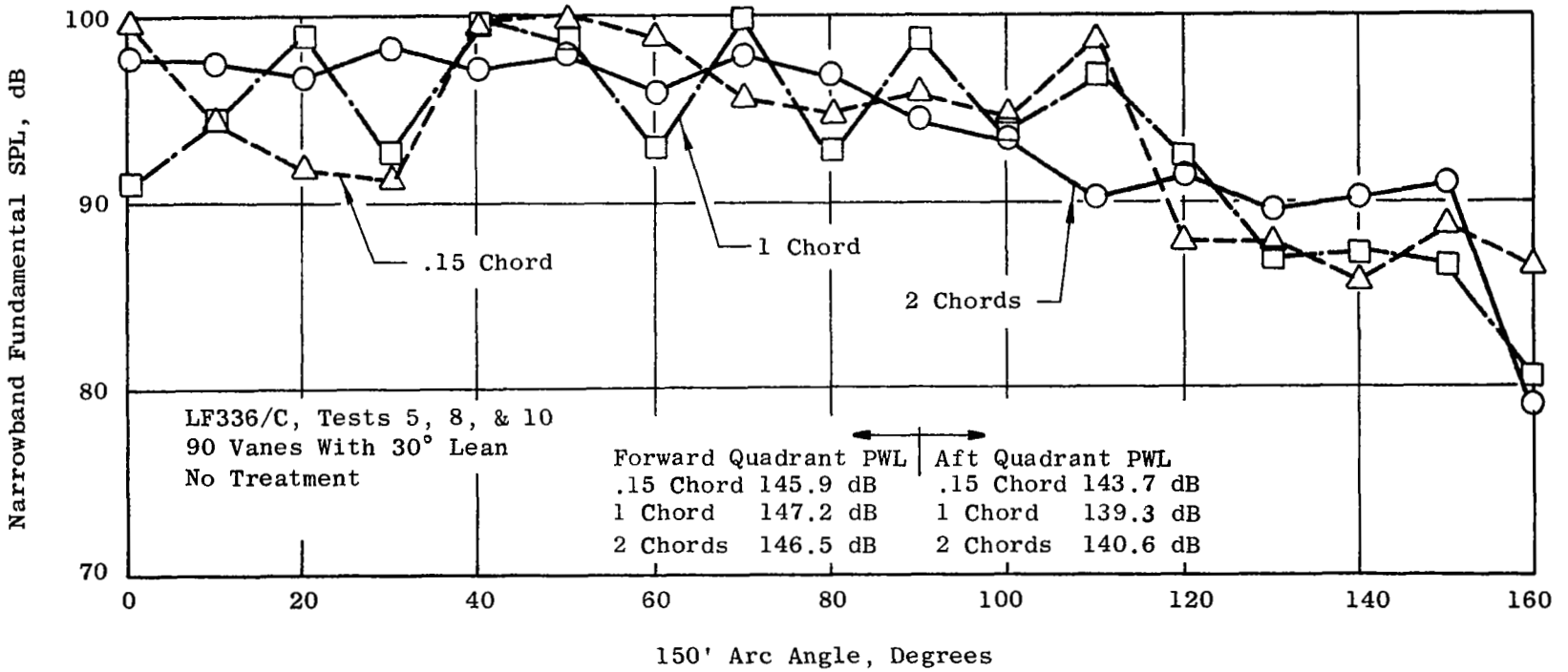

Figure 54. Effect of Spacing on Arc Fundamental SPL at 95% RPM

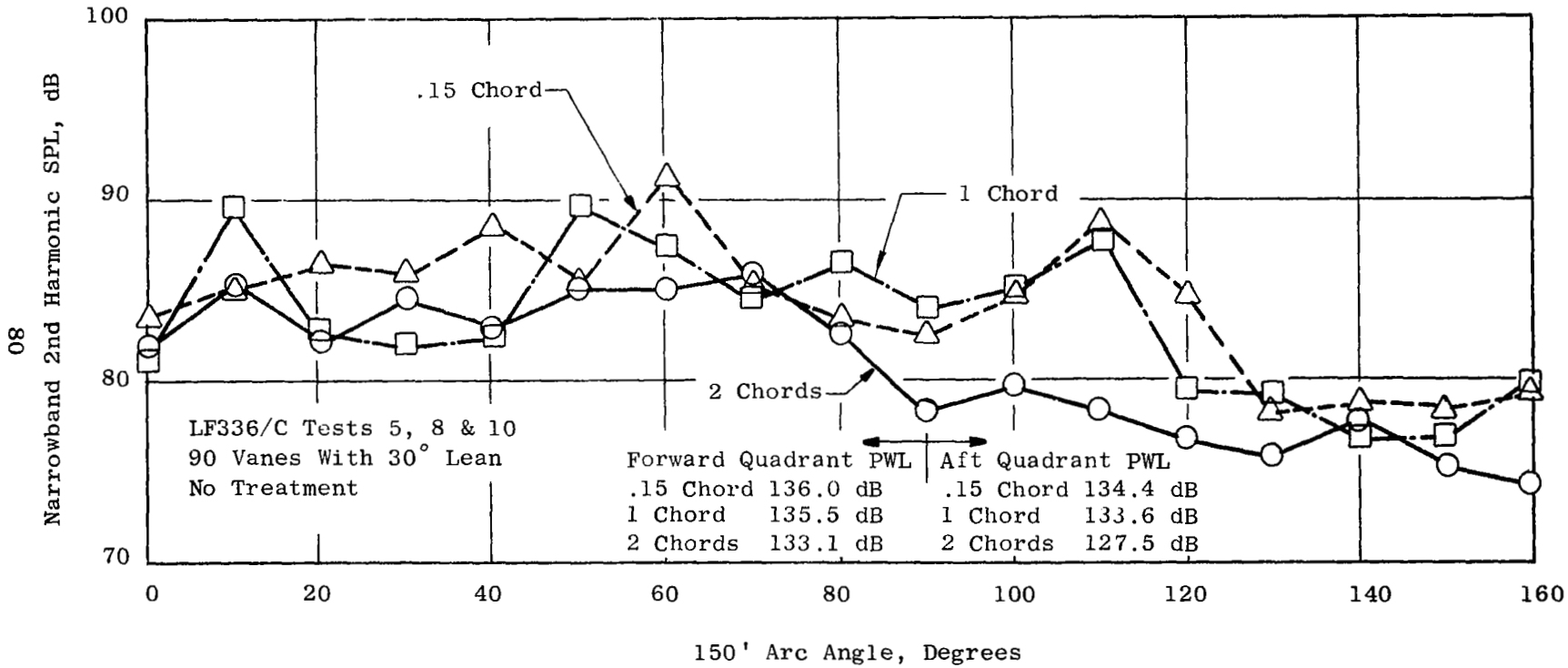

Figure 55. Effect of Spacing on Arc Second Harmonic SPL at 95% RPM

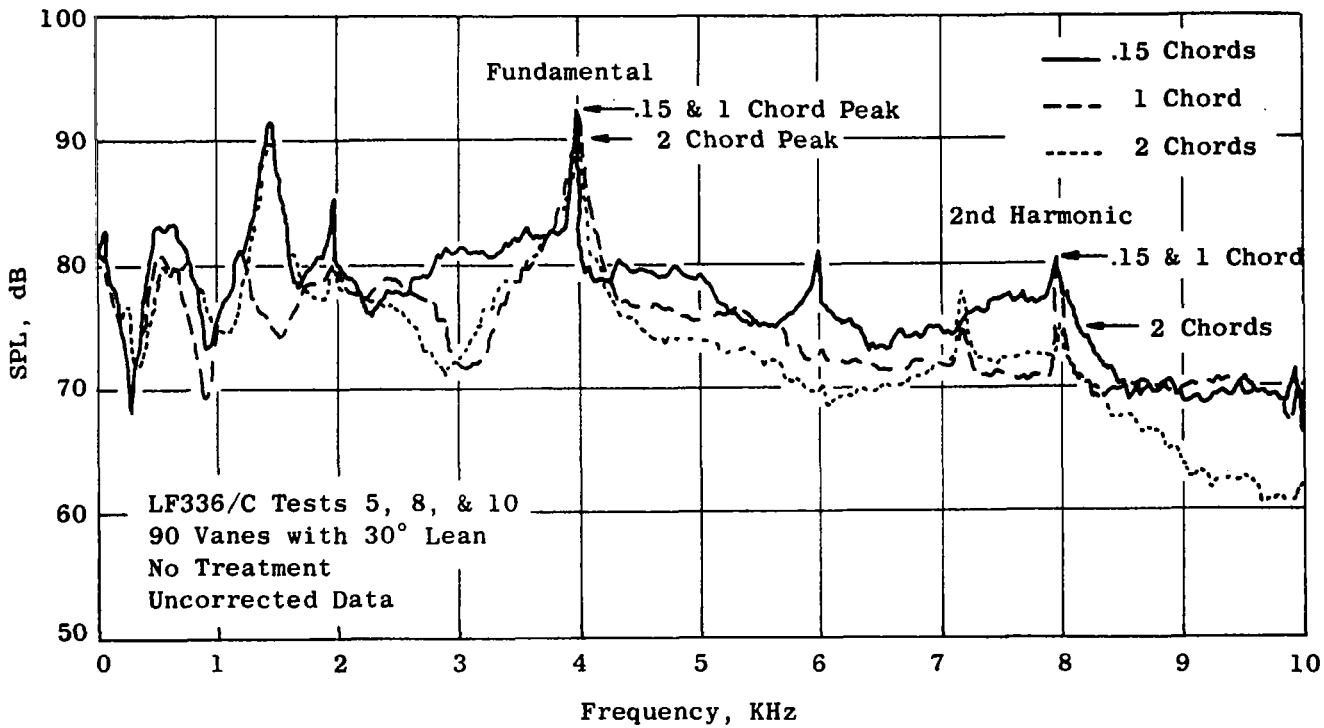

Figure 56. Effect of Spacing on SPL Spectrum at 100° Arc Angle at 95% RPM.

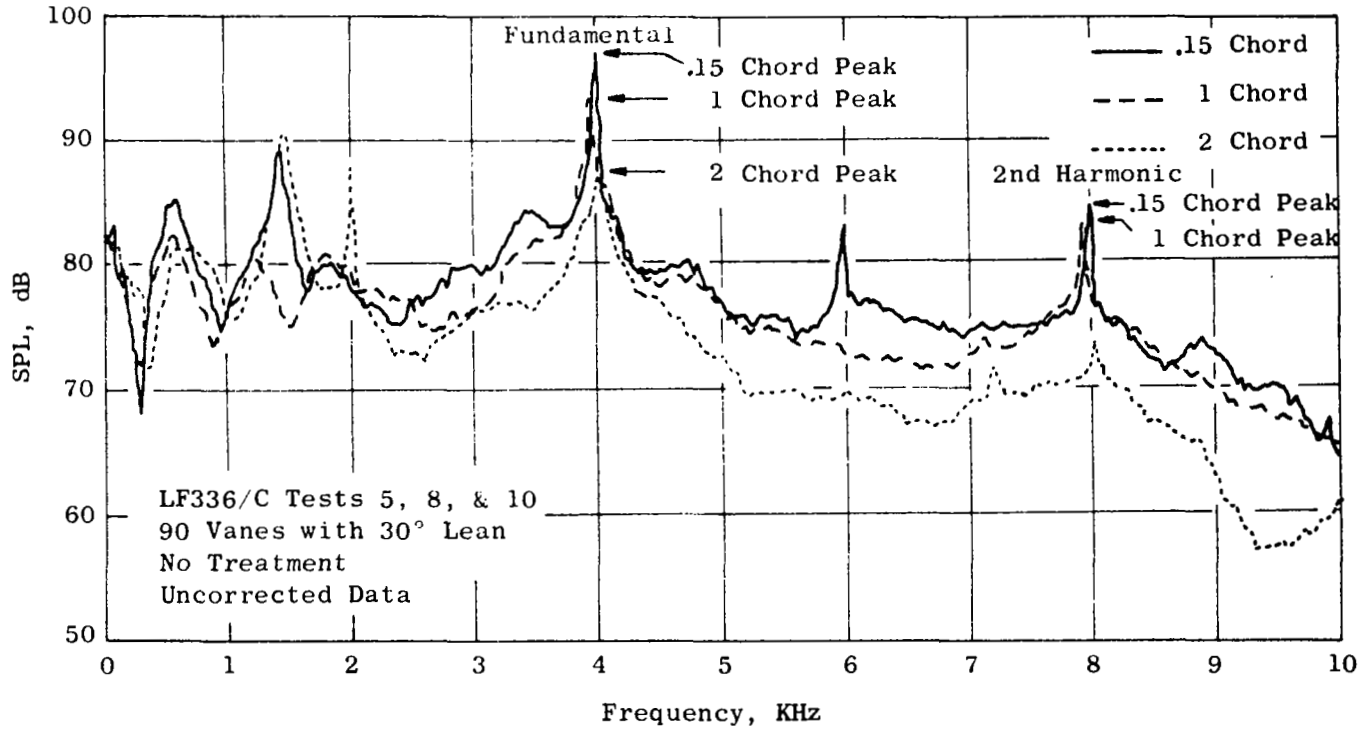

Figure 57. Effect of Spacing on SPL Spectrum at 110° Arc Angle at 95% RPM.

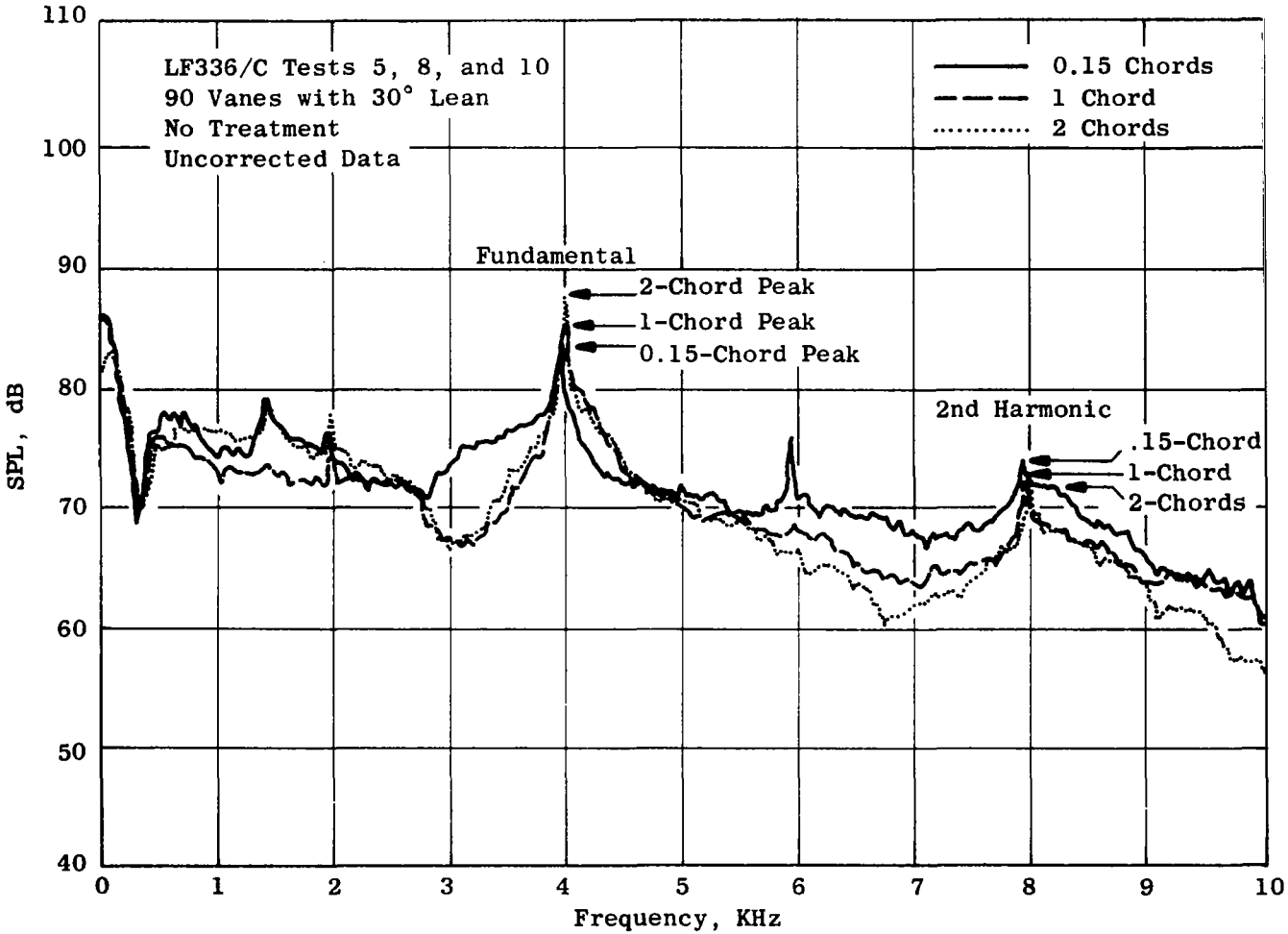

Figure 58. Effect on Spacing on SPL Spectrum at 140° Arc Angle at 95% RPM.

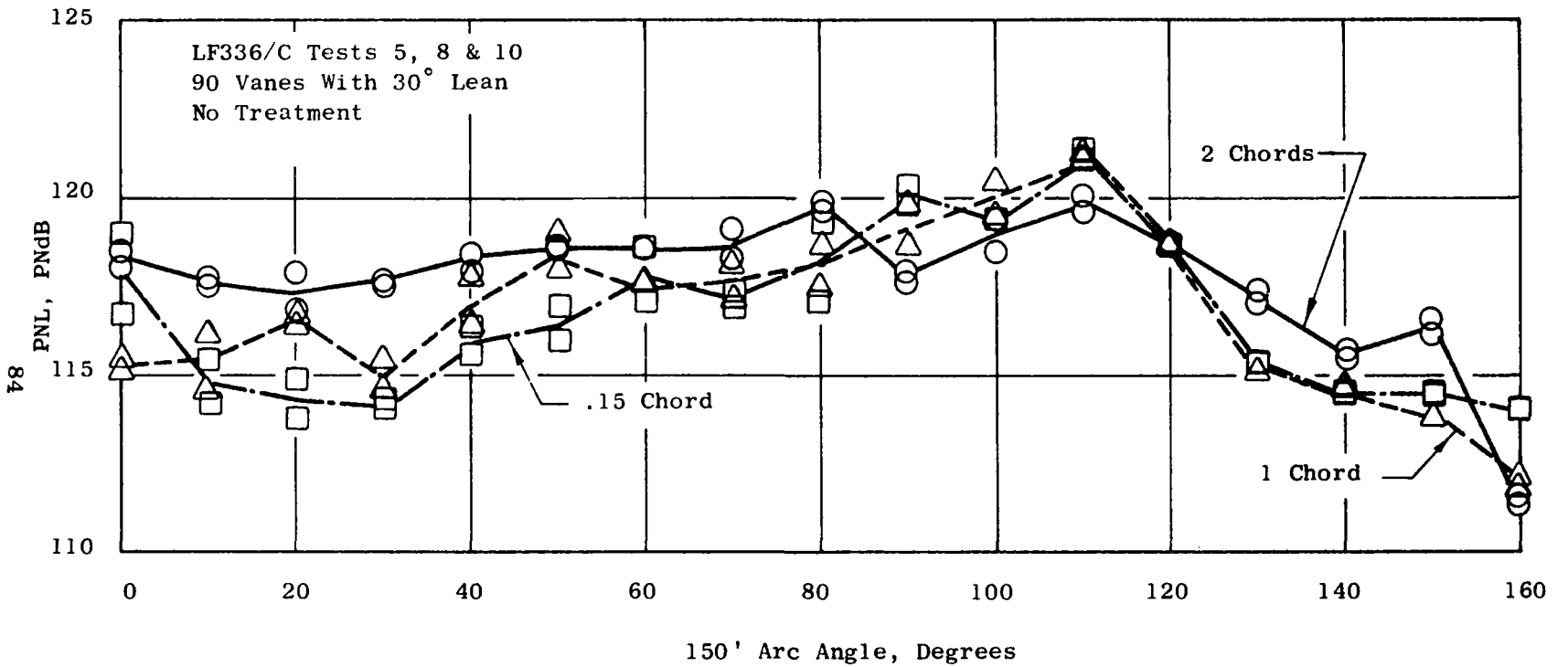

Figure 59. Effect of Spacing on Arc PNL at 95% RPM

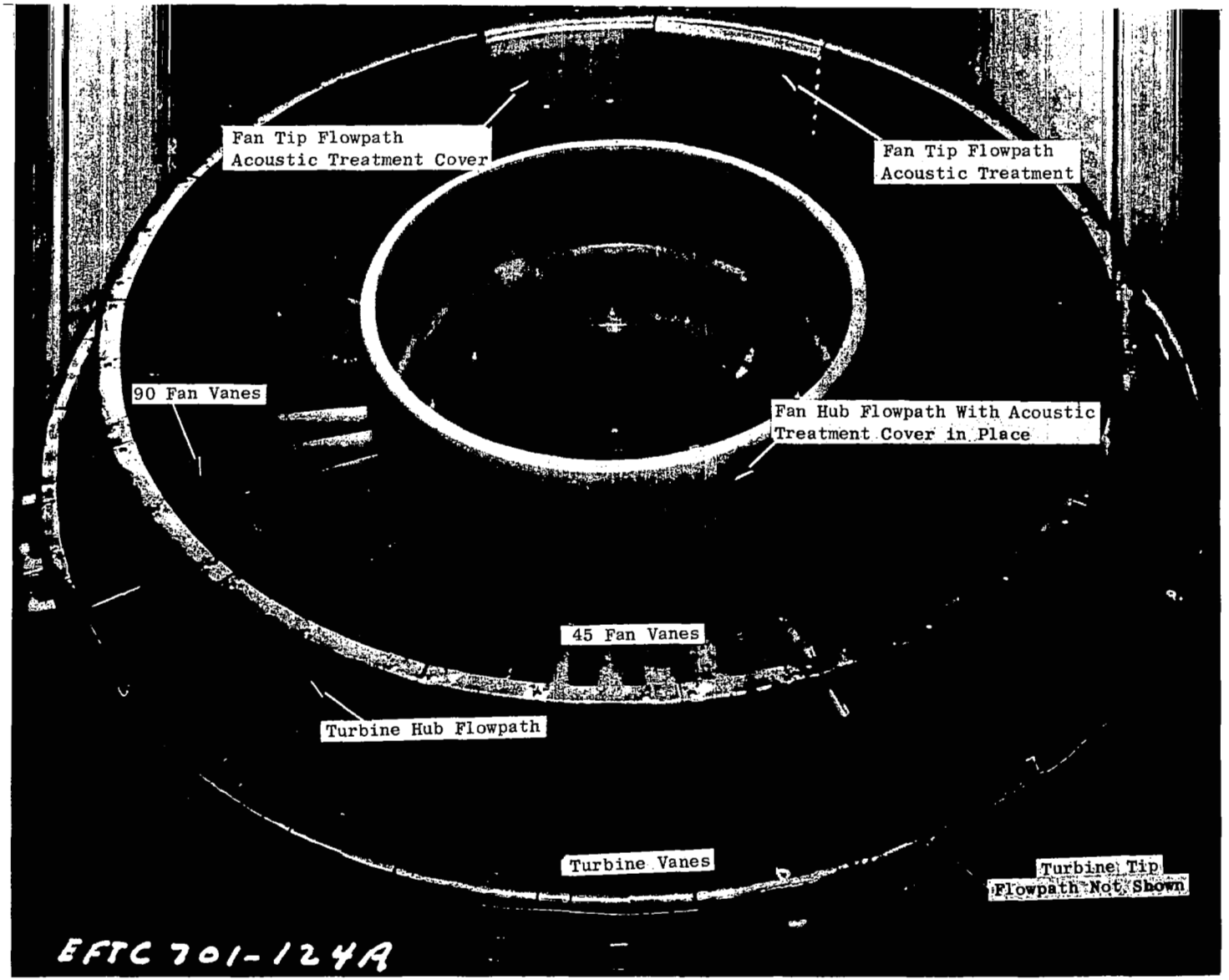

Figure 60. Two-Chords Spacing Hardware With Acoustic Treatment

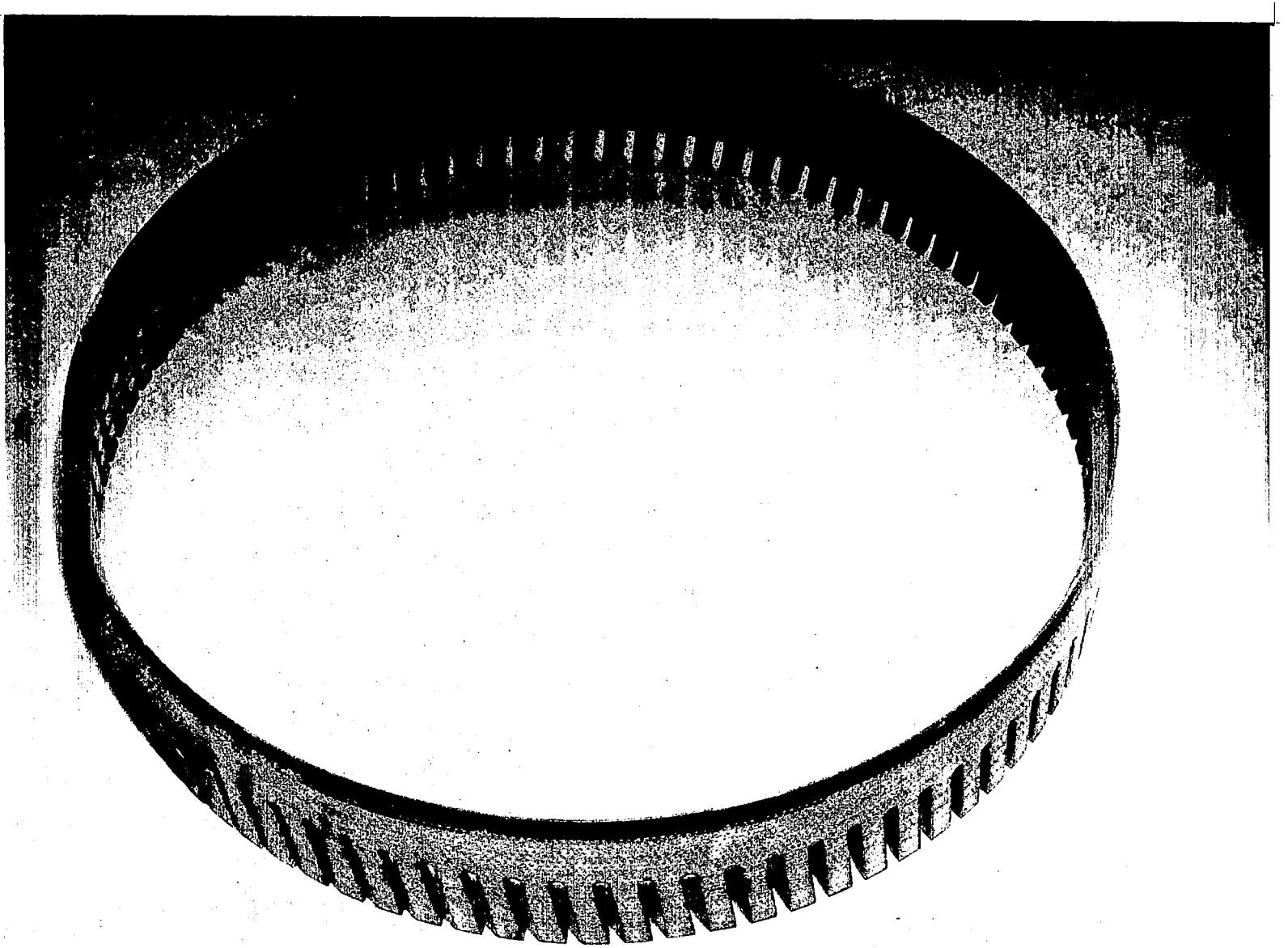

Figure 61. Acoustic Splitter

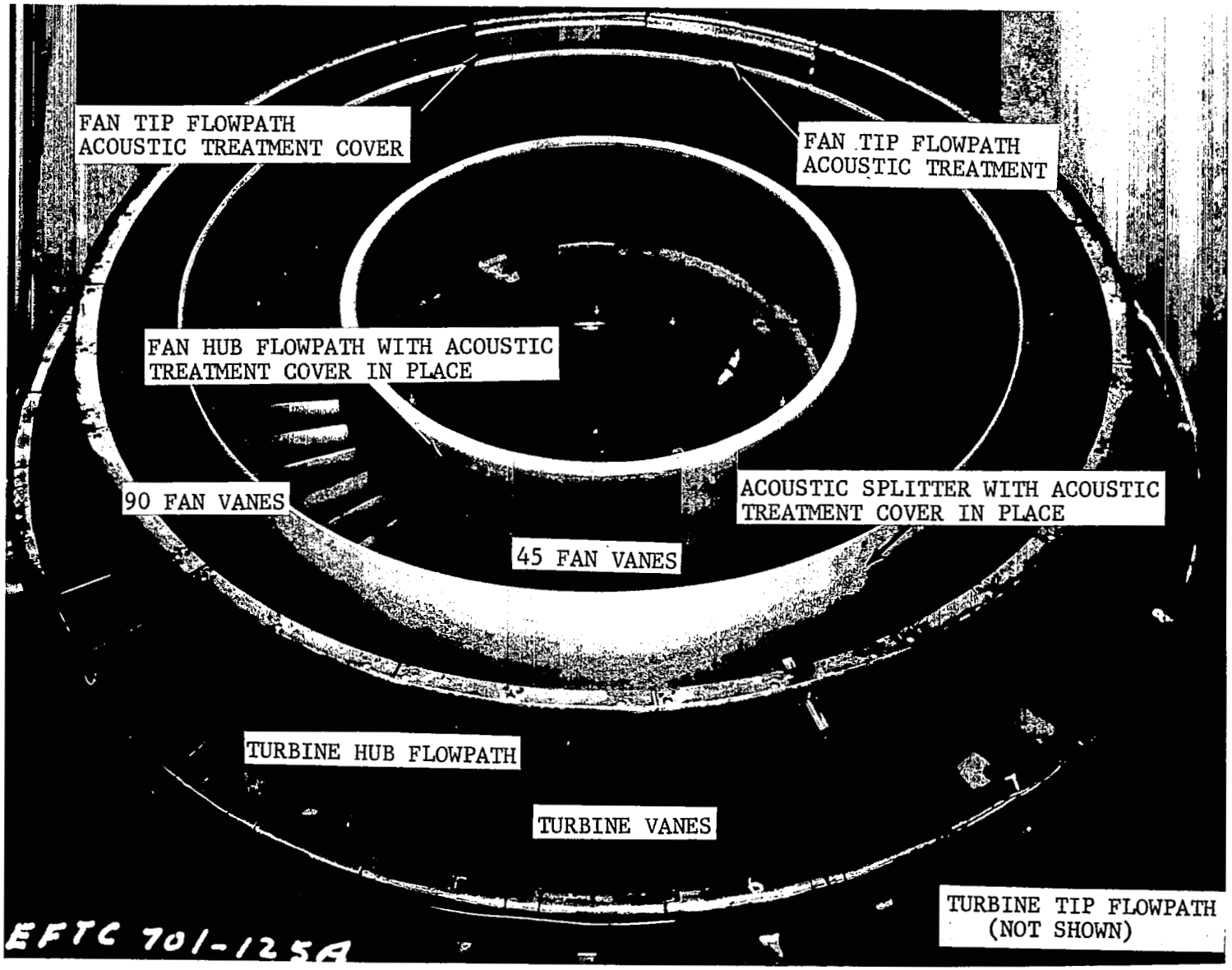

Figure 62. Acoustic Splitter Installed

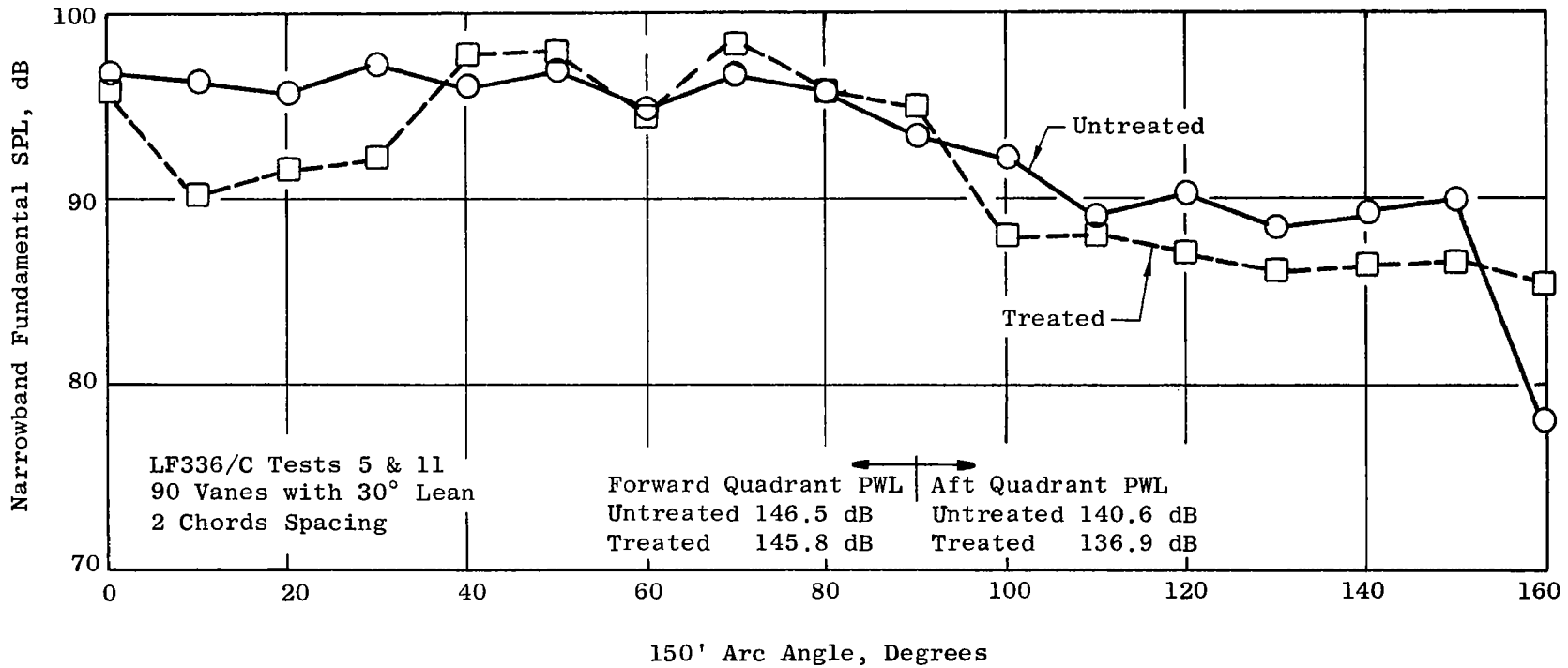

Figure 63. Effect of Treatment on Arc Fundamental SPL at 95% RPM

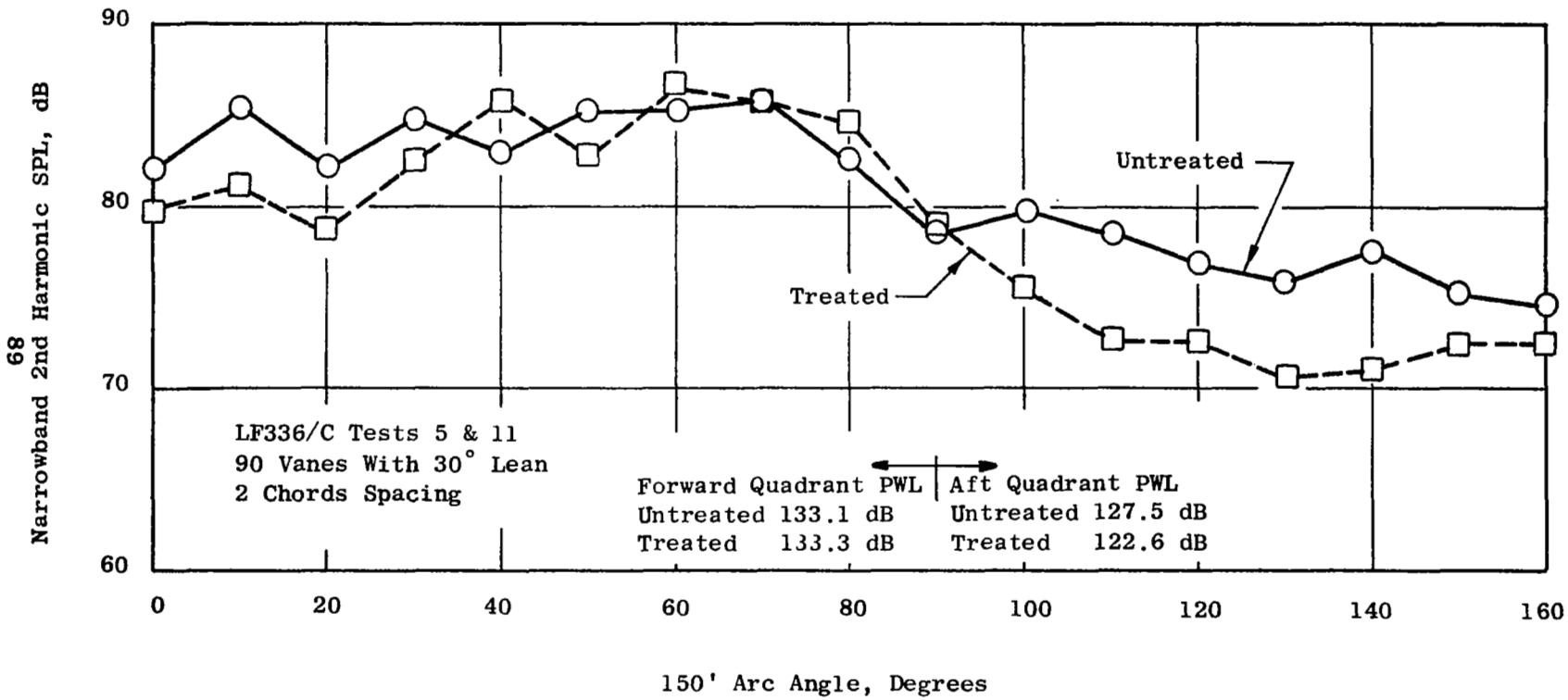

Figure 64. Effect of Treatment on Arc Second Harmonic SPL at 95% RPM

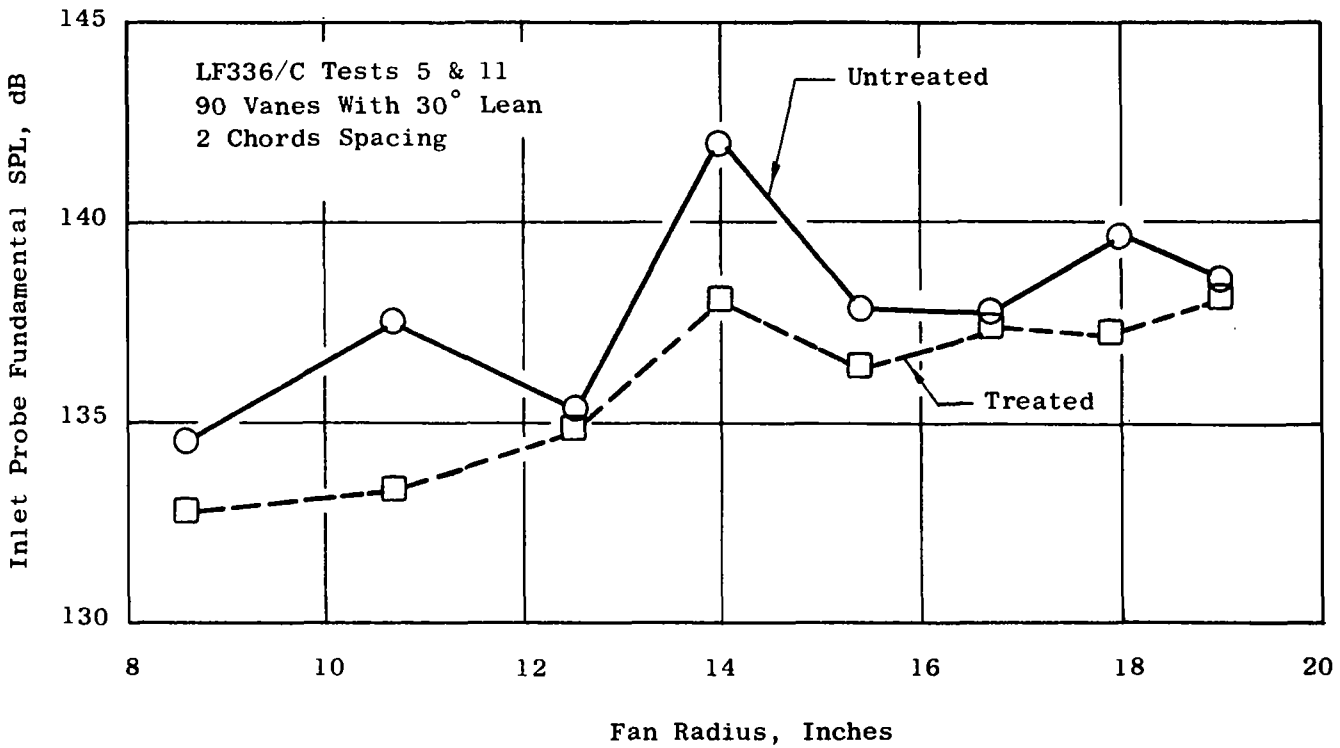

Figure 65 . Effect of Treatment on Inlet Probe Fundamental SPL at 95% RPM

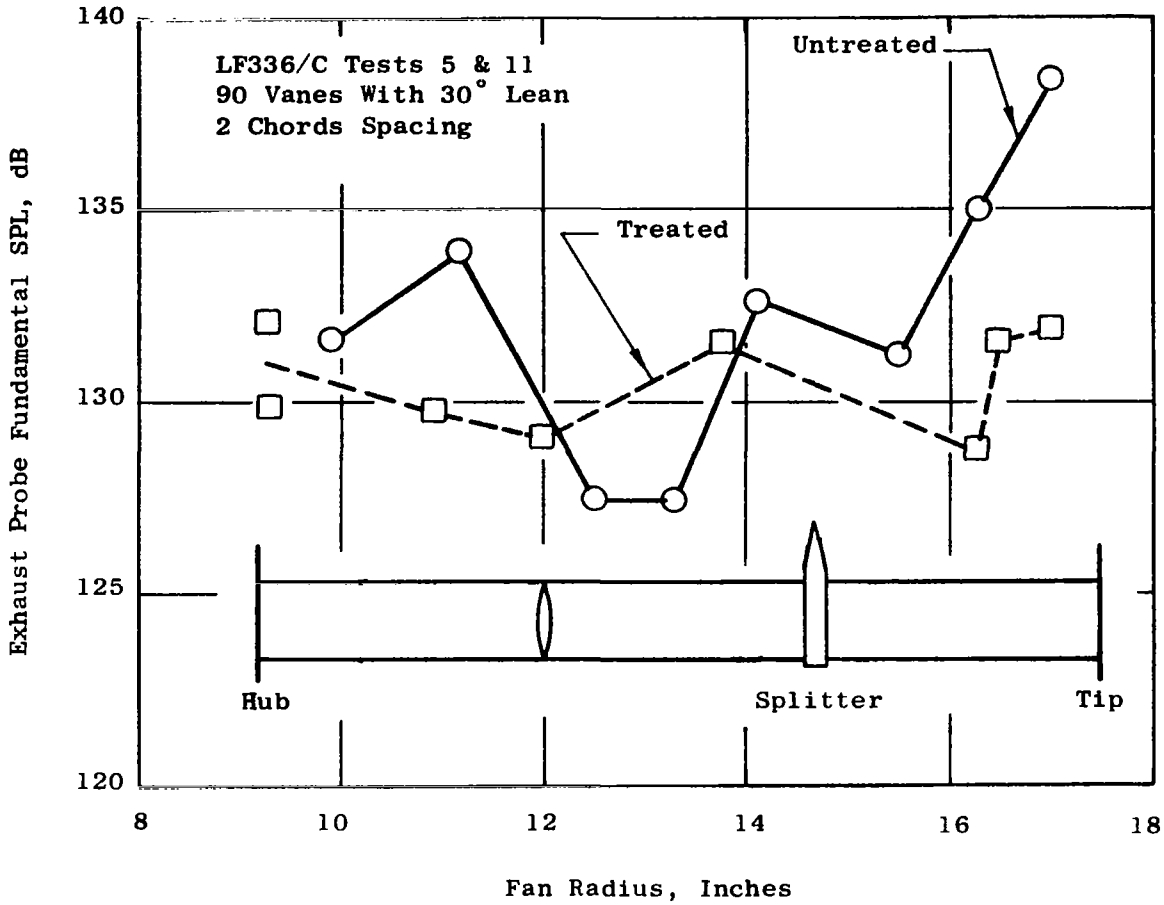

Figure 66. Effect of Treatment on Exhaust Probe Fundamental SPL at 95% RPM

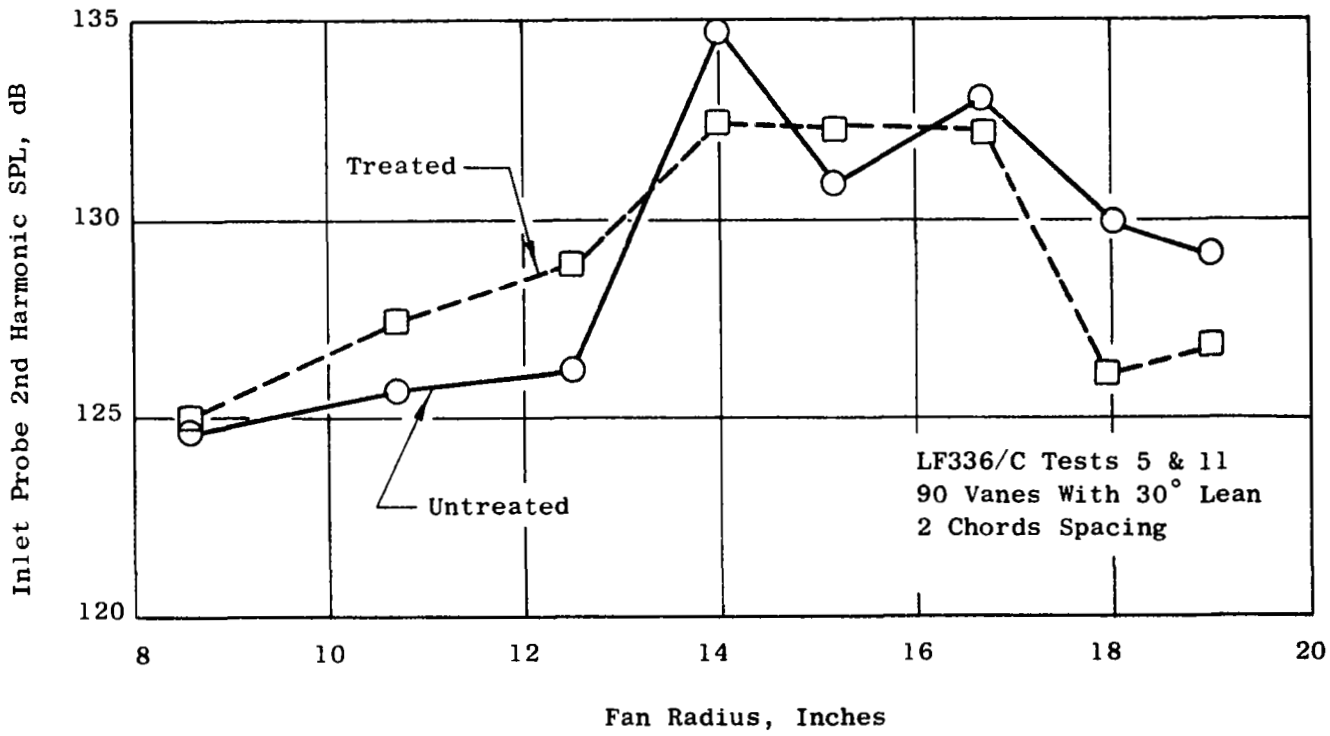

Figure 67. Effect of Treatment on Inlet Probe Second Harmonic SPL at 95% RPM

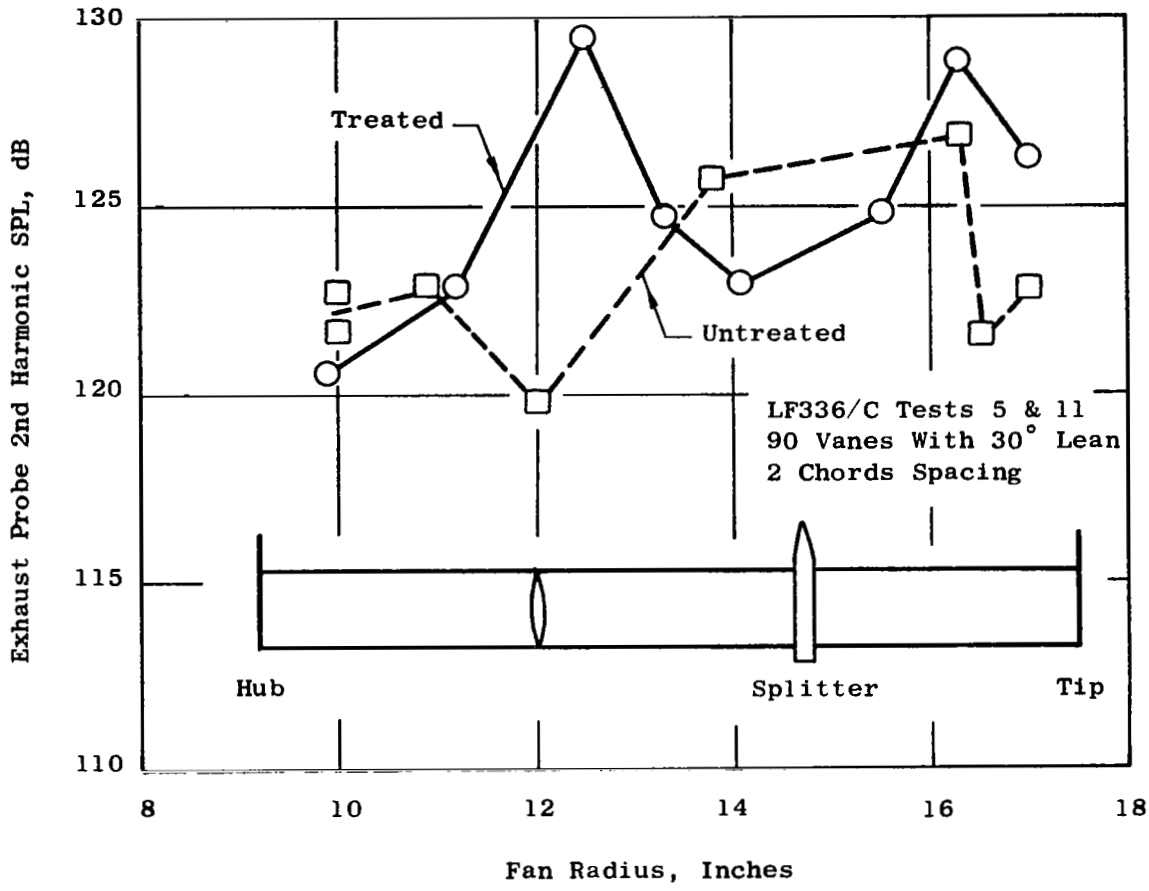

Figure 68. Effect of Treatment on Exhaust Probe Second Harmonic SPL at 95% RPM

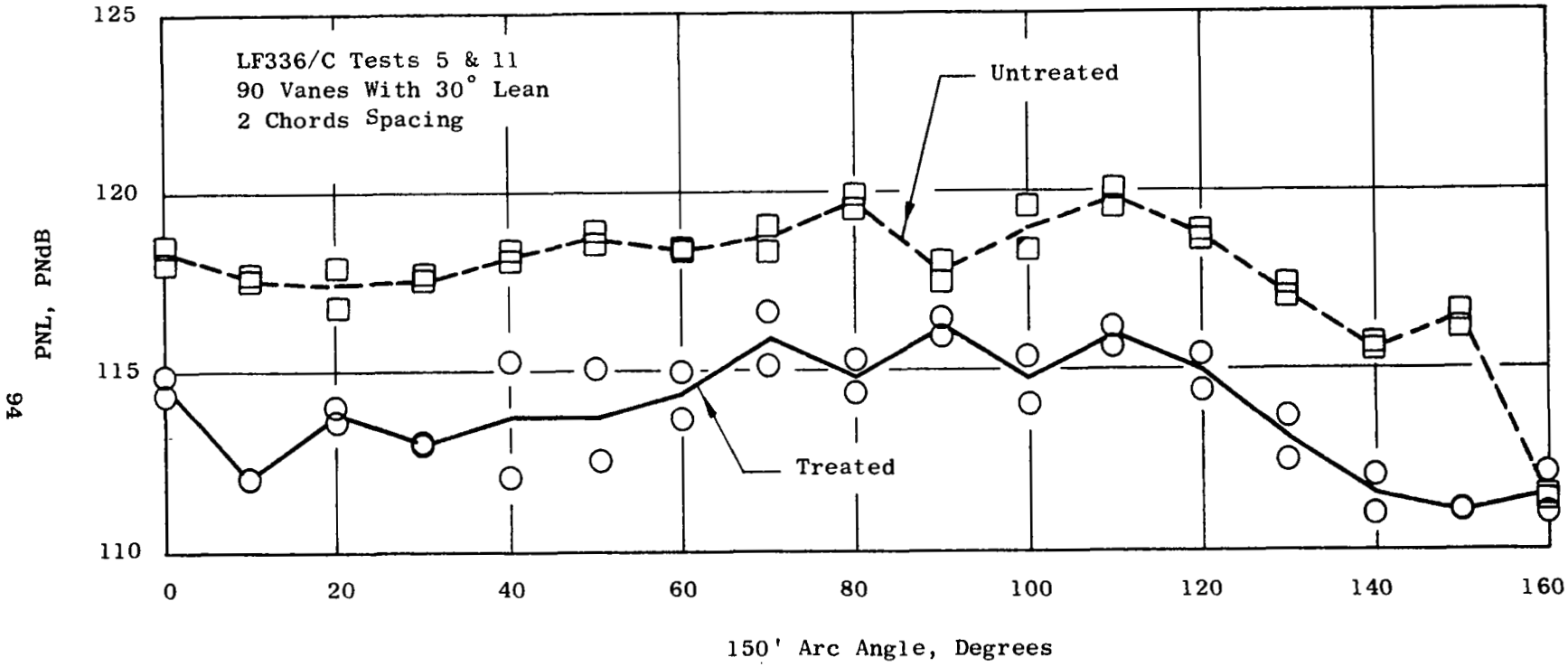

Figure 69. Effect of Treatment on Arc PNL at 95% RPM

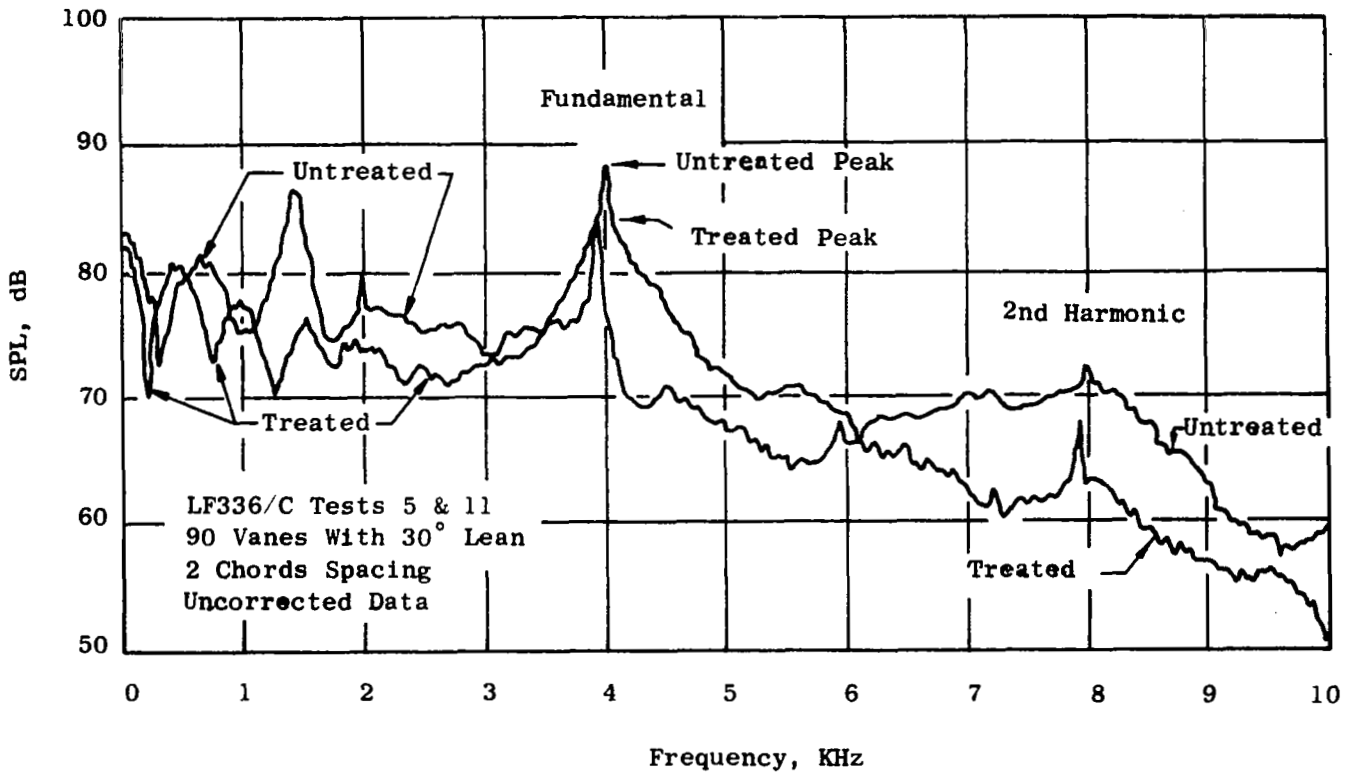

Figure 70. Effect of Treatment on SPL Spectrum at 120° Arc Angle at 95% RPM

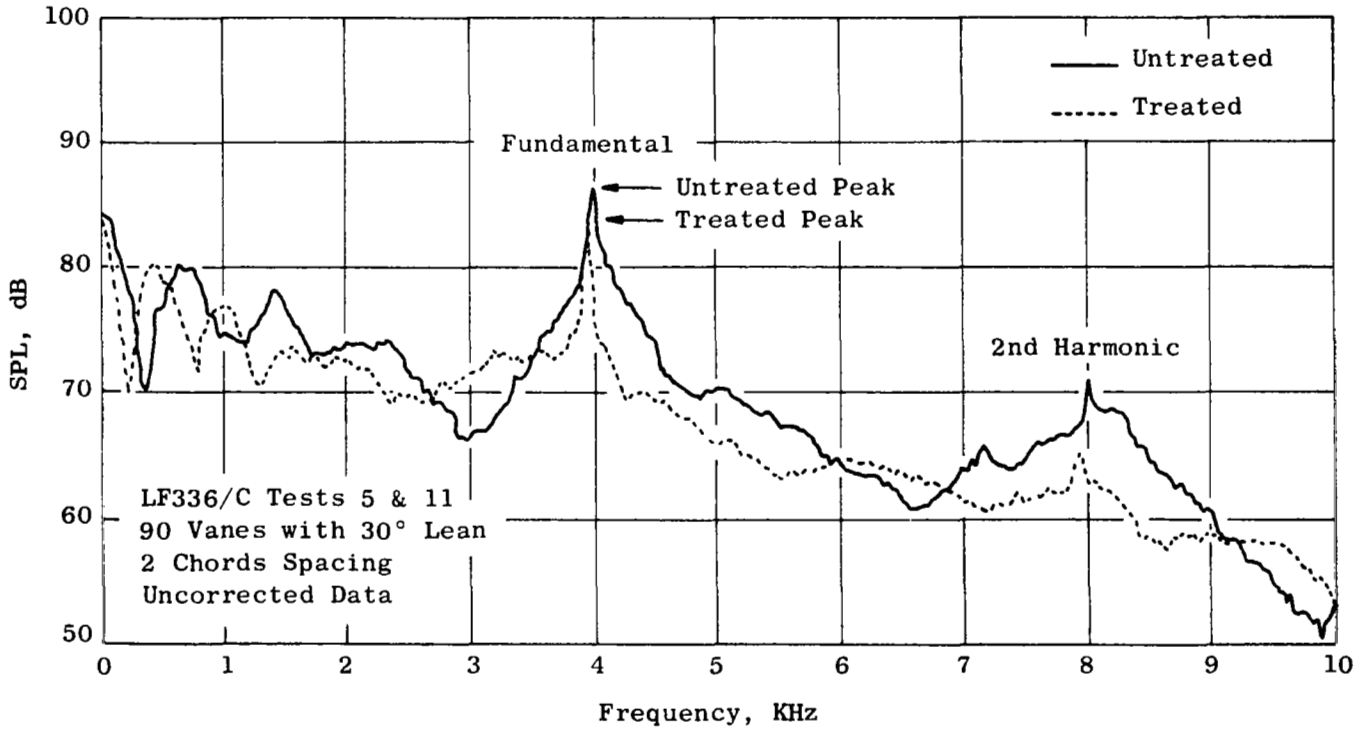

Figure 71. Effect of Treatment on SPL Spectrum at 130° Arc Angle at 95% RPM.

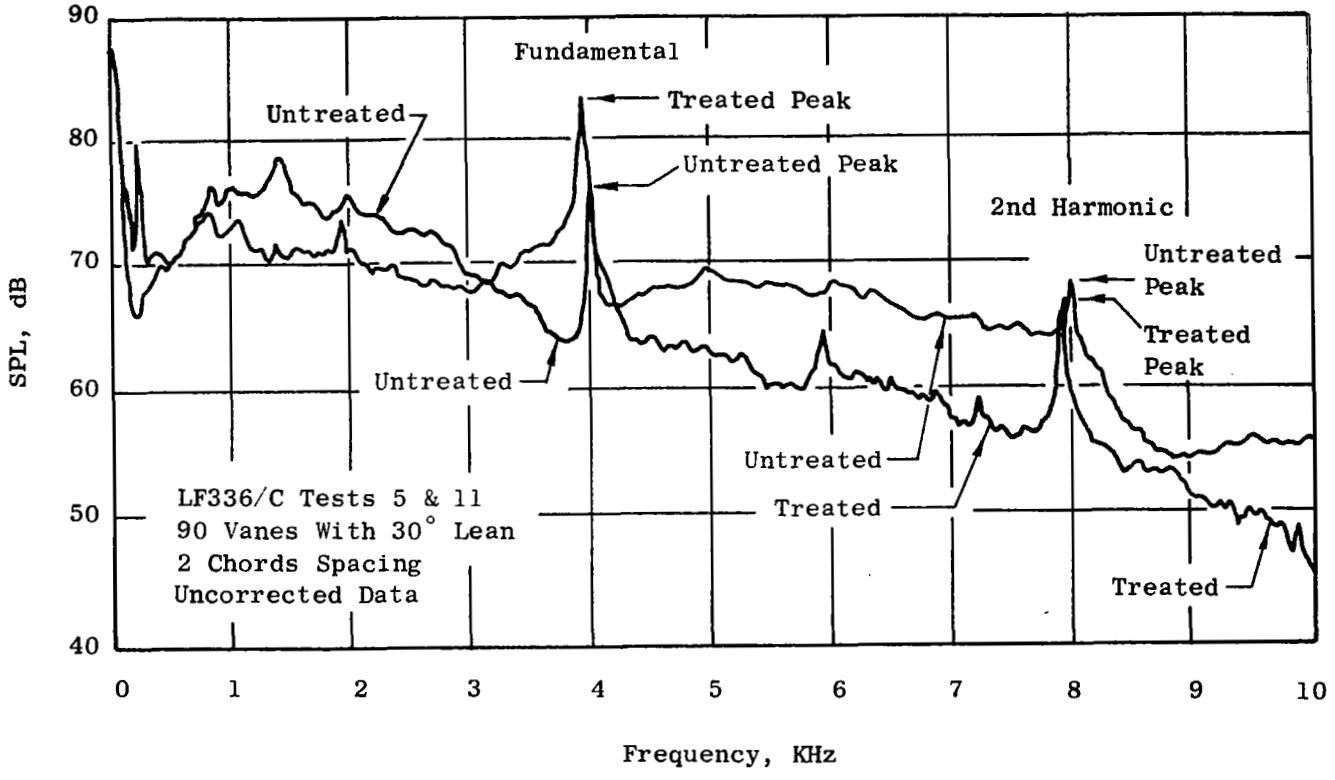

Figure 72. Effect of Treatment on SPL Spectrum at 160° Arc Angle at 95% RPM

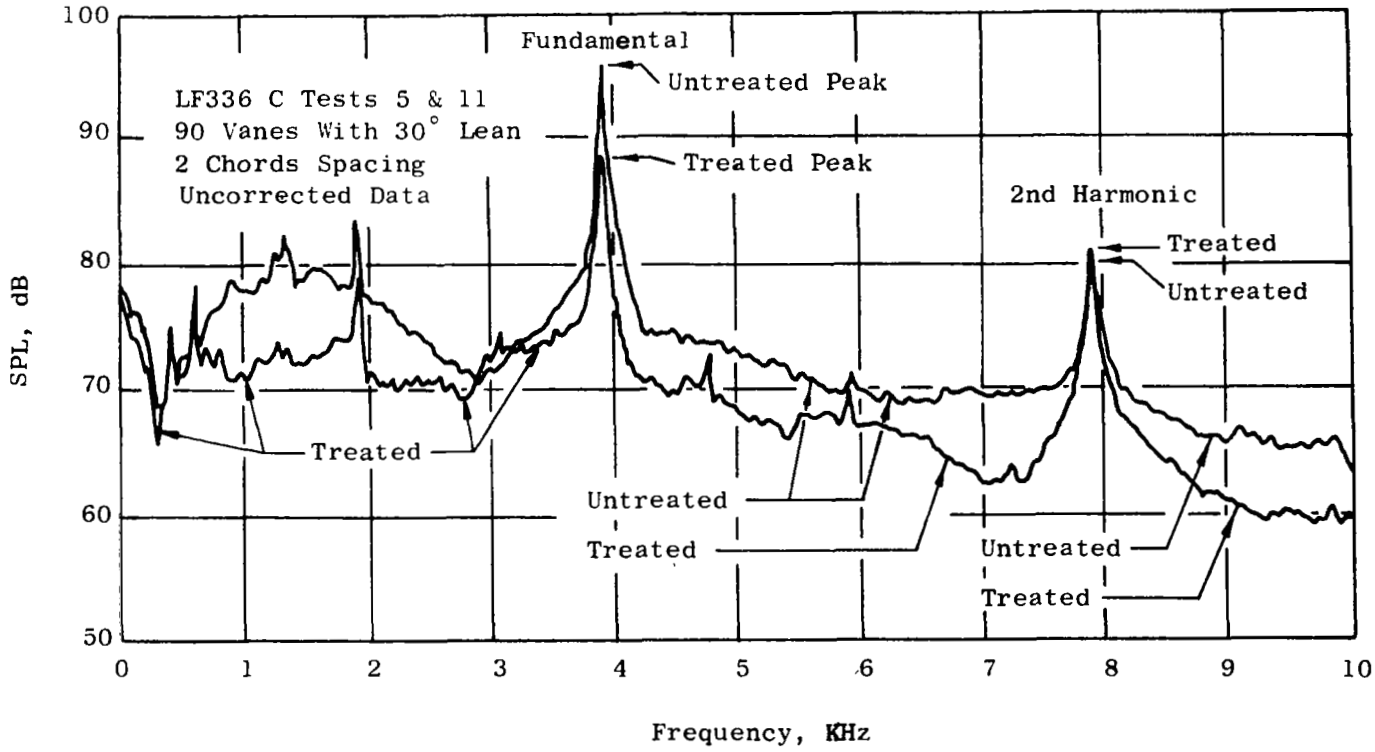

Figure 73. Effect of Treatment on SPL Spectrum at 60° Arc Angle at 95% RPM

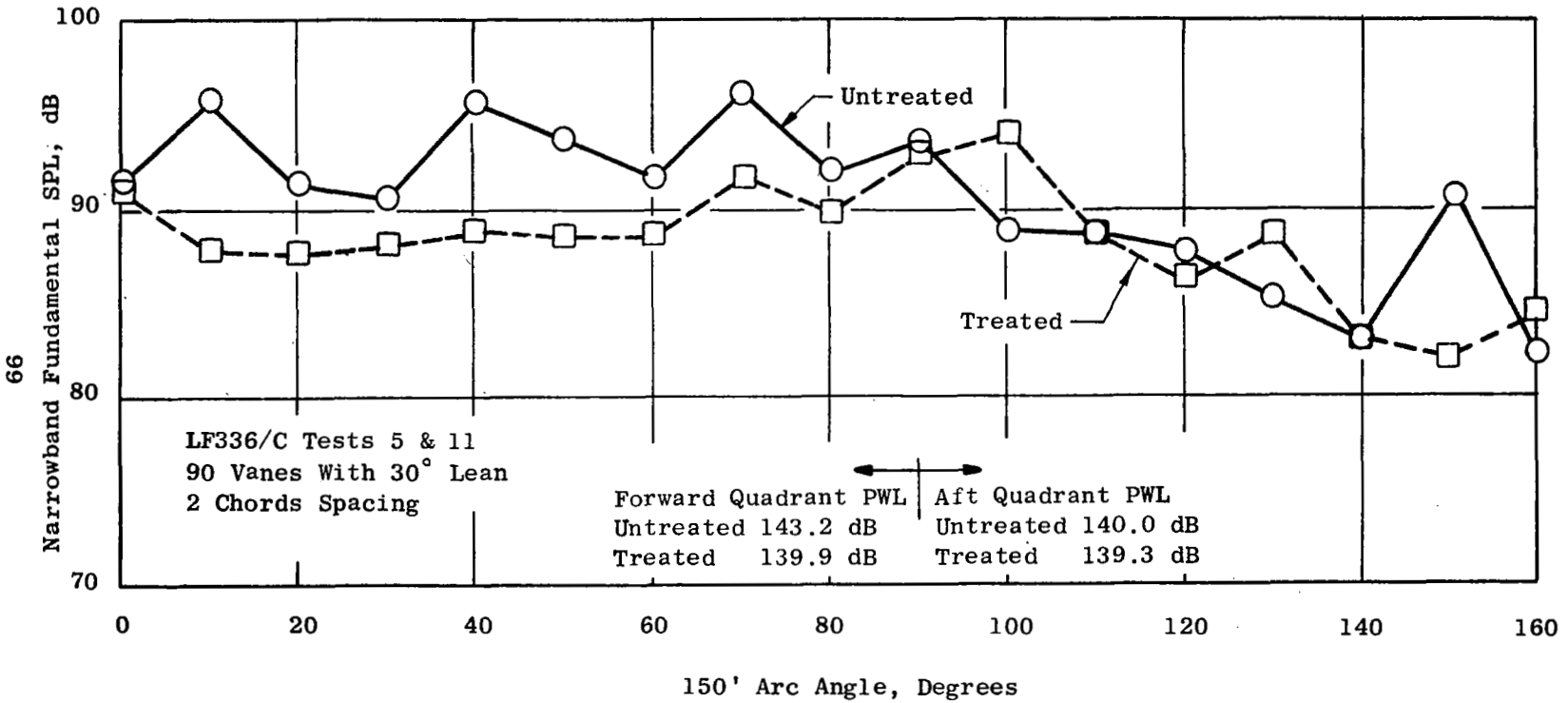

Figure 74. Effect of Treatment on Arc Fundamental SPL at 80% RPM

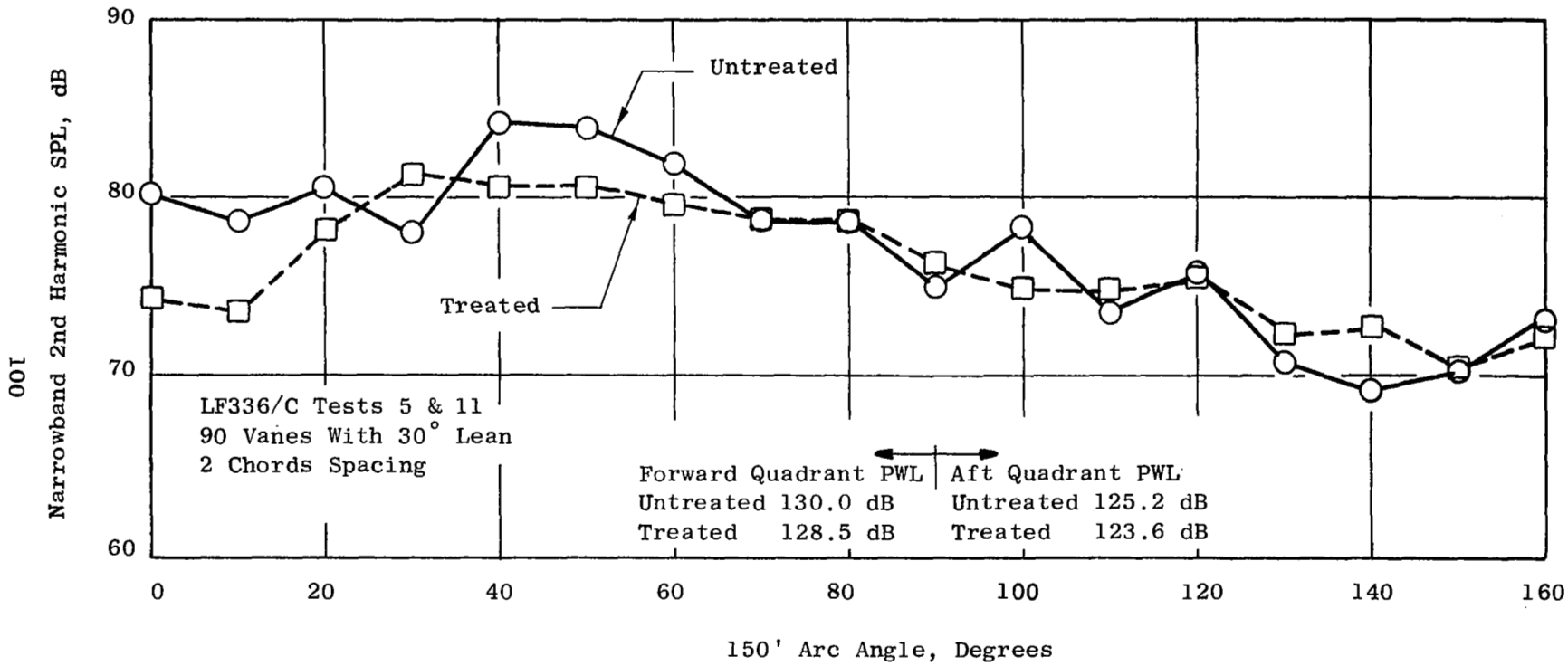

Figure 75. Effect of Treatment on Arc Second Harmonic SPL at 80% RPM

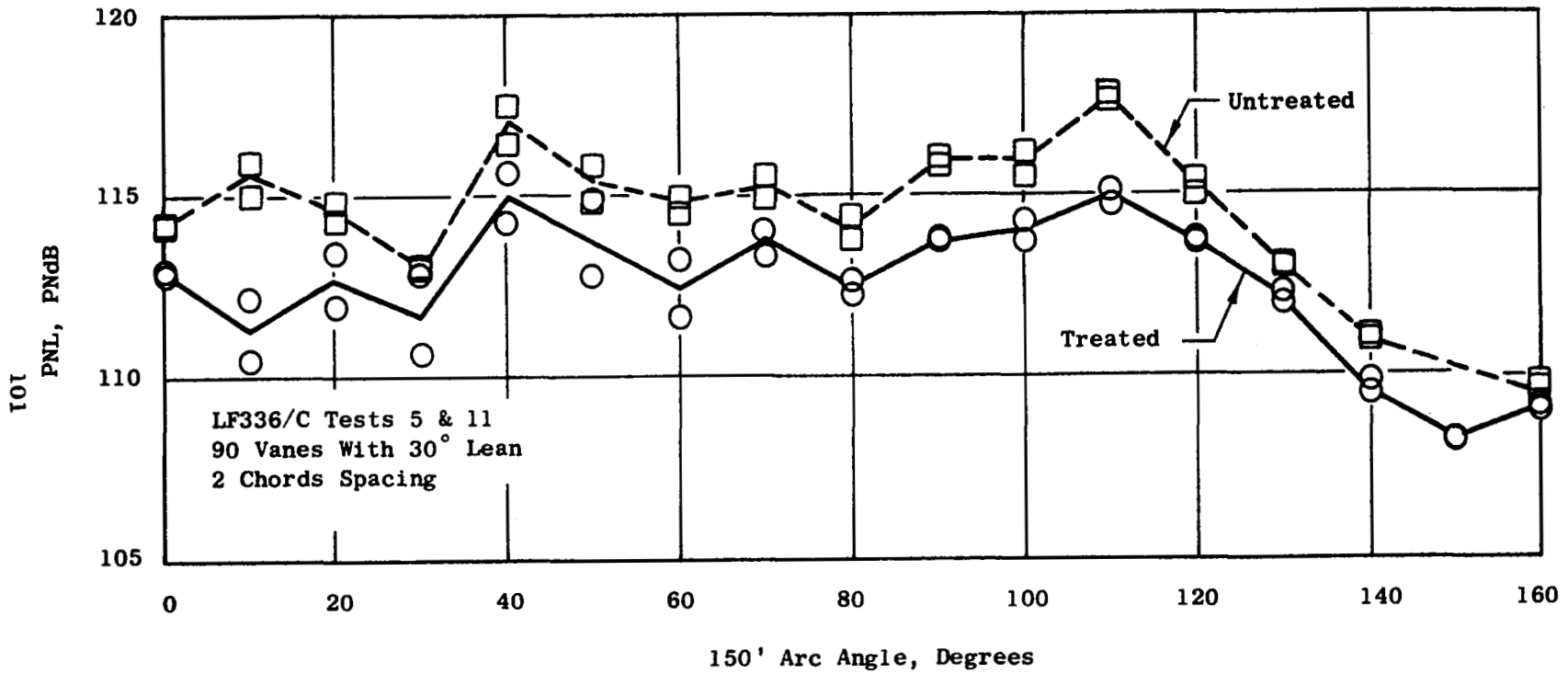

Figure 76. Effect of Treatment on Arc PNL at 80% RPM

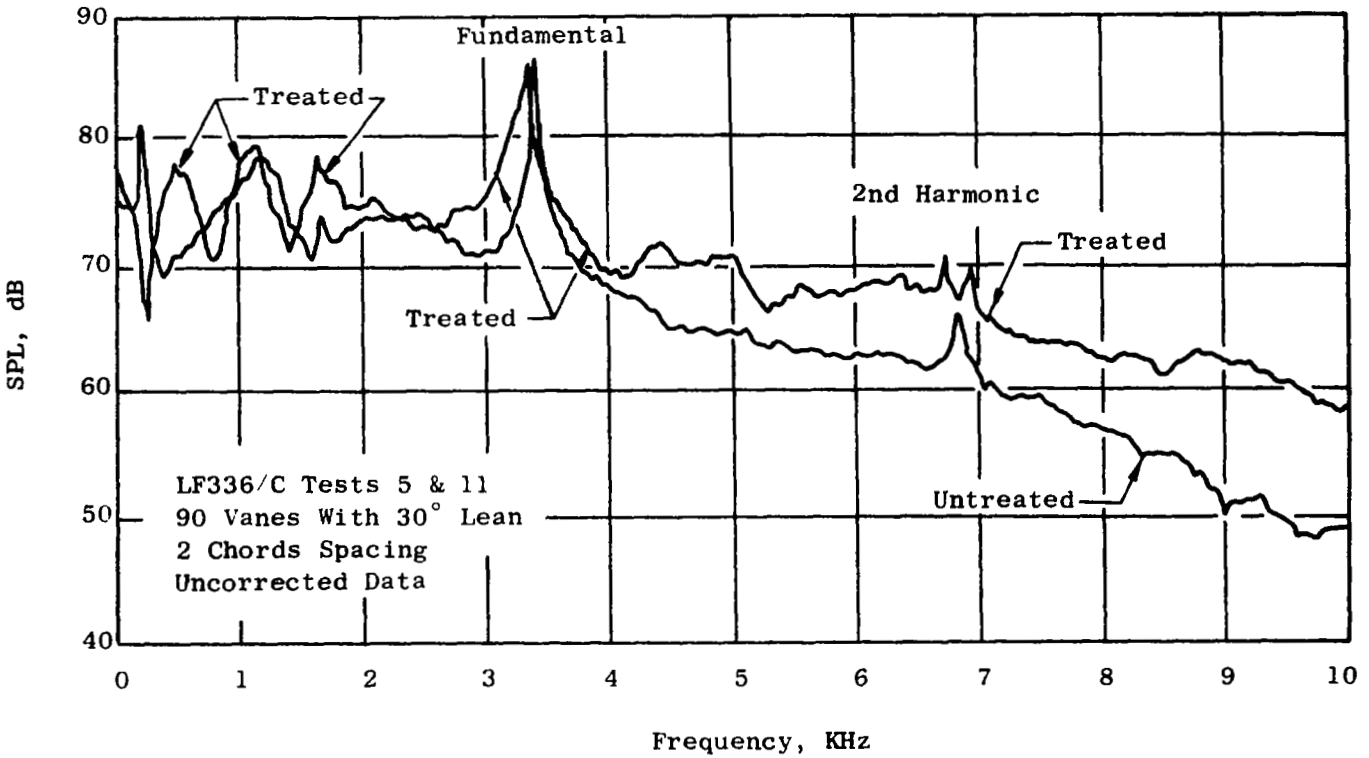

Figure 77. Effect of Treatment on SPL Spectrum at 110° Arc Angle at 80% RPM

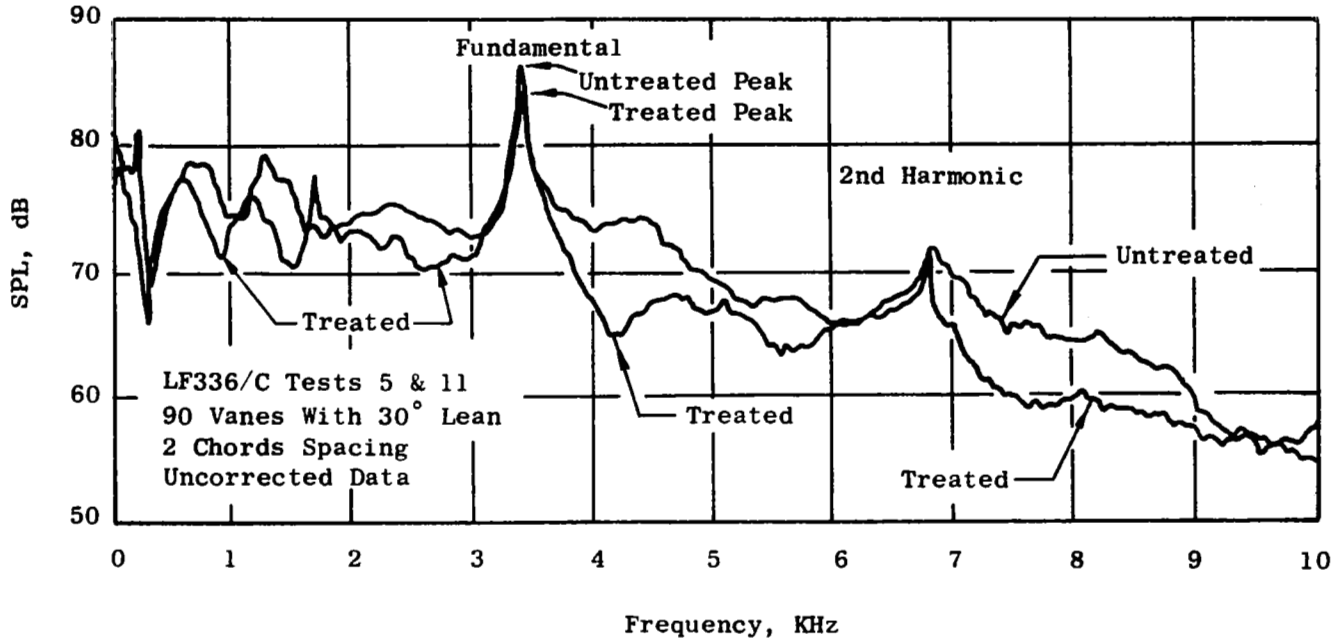

Figure 78. Effect of Treatment on SPL Spectrum at 120° Arc Angle at 80% RPM

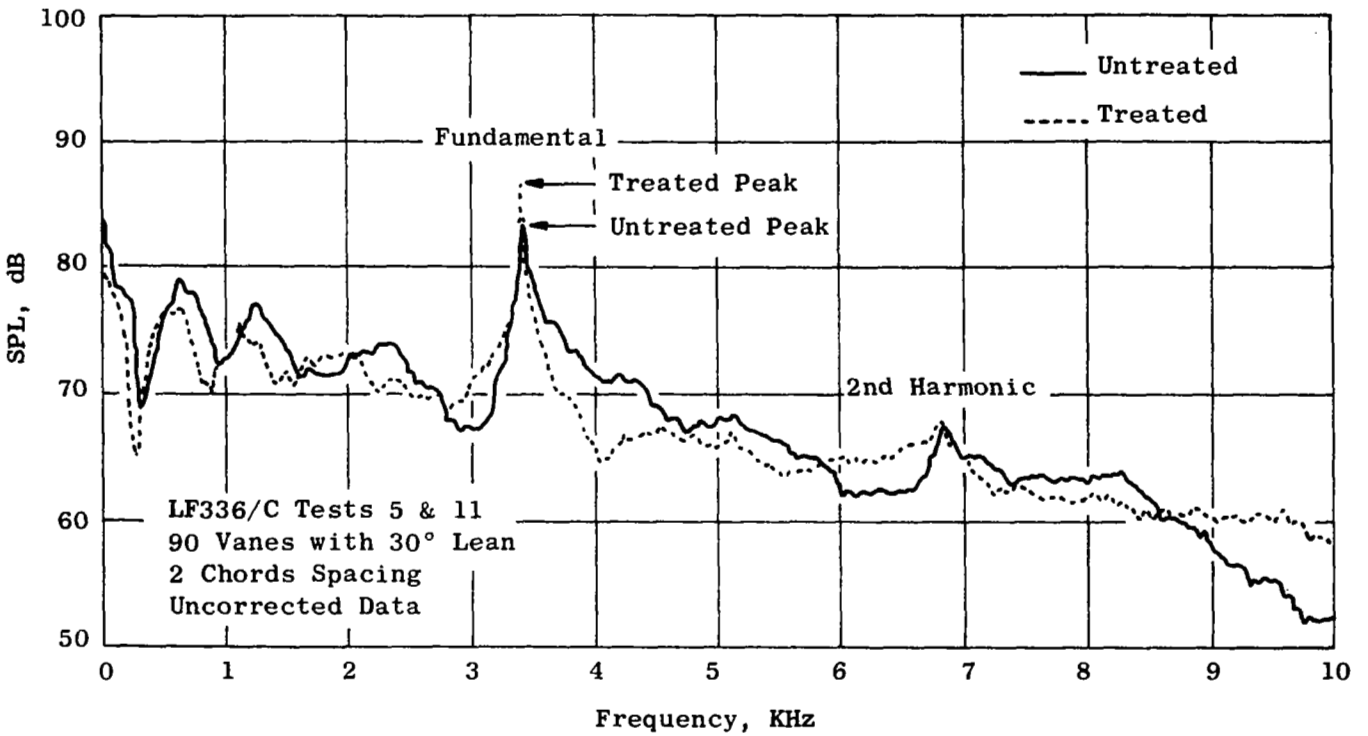

Figure 79. Effect of Treatment on SPL Spectrum at 130° Arc Angle at 80% RPM.

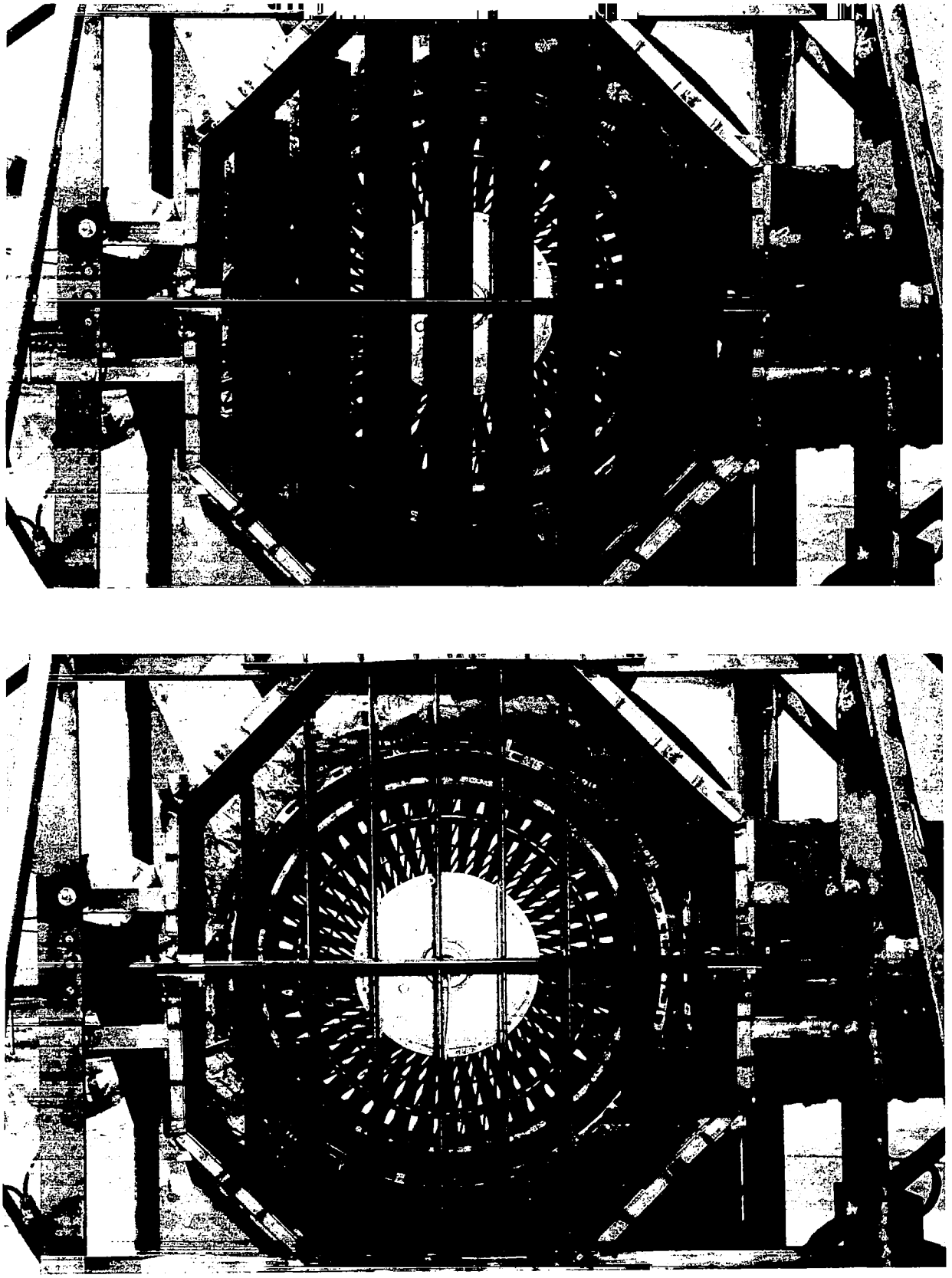

Figure 80. Acoustic Louvers Installed

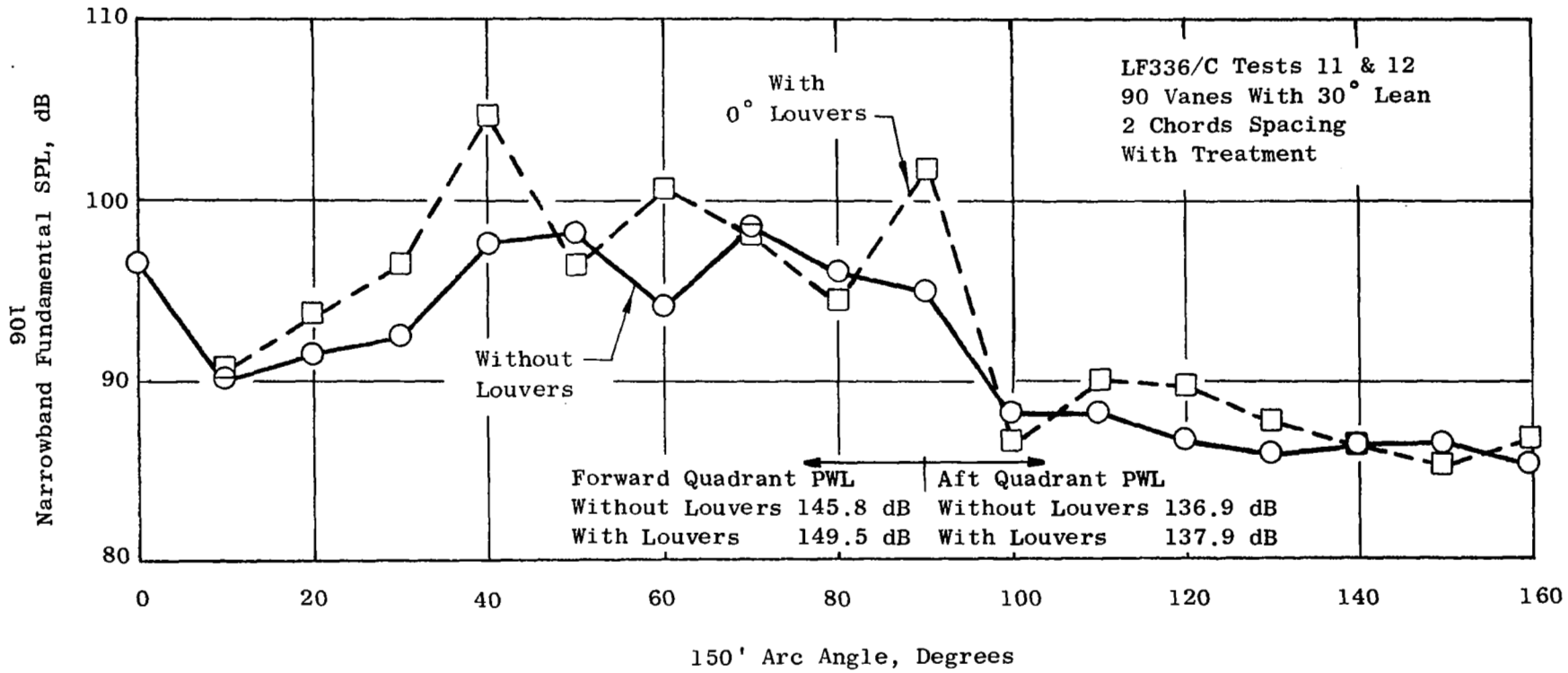

Figure 81. Effect of Acoustic Louvers on Arc Fundamental SPL at 95% RPM

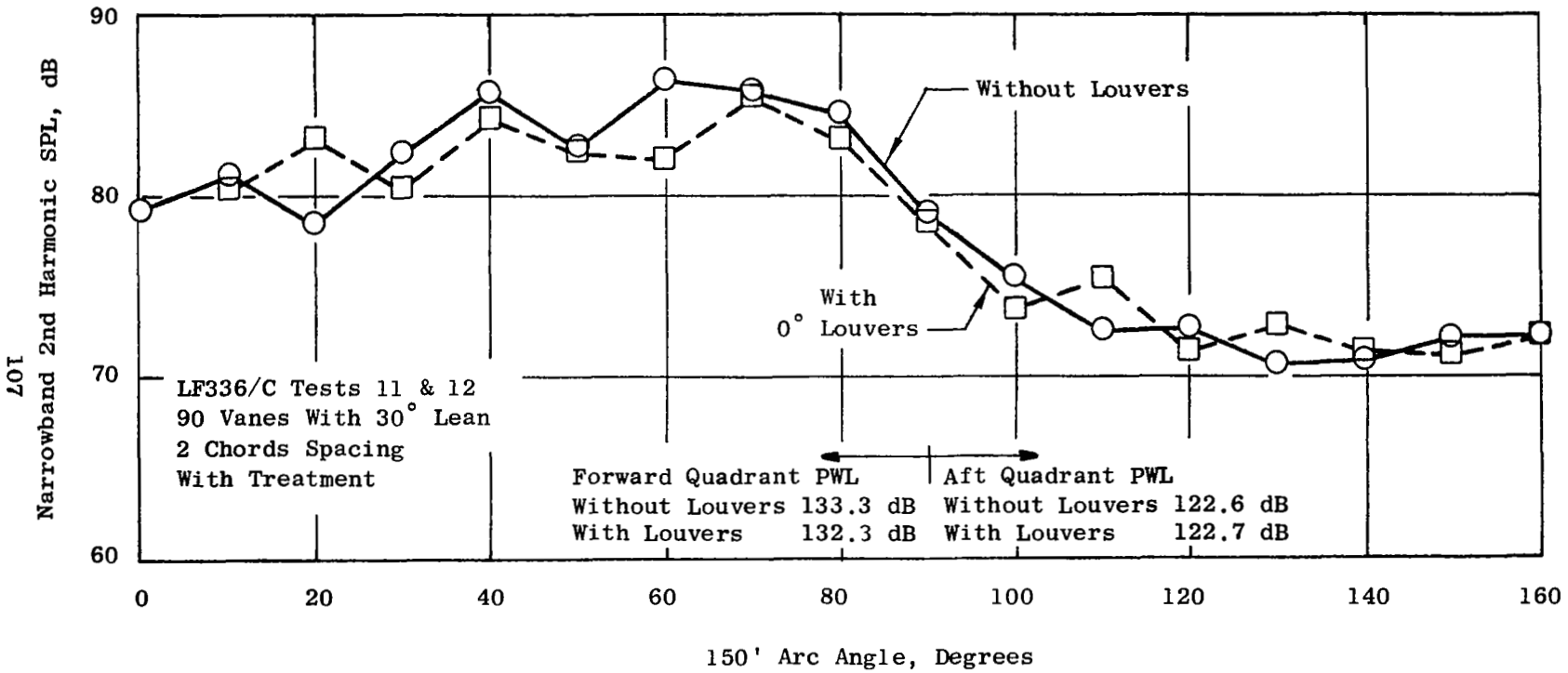

Figure 82. Effect of Acoustic Louvers on Arc Second Harmonic SPL at 95% RPM

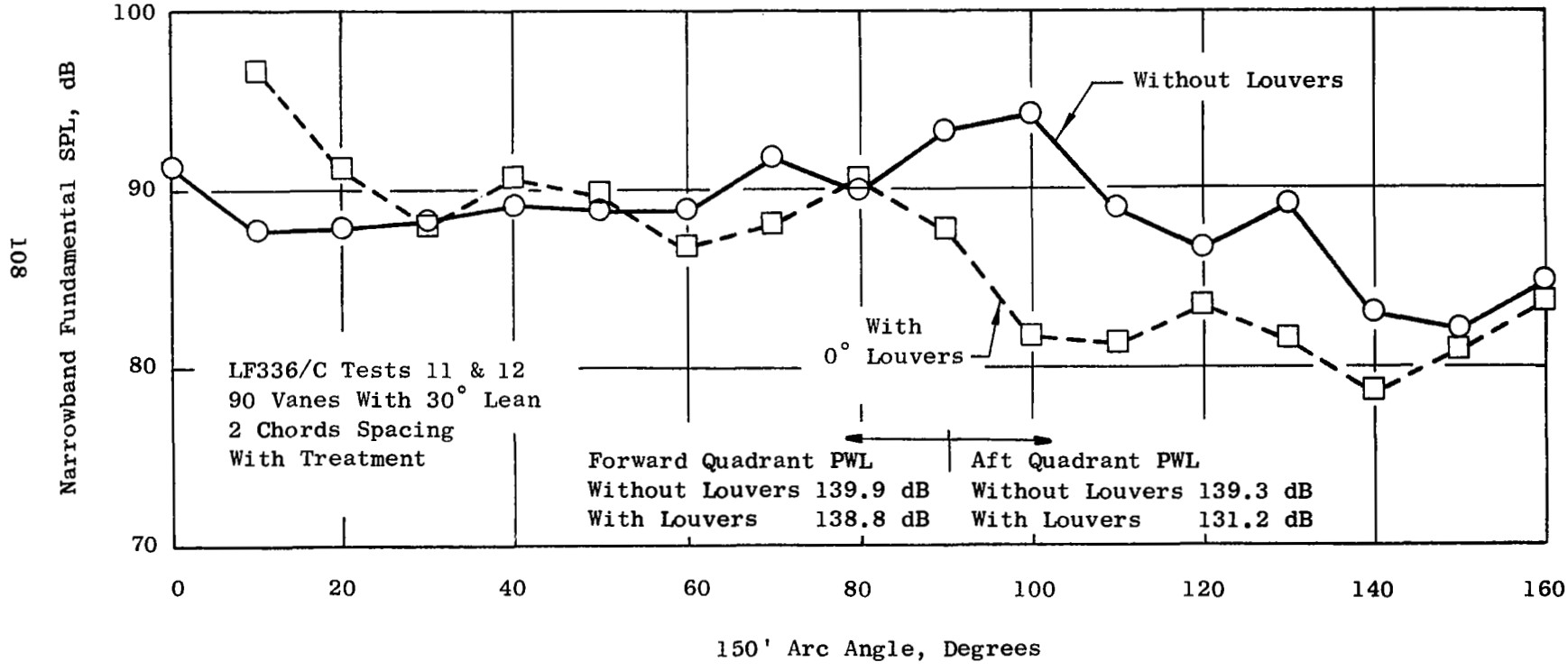

Figure 83. Effect of Acoustic Louvers on Arc Fundamental SPL at 80% RPM

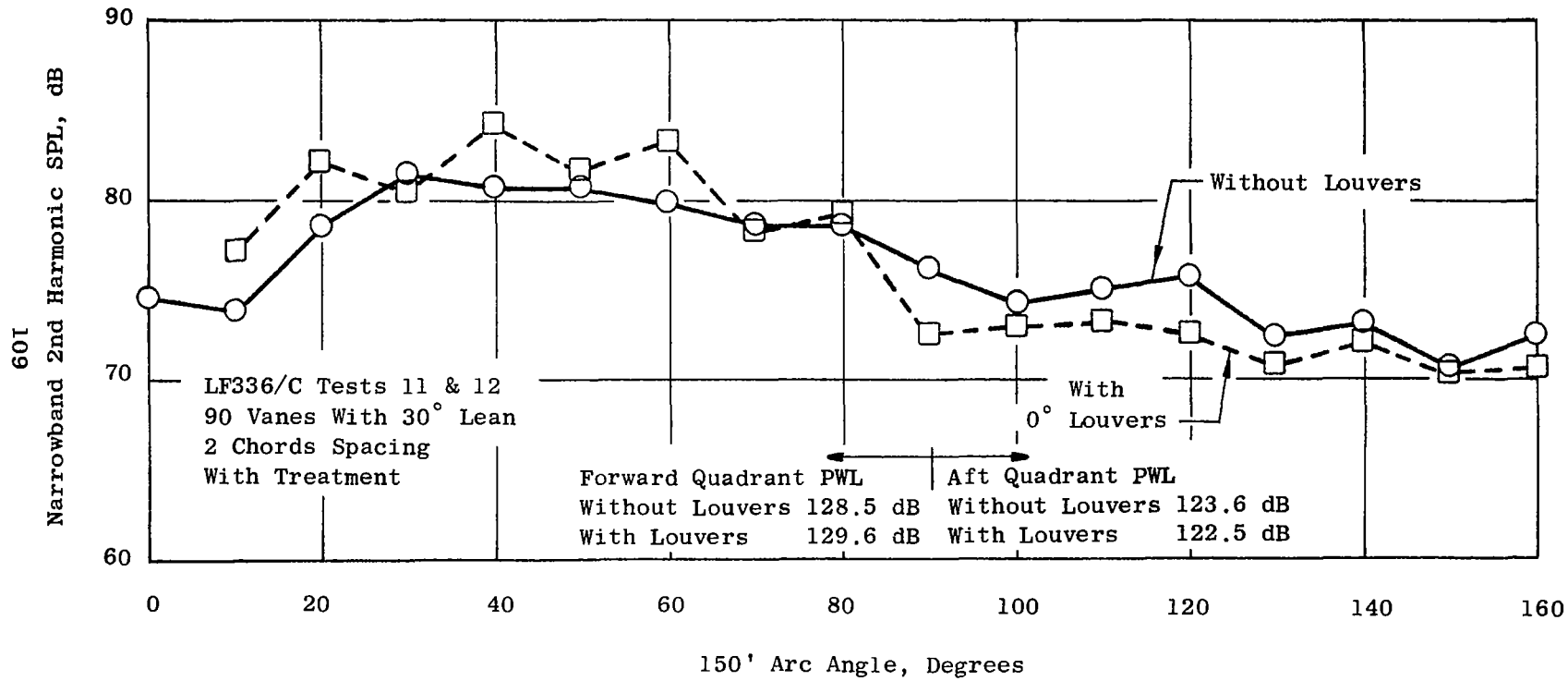

Figure 84. Effect of Acoustic Louvers on Arc Second Harmonic SPL at 80% RPM

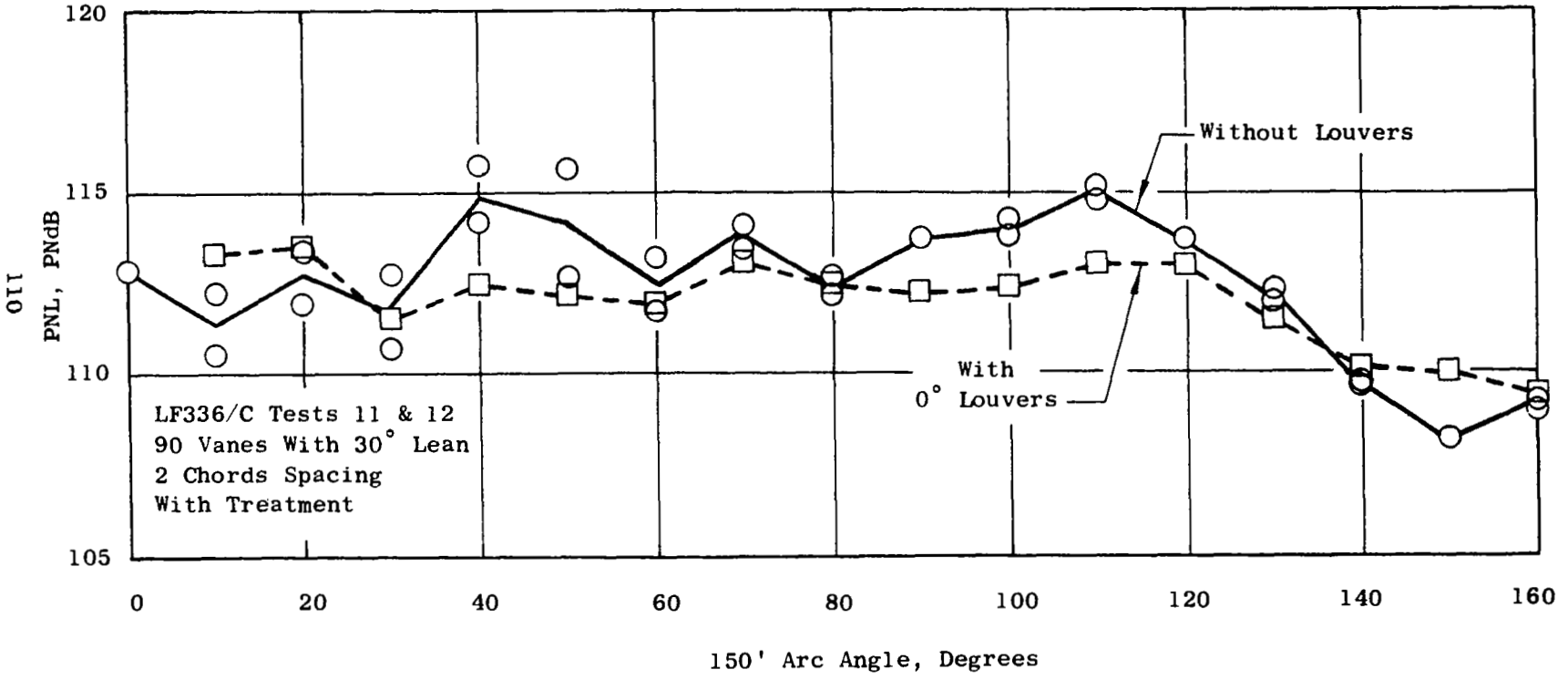

Figure 85. Effect of Acoustic Louvers on Arc PNL at 80% RPM

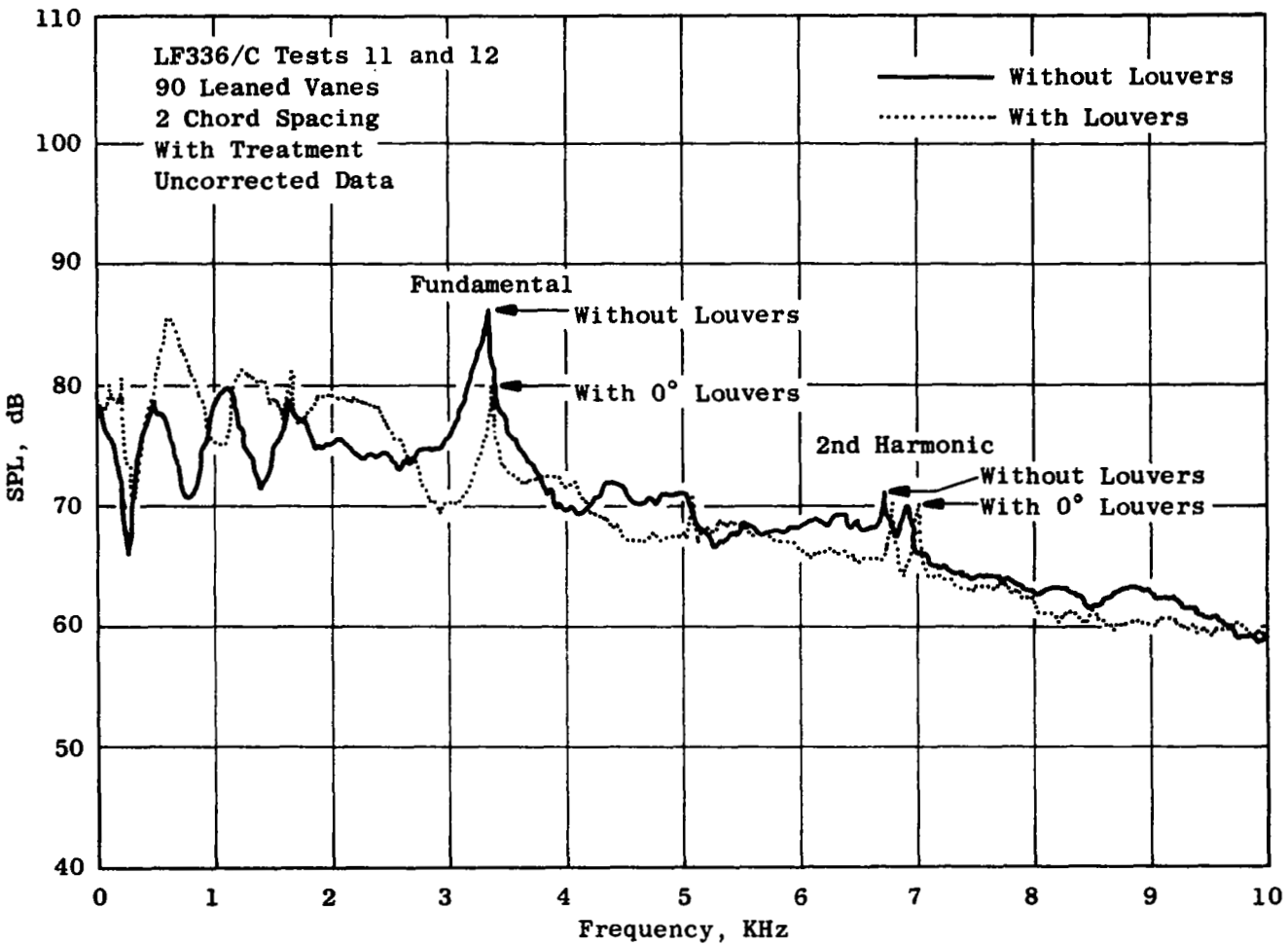

Figure 86. Effect of Acoustic Louvers on SPL Spectrum at 110° Arc Angle at 80% RPM.

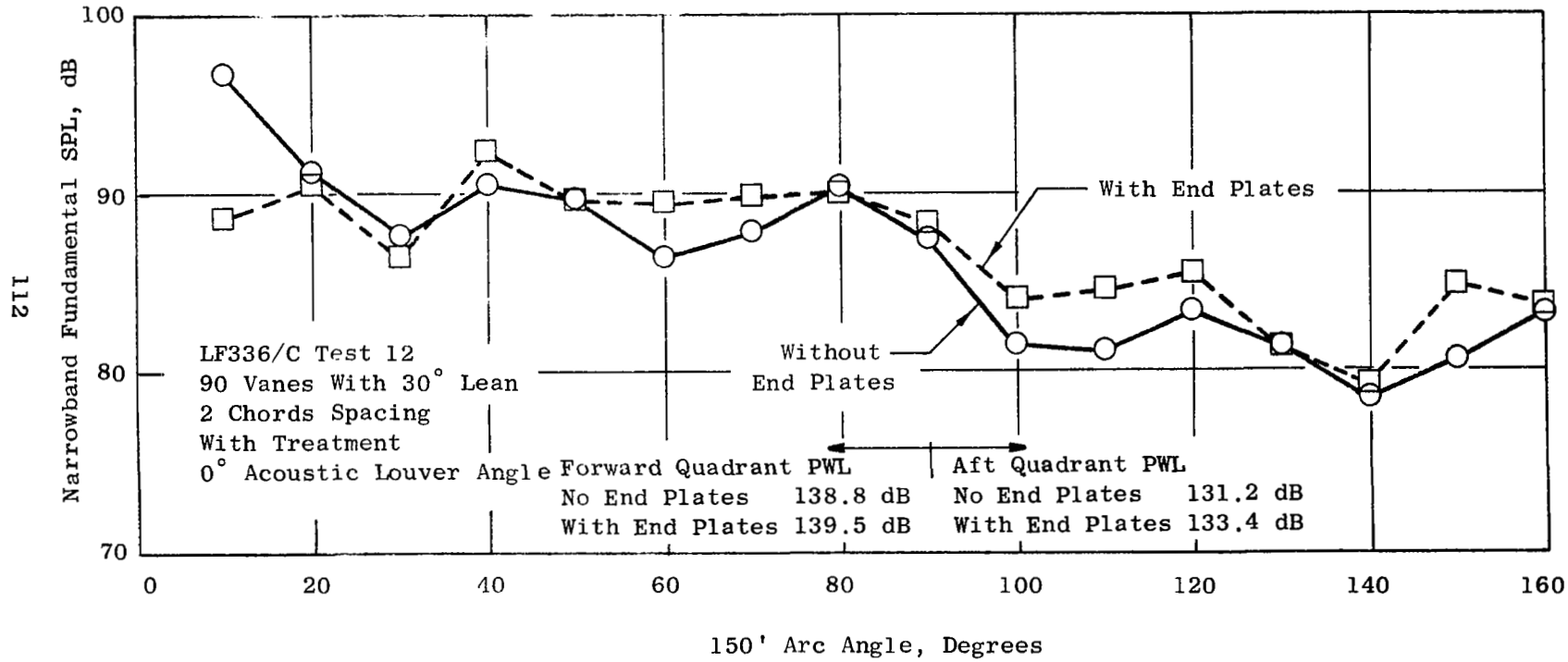

Figure 87. Effect of Acoustic Louver End Plates on Arc Fundamental SPL at 80% RPM

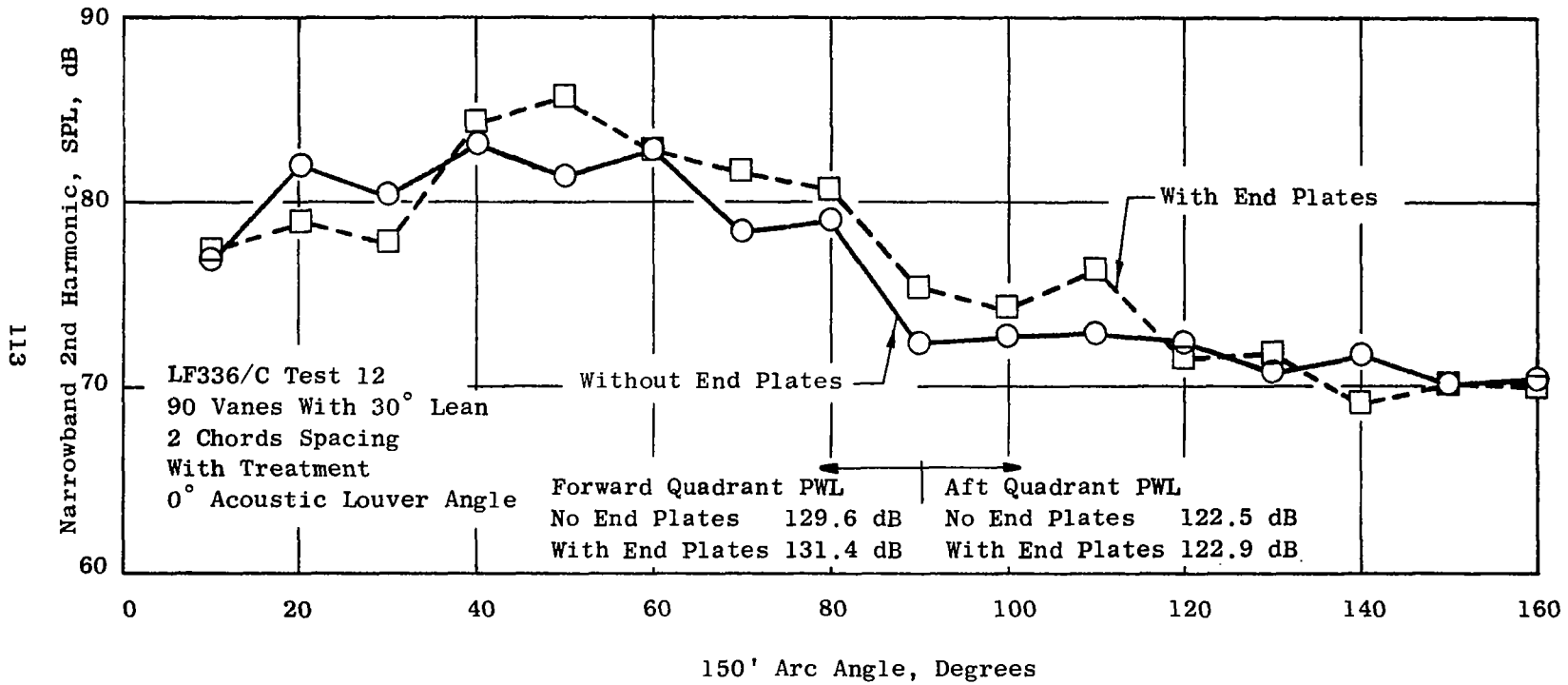

Figure 88. Effect of Acoustic Louver End Plates on Arc Second Harmonic SPL at 80% RPM

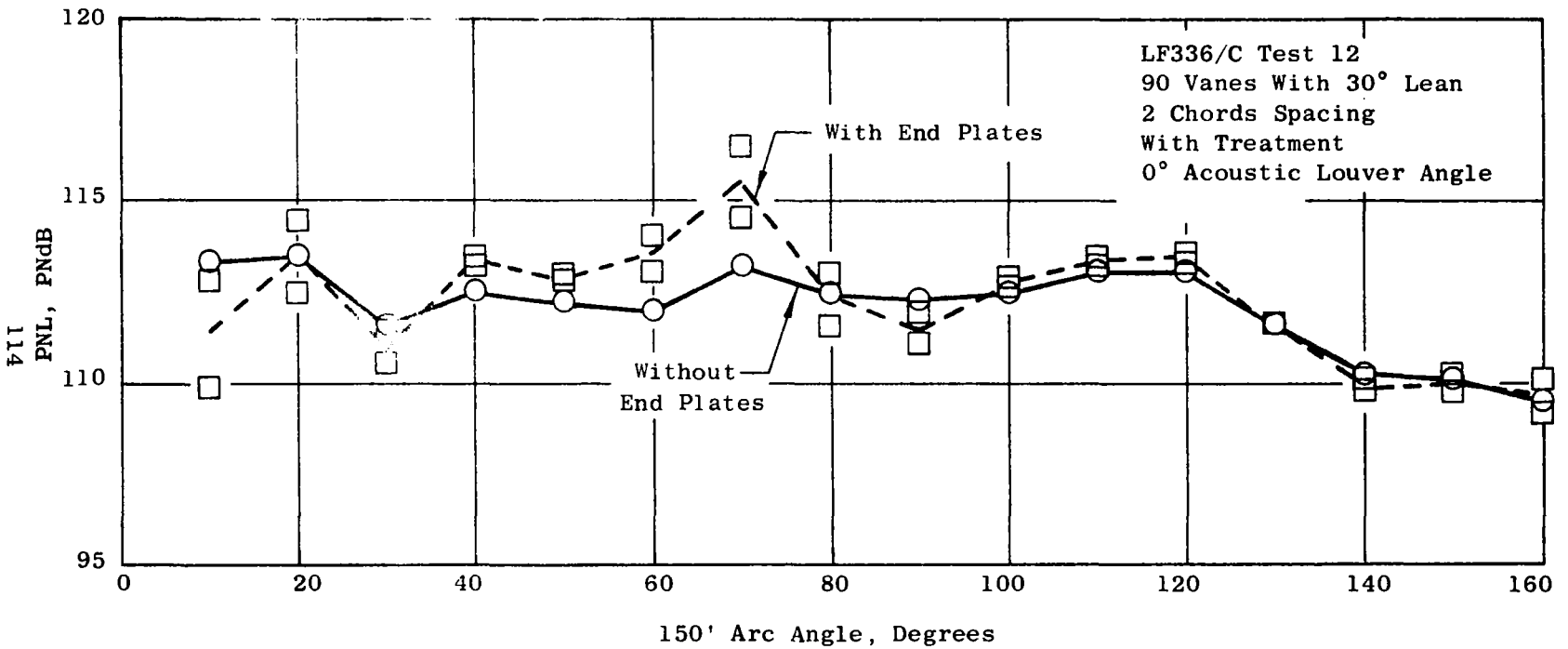

Figure 89. Effect of Acoustic Louver End Plates on Arc PNL at 80% RPM

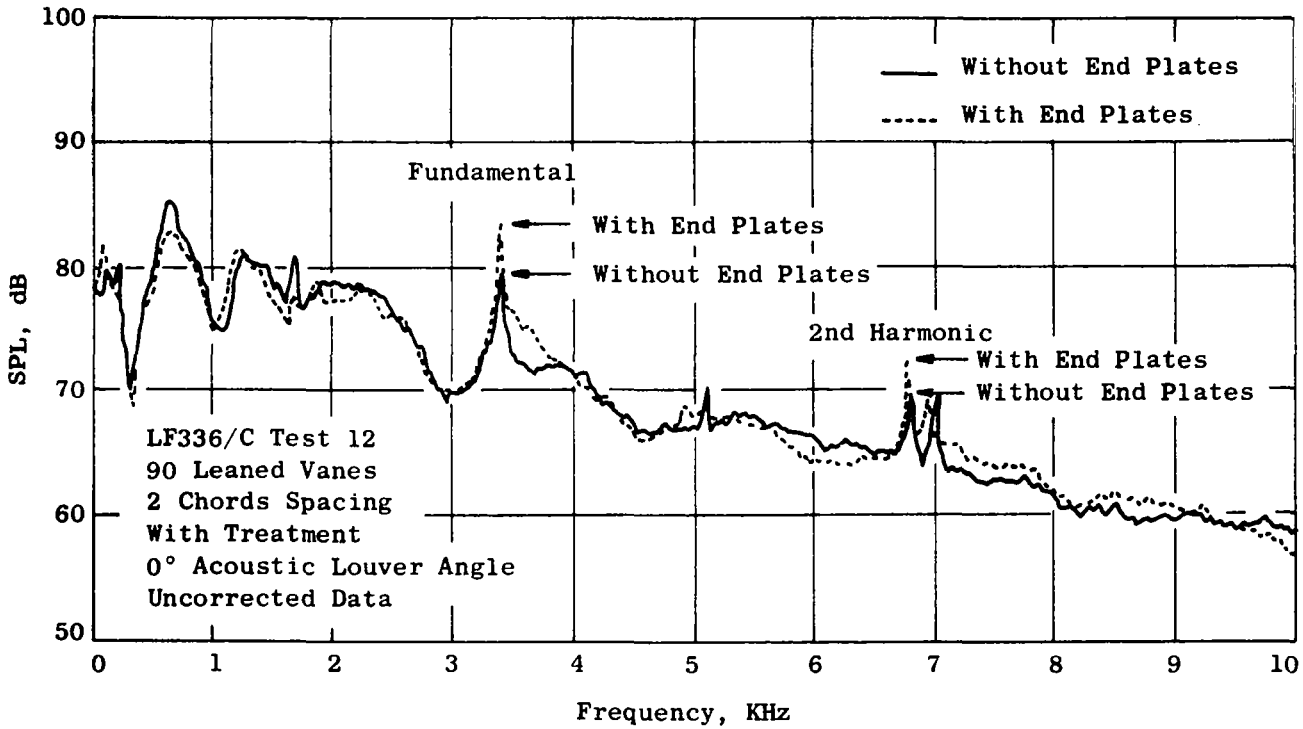

Figure 90. Effect of Acoustic Louver End Plates on SPL Spectrum at 110° Arc Angle at 80% RPM.

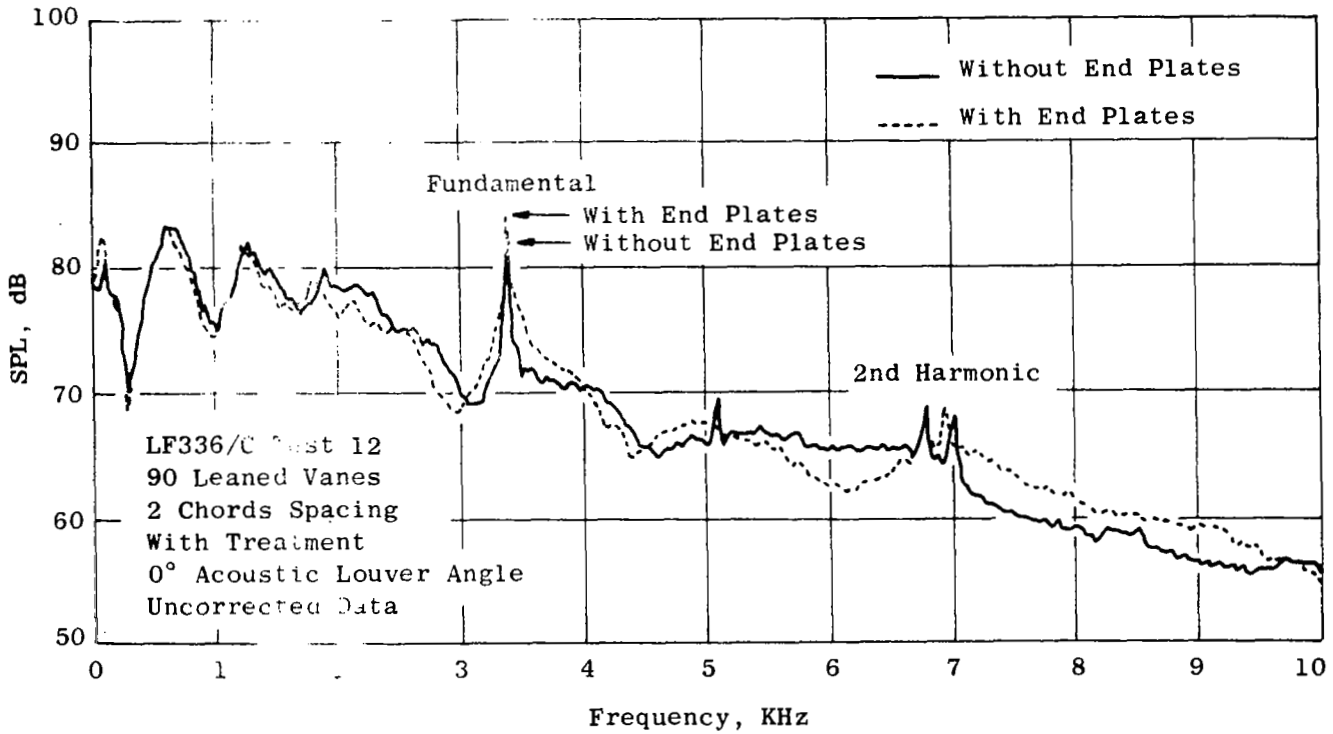

Figure 91. Effect of Acoustic Louver End Plates on SPL Spectrum at 120° Arc Angle at 80% RPM

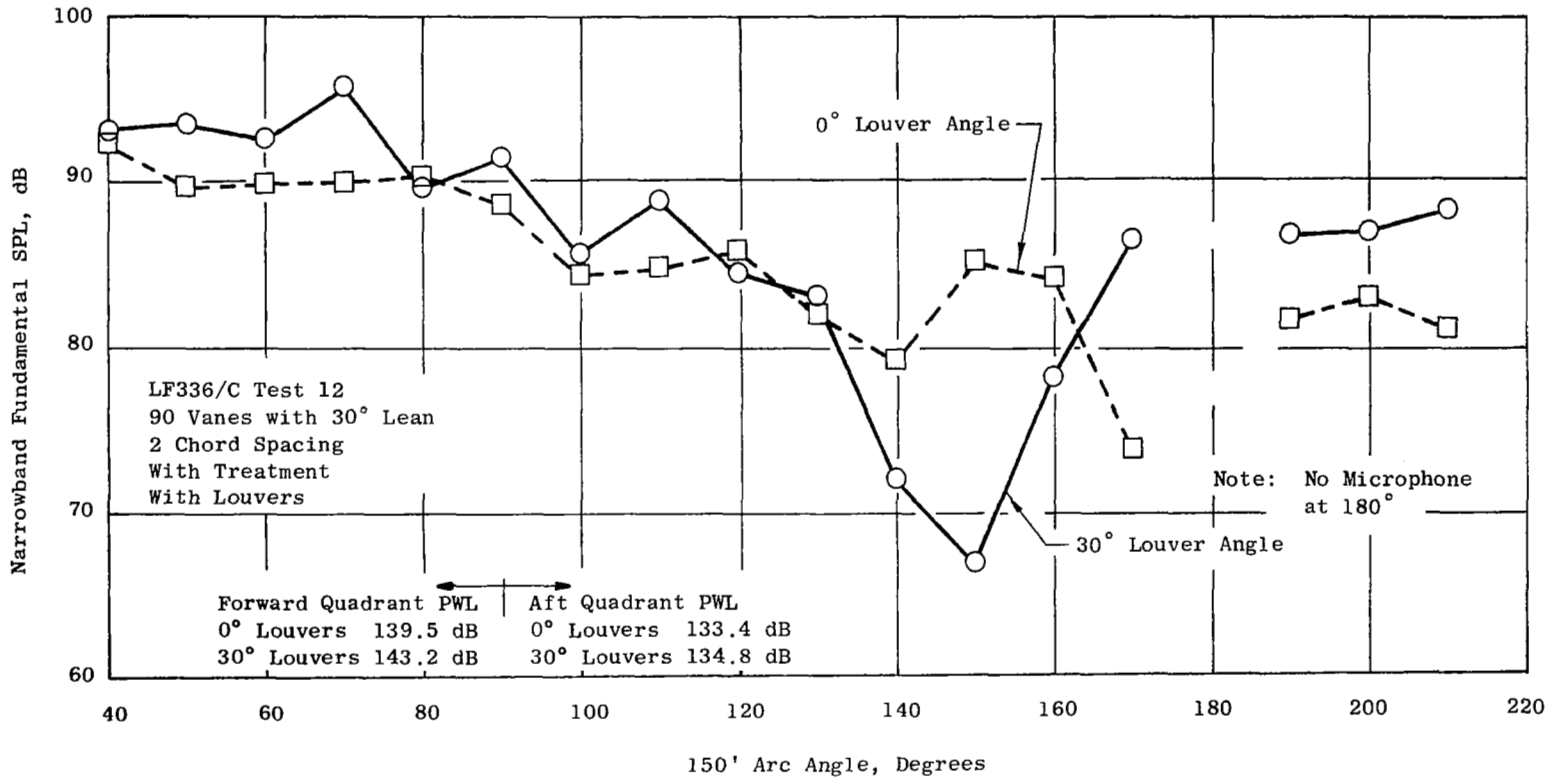

Figure 92. Effect of Acoustic Louver Angle on Arc Fundamental SPL at 80% RPM

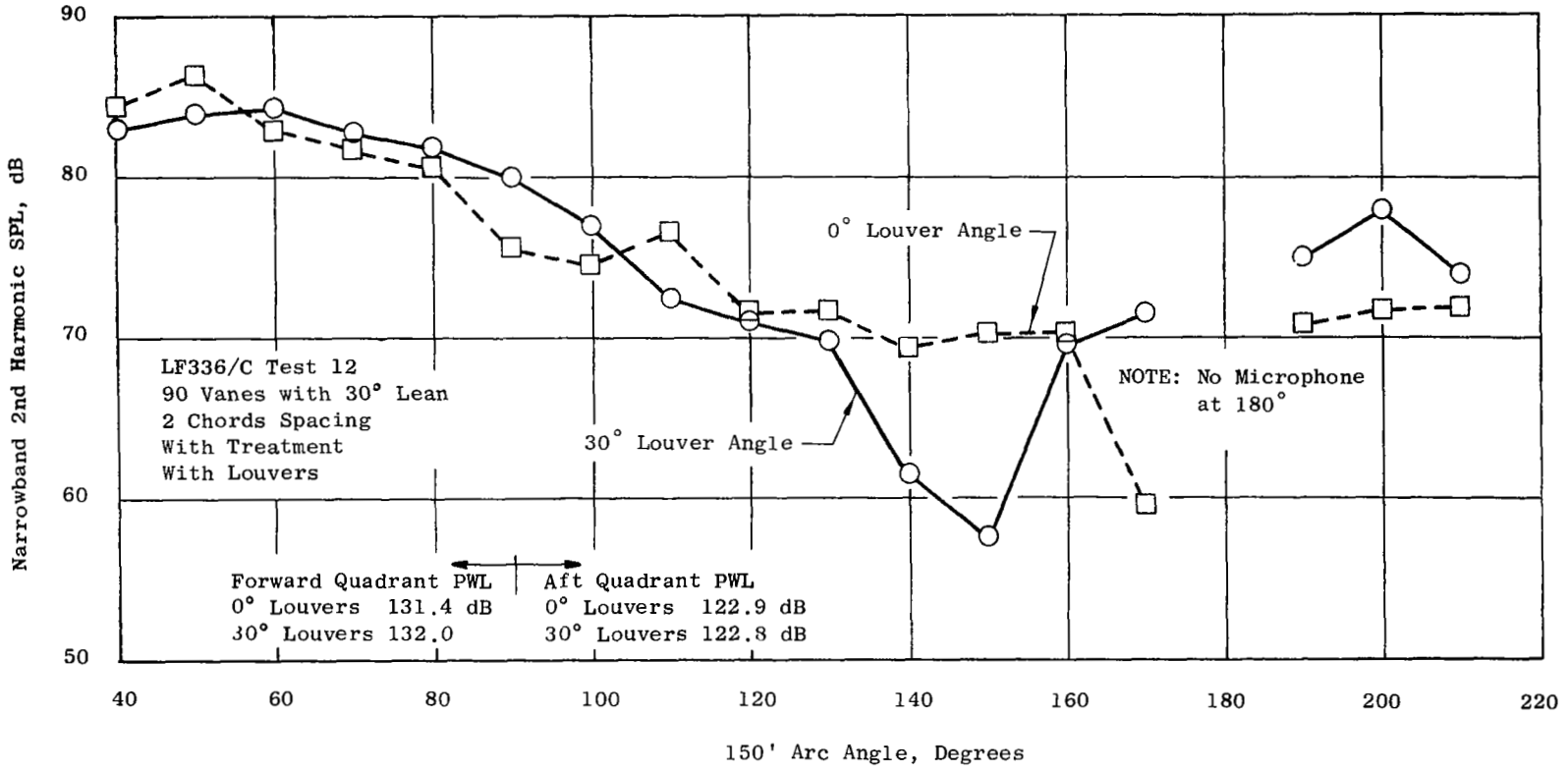

Figure 93. Effect of Acoustic Louver Angle on Arc Second Harmonic SPL at 80% RPM

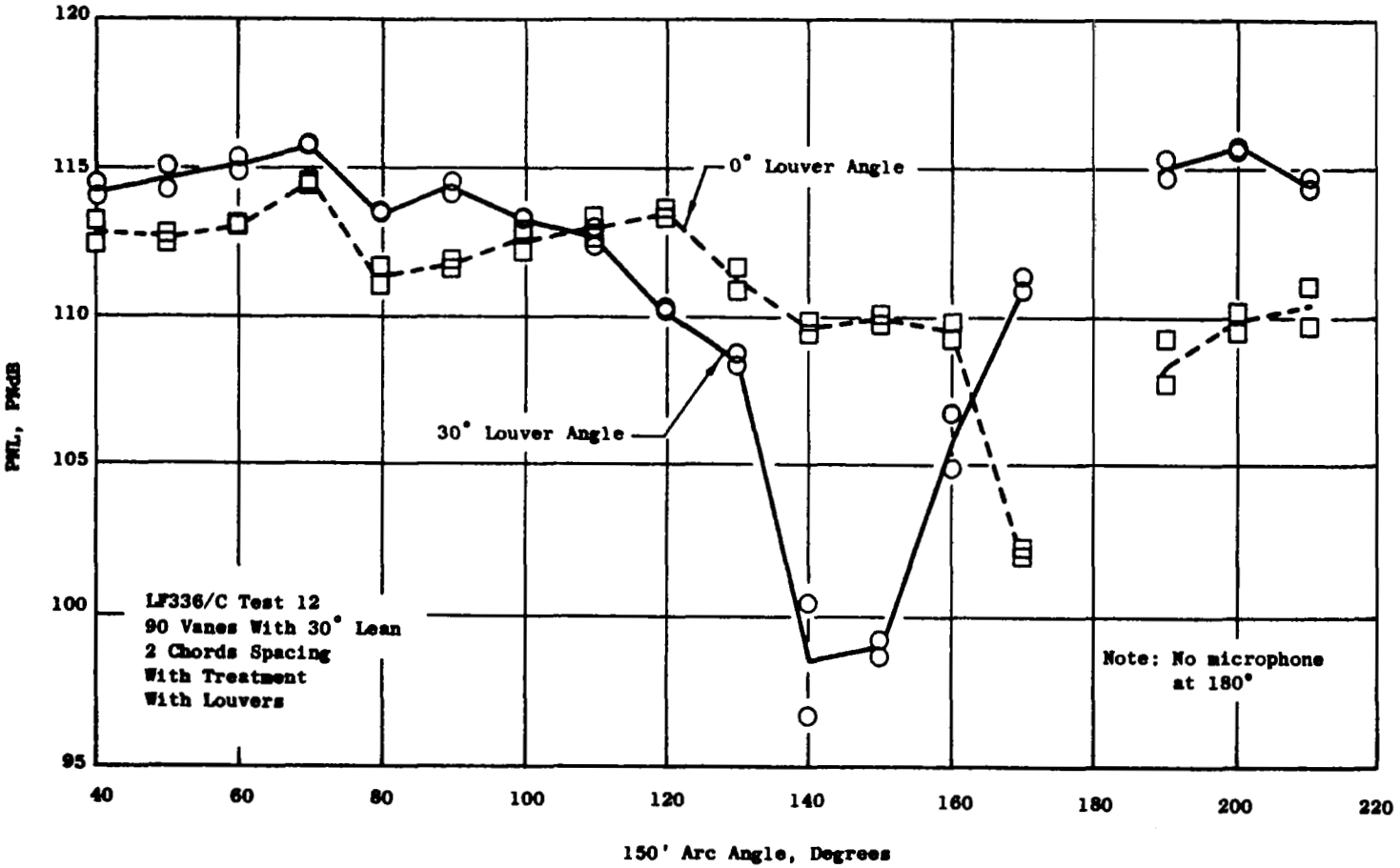

Figure 94. Effect of Acoustic Louver Angle on Arc PNL at 80% RPM

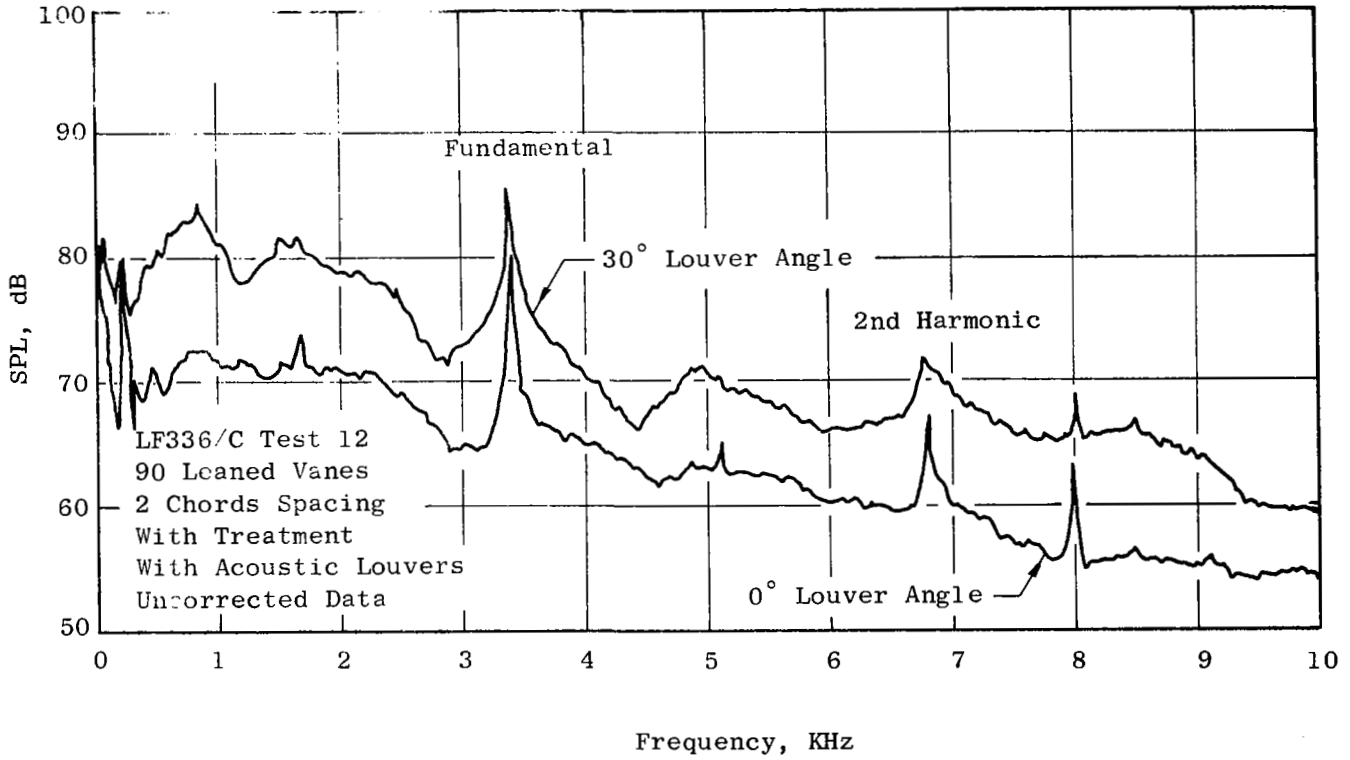

Figure 95. Effect of Acoustic Louver Angle on SPL Spectrum at 190° Arc Angle at 80% RPM

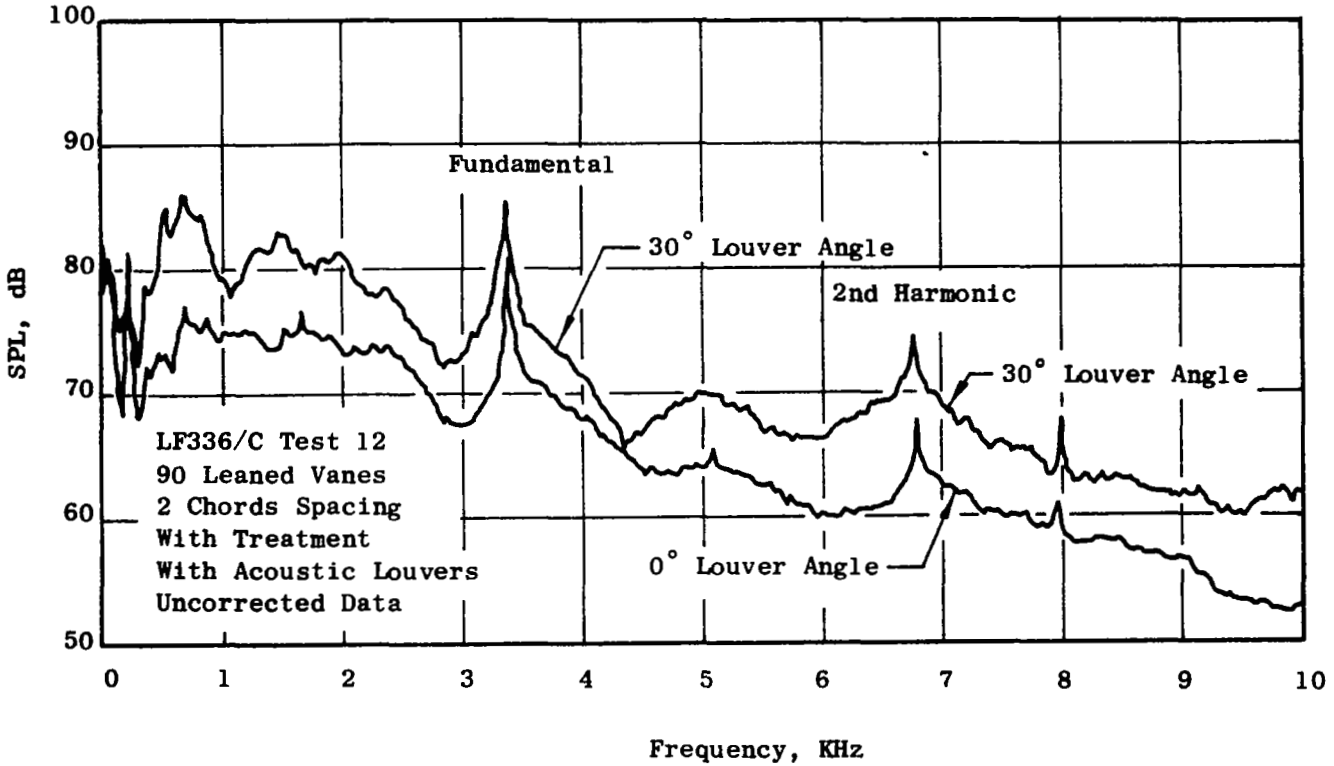

Figure 96. Effect of Acoustic Louver Angle on SPL Spectrum at 200° Arc Angle at 80% RPM

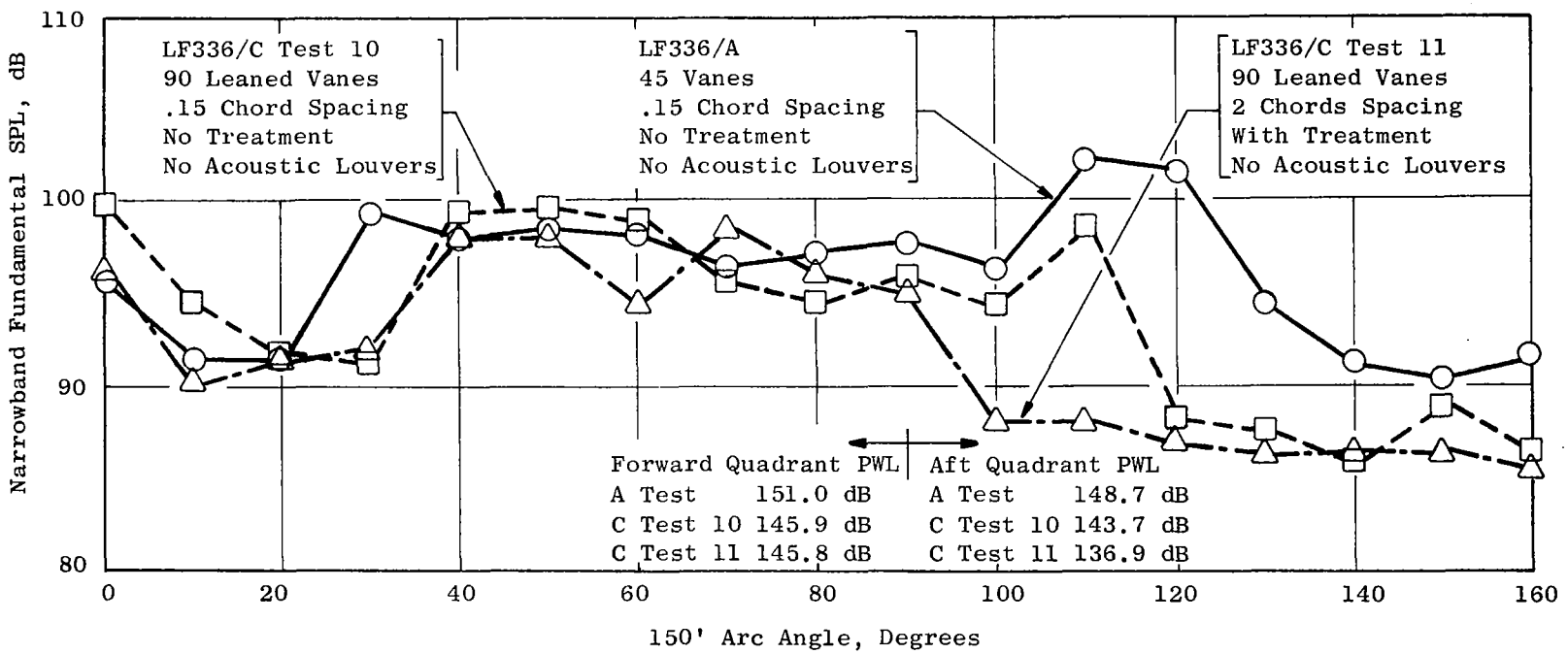

Figure 97. Arc Fundamental SPL for Three Fan Configurations at 95% RPM

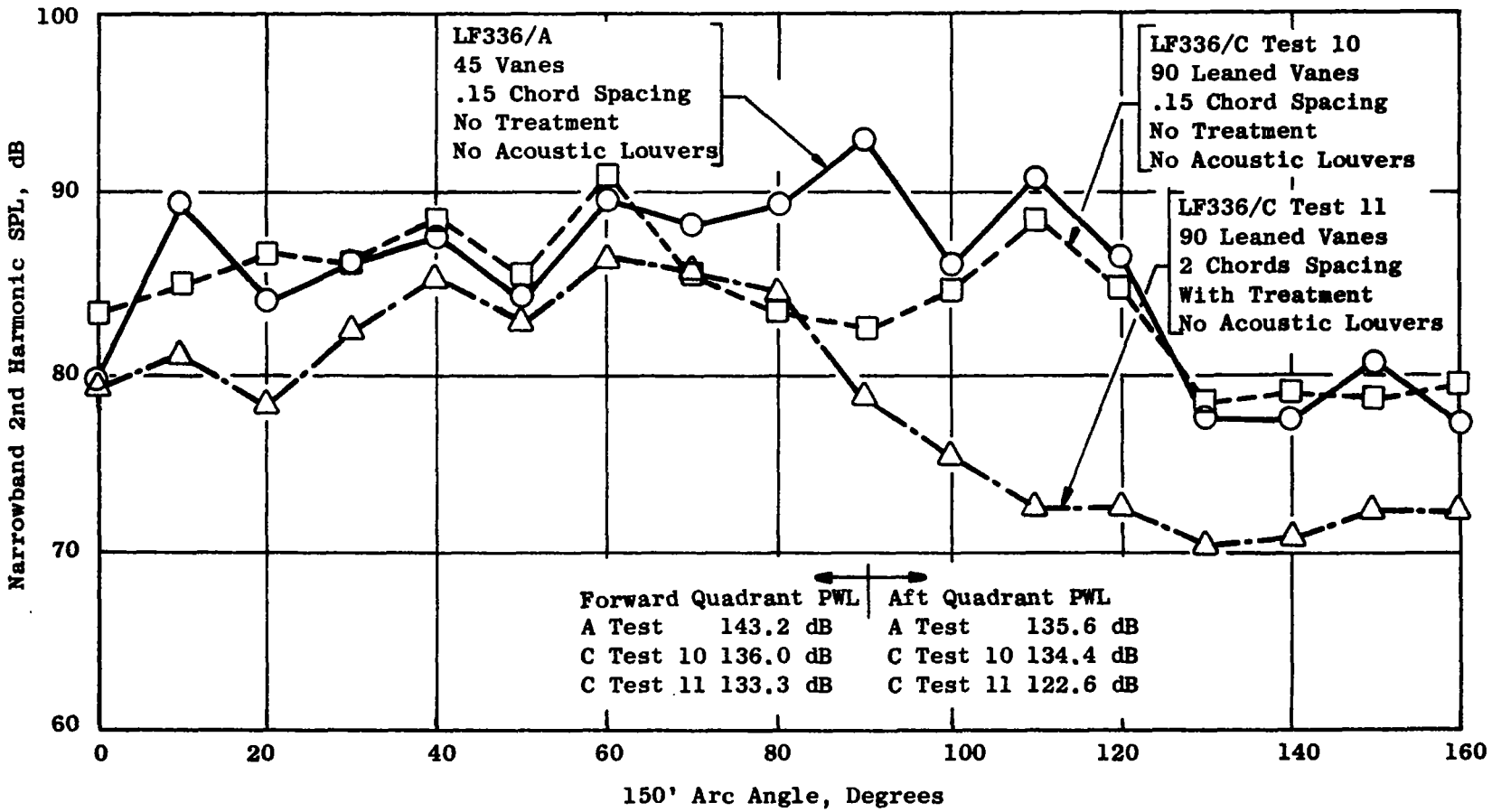

Figure 98. Arc Second Harmonic SPL for Three Fan Configurations at 95% RPM

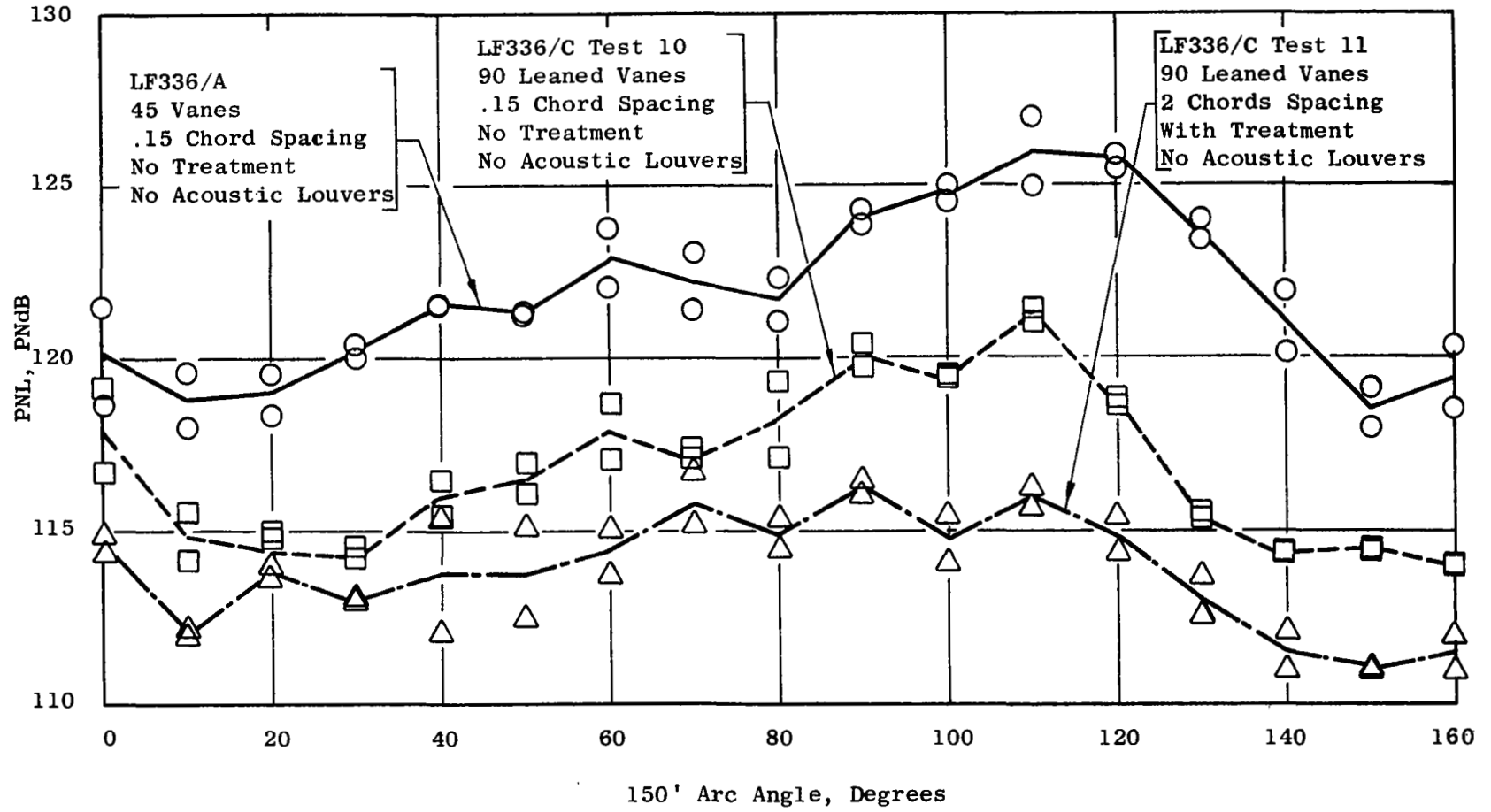

Figure 99. Arc PNL For Three Fan Configurations at 95% RPM

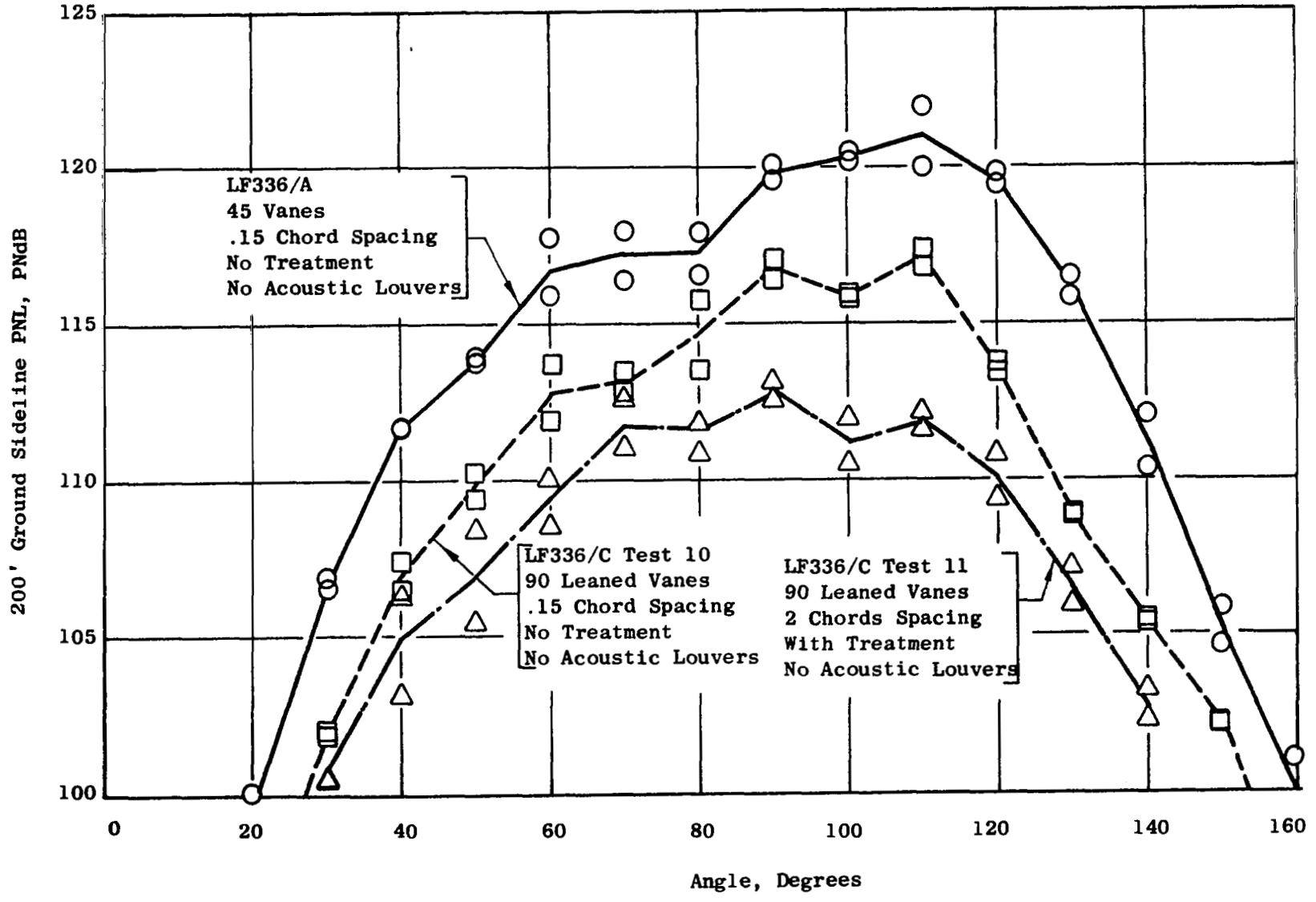

Figure 100. 200' Sideline PNL For Three Fan Configurations at 95% RPM

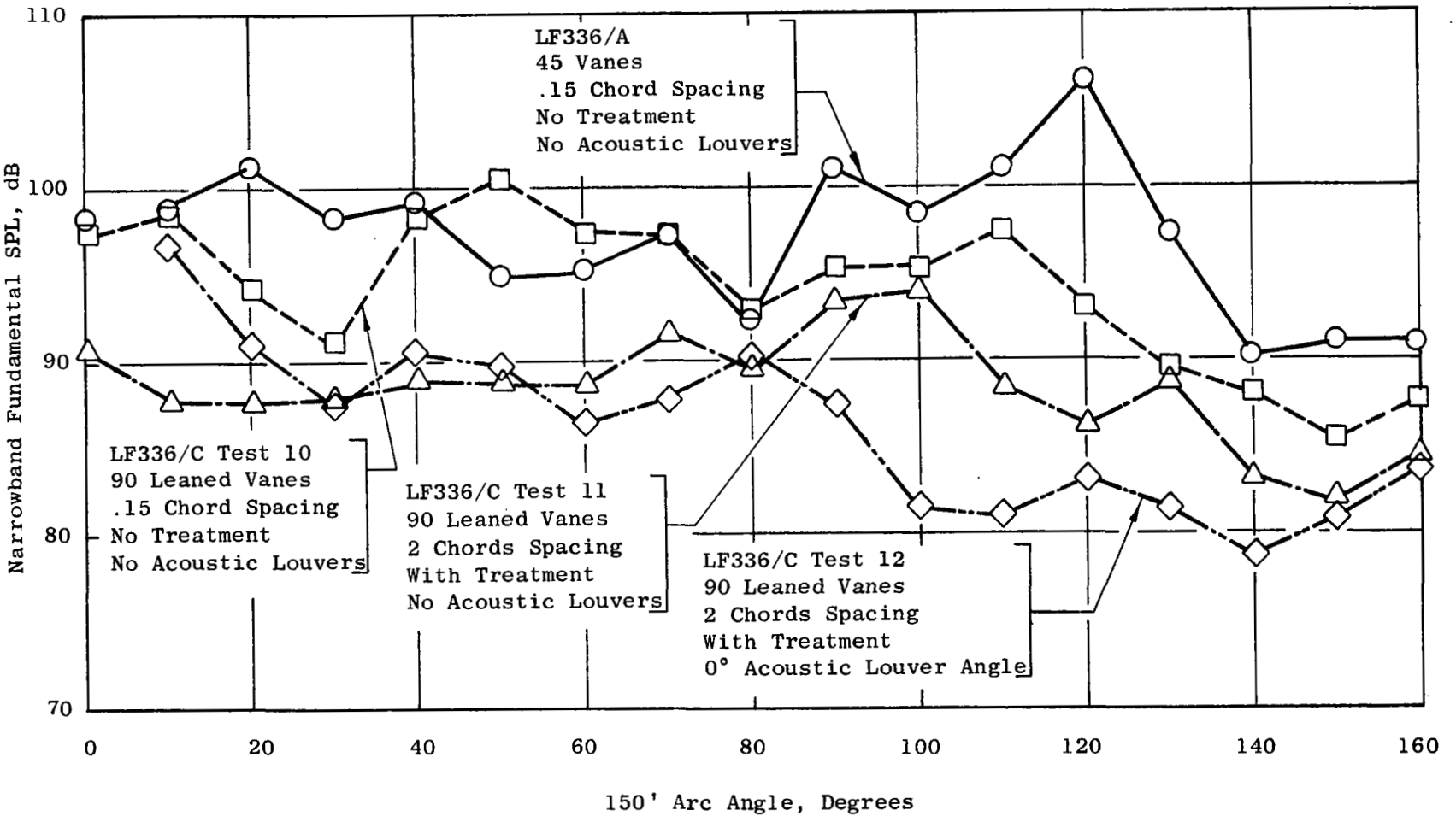

Figure 101. Arc Fundamental SPL For Four Fan Configurations at 80% RPM

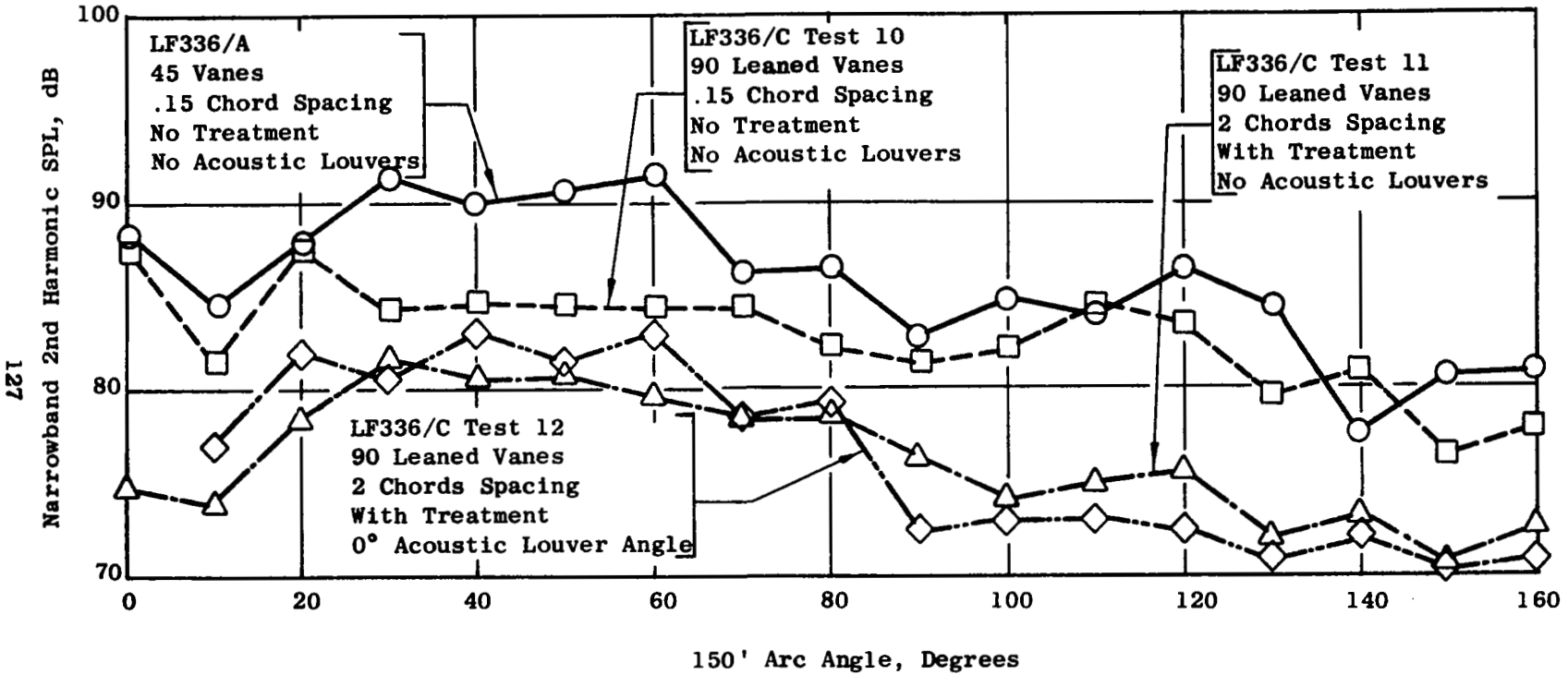

Figure 102. Arc Second Harmonic SPL For Four Fan Configurations at 80% RPM

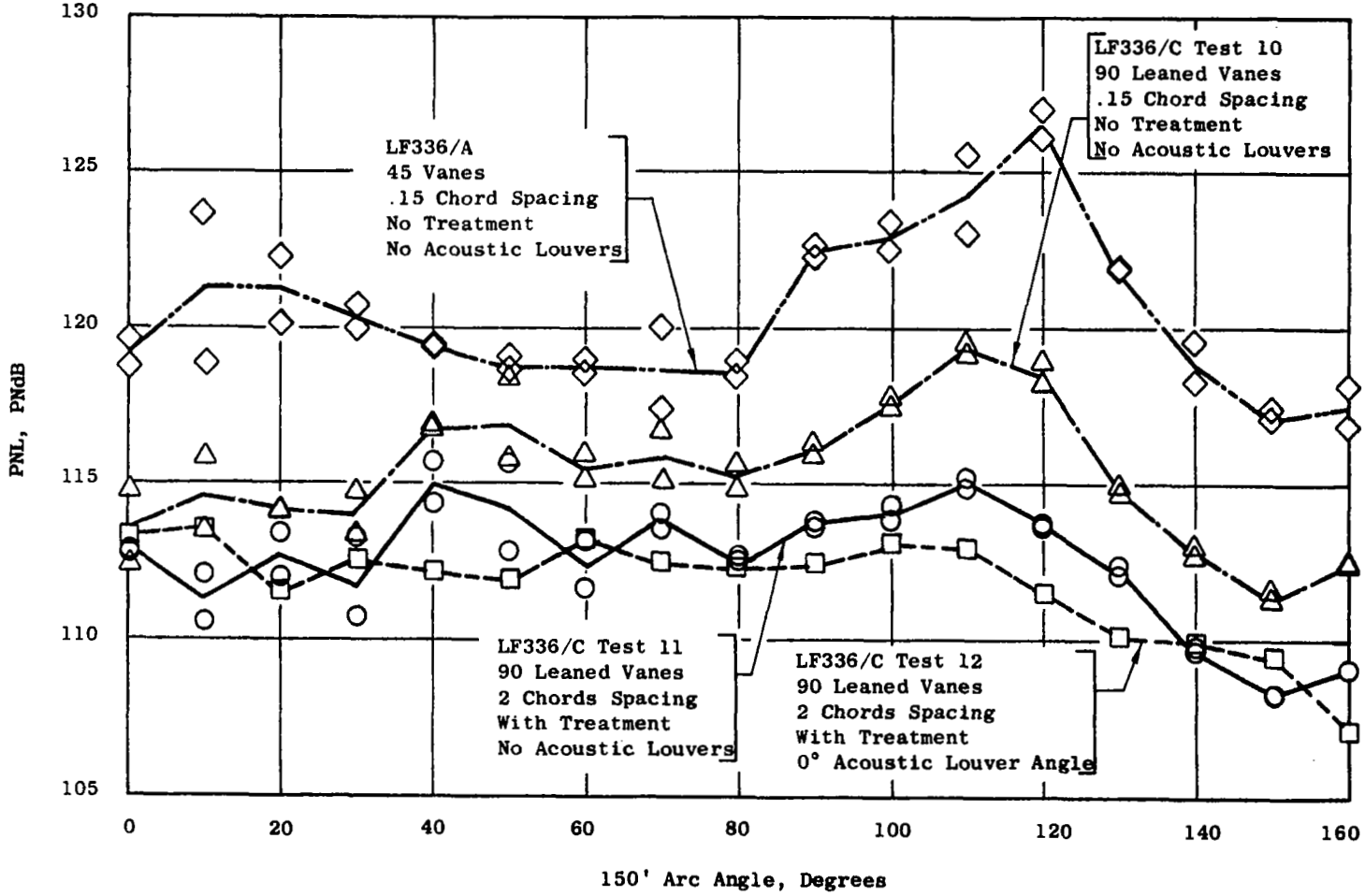

Figure 103. Arc PNL For Four Fan Configurations at 80% RPM

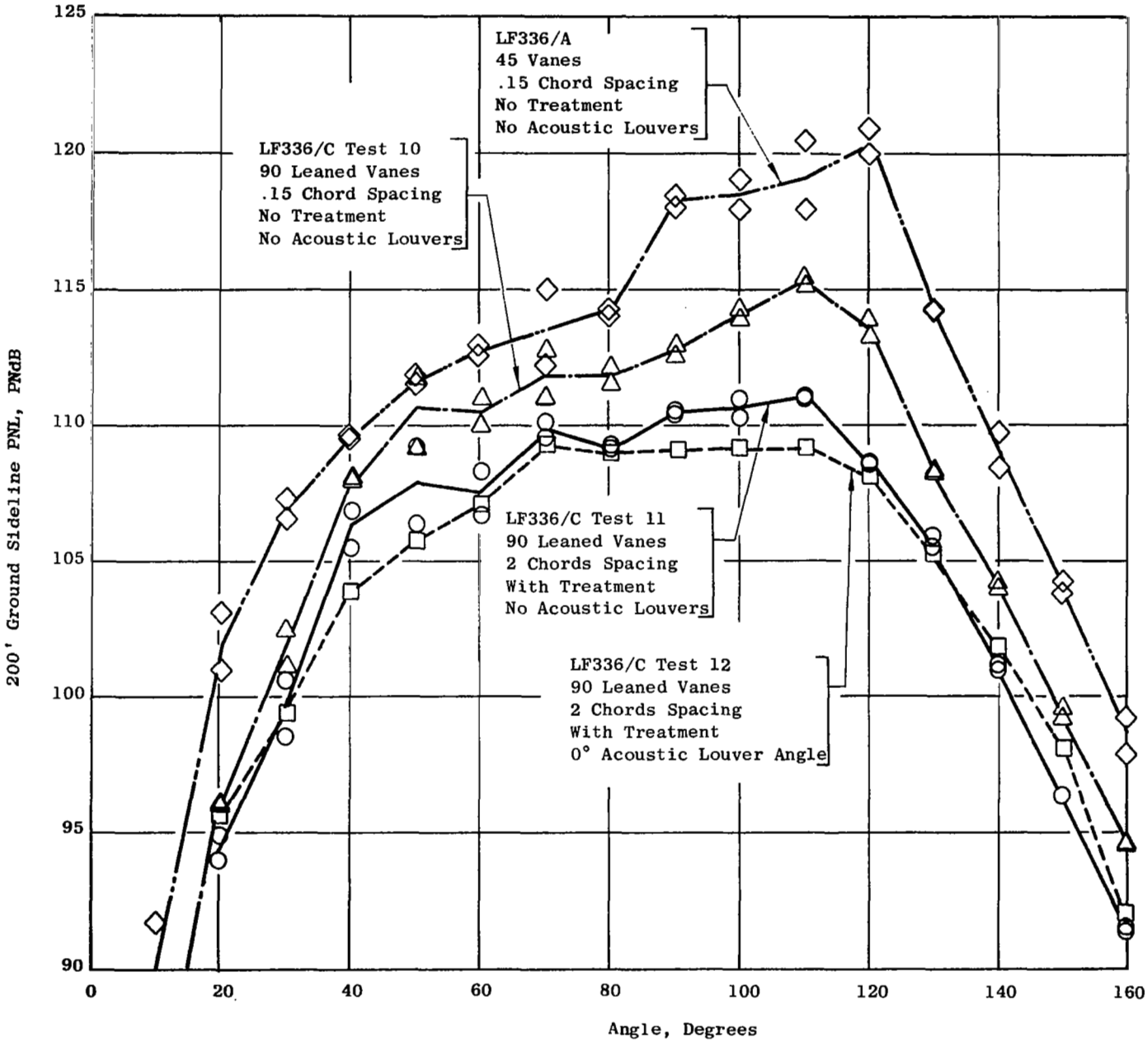

Figure 104. 200' Sideline PNL for Four Fan Configurations at 80% RPM

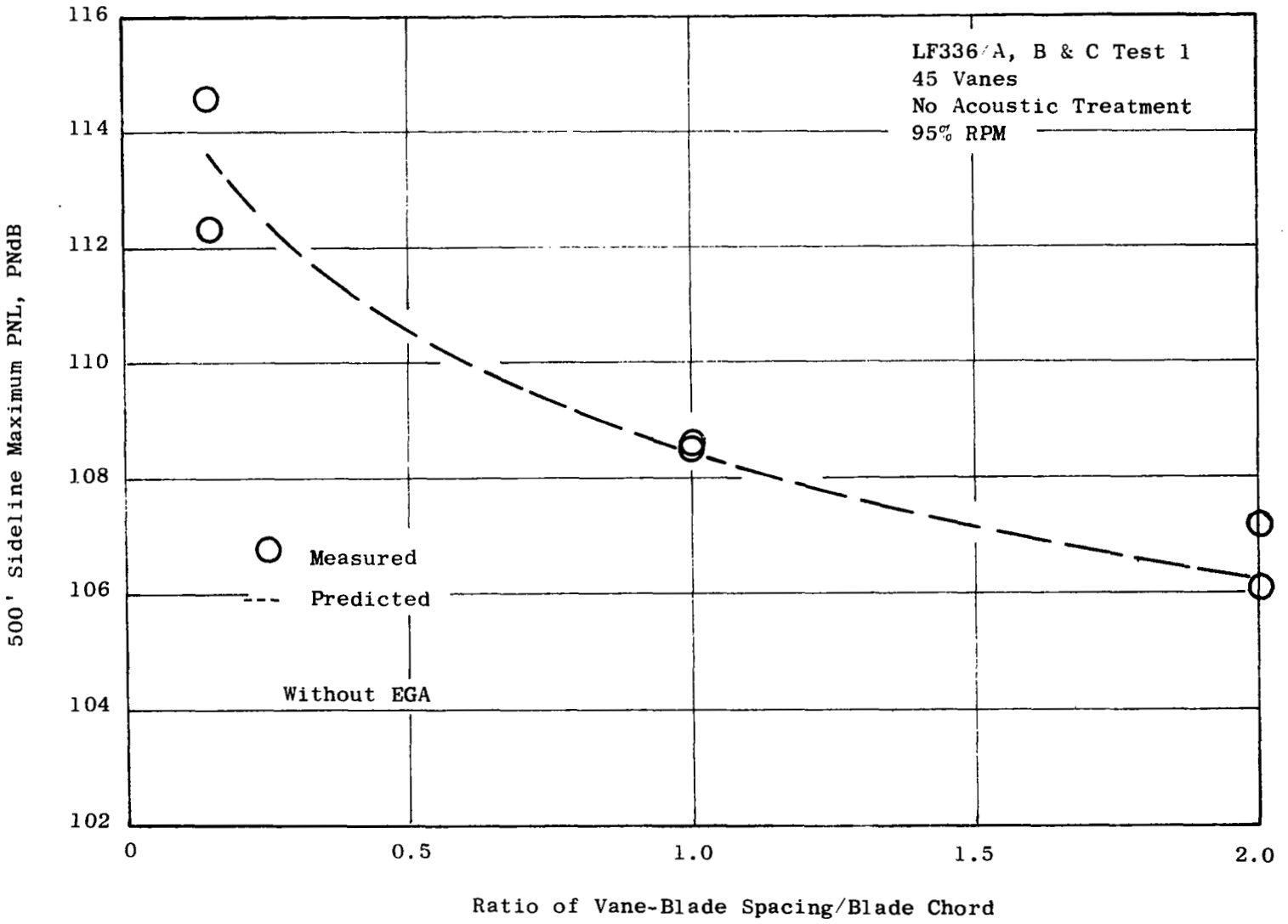

Figure 105. Comparison Between Measured and Predicted 500' Sideline PNL Versus Spacing

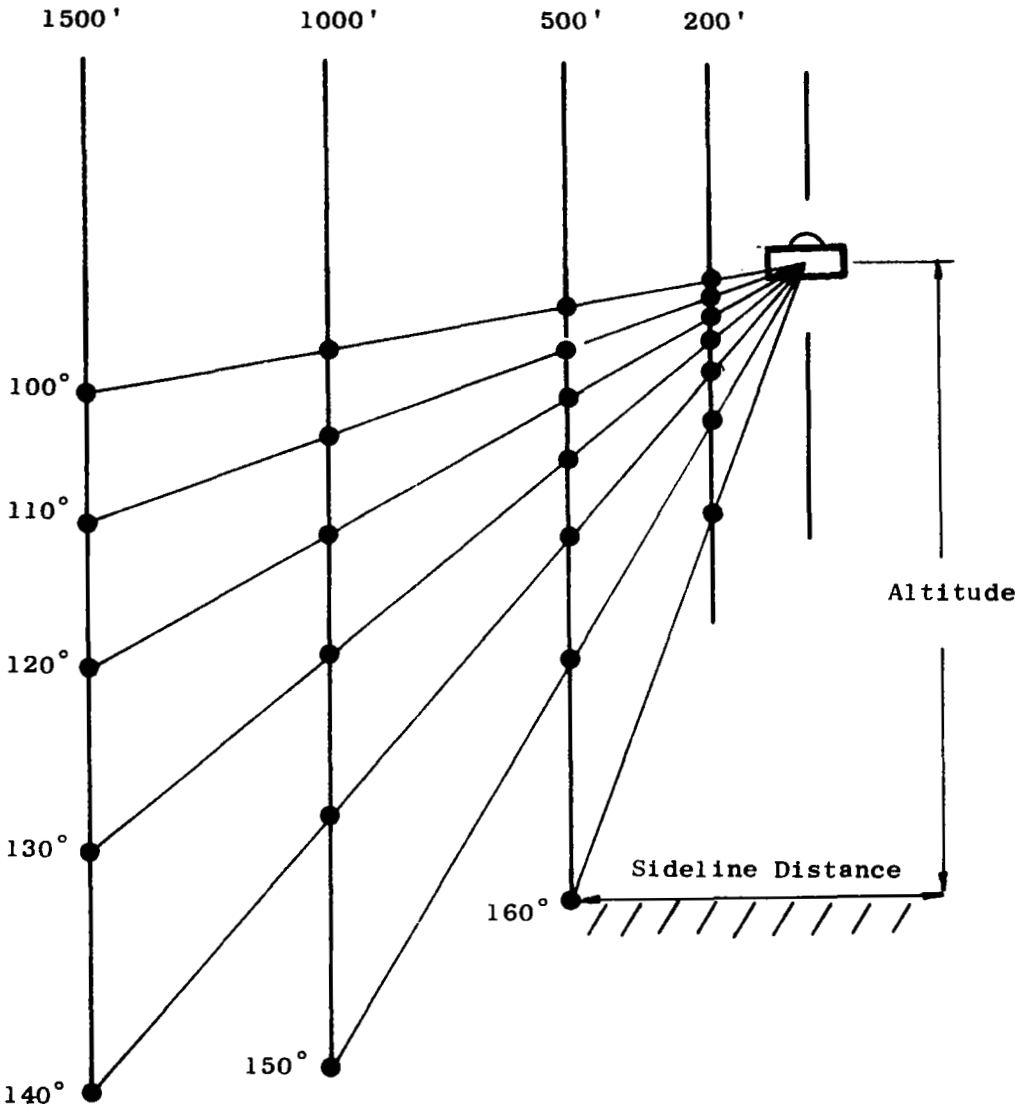

Figure 106. Flight Sideline Definitions

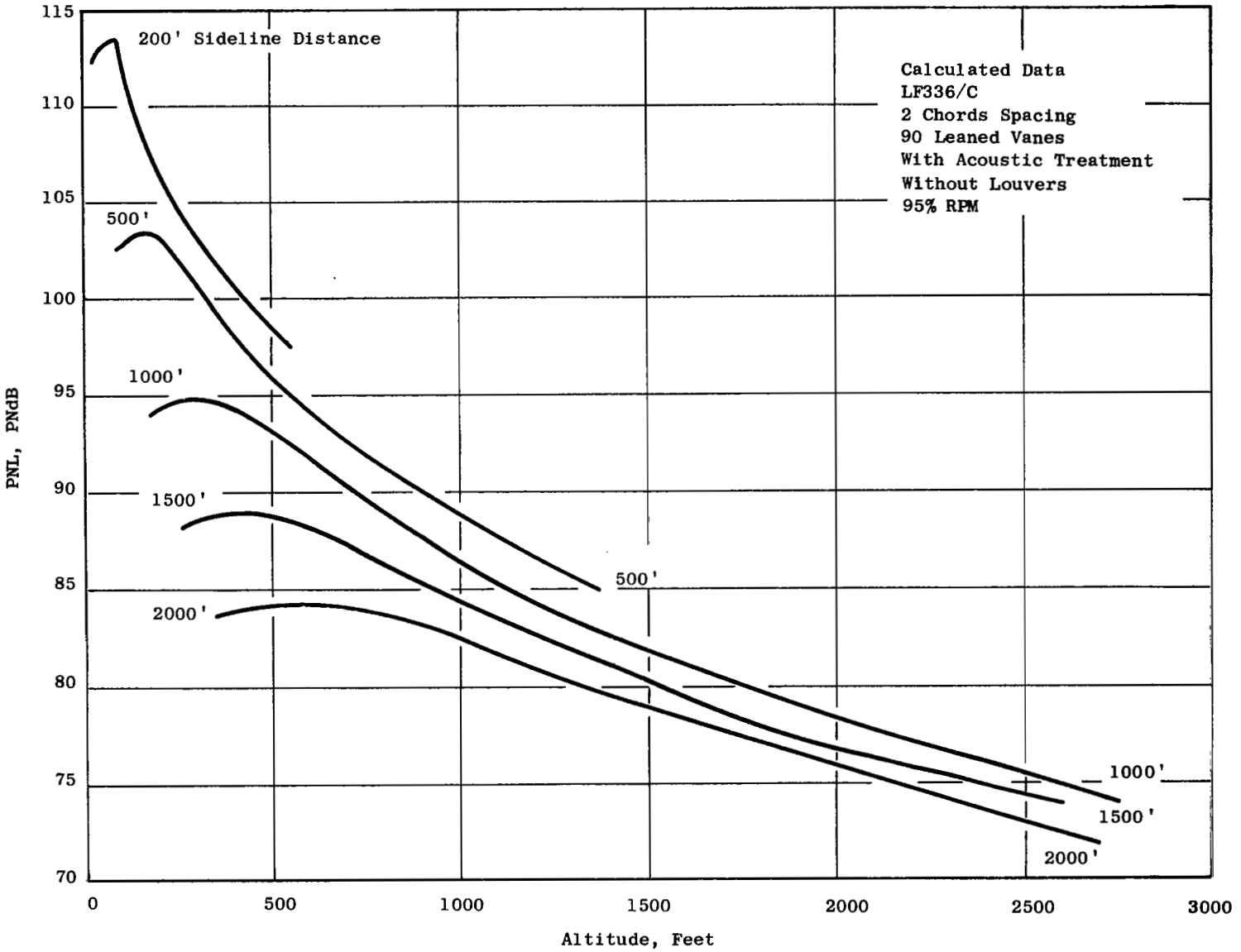

Figure 107. Calculated PNL Versus Altitude and Sideline Distance for 95% RPM

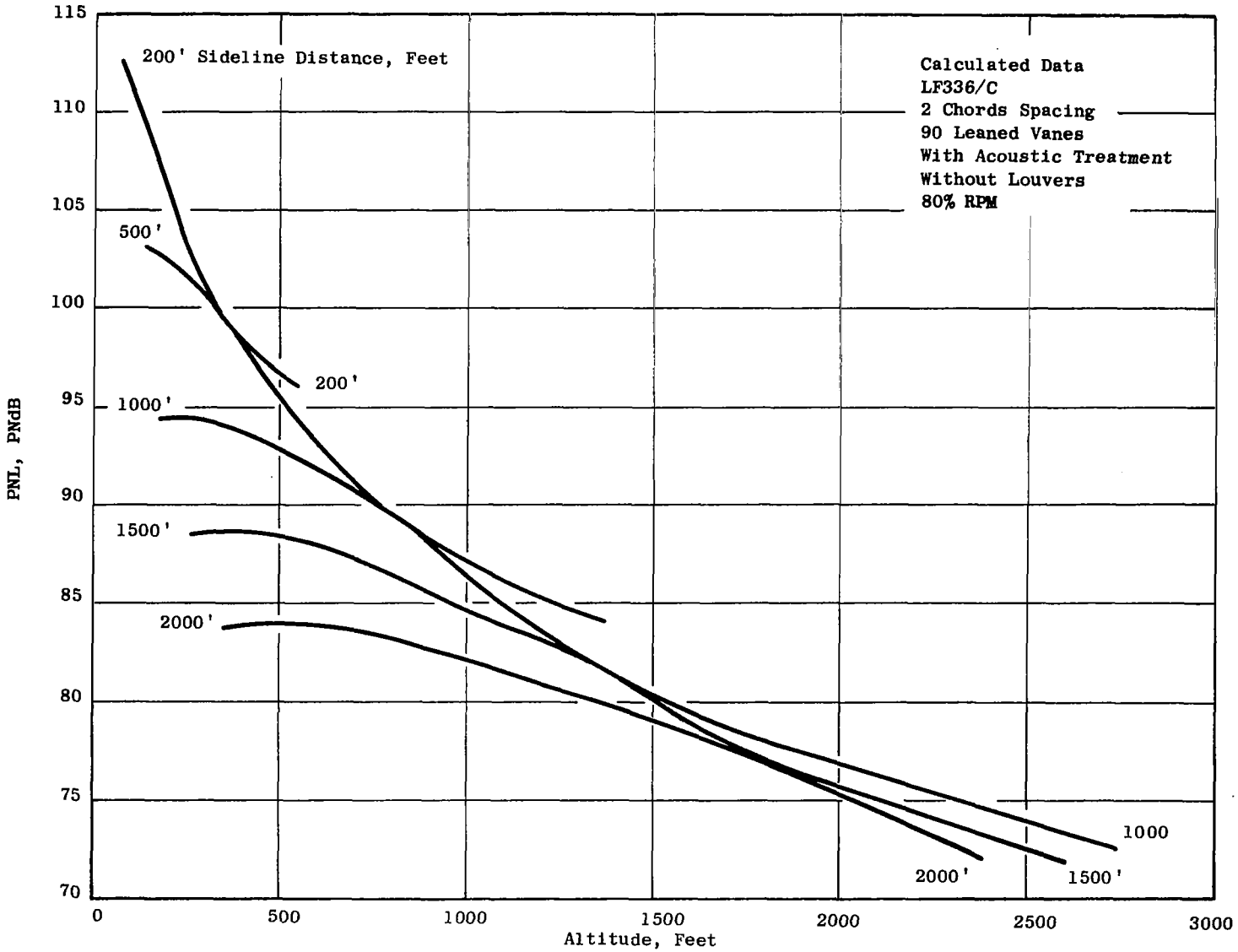

Figure 108. Calcualted PNL Versus Altitude and Sideline Distance for 80% RPM